Università
degli Studi
della Campania
Luigi Vanvitelli

DOTTORATO DI RICERCA IN
"SCIENZE BIOCHIMICHE E BIOTECNOLOGICHE"
XXXV CICLO

SETTORE SCIENTIFICO-DISCIPLINARE BIO/12

Curriculum: Biologia, Biochimica e Biotecnologie Mediche

ANNO ACCADEMICO 2021/2022

Integrating Gemcitabine based-therapy with AdipoRon in PDAC treatment & the inheritance of centromere in genome stability: possible therapeutic approaches for cancer care in Precision Medicine

Dottoranda: **Dott.ssa Angela Ragone**

Docente guida: **Prof. Silvio Naviglio**

Tutor di laboratorio: **Dr. Luigi Sapio**

Coordinatore: **Prof. Fulvio Della Ragione**

TABLE OF CONTENTS

SUMMARY I

PART I

1 INTRODUCTION TO INTEGRATING GEMCITABINE BASED-THERAPY WITH ADIPORON IN PDAC TREATMENT 1

1.1 Pancreatic cancer 1

1.1.1 Pancreatic cancer: an overview 1

1.1.2 PDAC: prevention, diagnosis and treatment 3

1.1.3 Gemcitabine and combination therapy 4

1.1.4 Clinical challenges in PDAC care 6

1.2 AdipoRon 8

1.2.1 Characteristics and possible therapeutic uses 8

1.2.2 AdipoRon as anticancer molecule: evidence from literature 9

2 RESULTS 11

2.1 Effects of AdipoRon and Gemcitabine on PDAC cells 11

2.2 Effects of combination AdipoRon plus Gemcitabine on PDAC cells 13

2.2.1 Combination improves single outcomes 13

2.2.2 Combination minimizes the clonogenic potential 16

2.2.3 Combination differently affects cell cycle 17

2.3 Involvement of p44/42 MAPK pathway in Combination outcome in PDAC cells 20

2.3.1 Combination activates p44/42 MAPK 20

2.3.2 p44/42 MAPK pathway perturbation counterparts Combination effectiveness 21

2.4 Combination effectiveness in Gemcitabine-resistant cells 23

3 DISCUSSION 26

4 CONCLUSION 30

5 MATERIAL & METHODS 31

5.1 Chemicals & Antibodies 31

5.2 Cell culture and experimental procedures 31

5.3 Development of Gemcitabine-resistant MIA PaCa-2 cells 32

5.4 Assessment of drug-mediated effect on alive and dead cells 32

5.5 Flow cytometry analysis 33

5.6 Colony forming assay 33

5.7 Western Blotting 34

5.8 Protein extraction and western blotting samples preparation 34
5.9 Statistical analysis 35

PART II

6 INTRODUCTION TO THE INHERITANCE OF CENTROMERE IN GENOME STABILITY .. 36
6.1 The centromere 36
6.2 CENP-A 38
6.3 The propagation of centromeric chromatin 41
6.4 The genome instability 45
6.5 CENP-A in cancer care 46
6.6 Objectives of the Project 48
7 RESULTS 51
7.1 Generation of CENP-A-SNAP RPE-1 stable cell line 51
7.2 Labelling of CENP-A-SNAP protein in RPE-1cells 52
7.3 Standardization of the synchronization protocol for labelling of CENP-A-SNAP in RPE-1 cells 54
8 DUSCUSSION AND FUTURE PERSPECTIVES 60
9 MATERIAL & METHODS 63
9.1 Chemicals & Antibodies 63
9.2 Cell culture and synchronization 63
9.3 Immunofluorescence 64
9.4 Chromatin purification 64
9.5 Co-Immunoprecipitation and sample preparation 65
9.6 Western Blotting 65
9.7 Flow cytometry analysis 66

BIBLIOGRAPHY 67

SUMMARY

Accross the years, Precision Medicine has gained great importance establishing itself as “the future of medicine”. In respect of the traditional therapeutic approach, which is universal and proposes an equal cure for all people using strategies of treatment and prevention based on meta-analysis of data patients, Precision Medicine offers a personalized therapy which takes into account the individuality of each case. Despite challenging, this therapeutic approach is now employed in different medical fields, especially in cancer care where a whole revolution has been initiated. Actually, the most used types of treatment belonging to Precision Medicine in cancer care are: i) targeted drug therapy, which makes use of the drugs designed to hit a specific target on cancer cells; ii) immunotherapy, which is used to help the patient immune system attack cancer. Unfortunately, whilst certain types of cancer have limited response to immunotherapy, identification of new targets is particularly slow due to both high failure rate and excessive costs. Therefore, discovering novel therapeutic approaches is mandatory in clinical practice for cancer cure. Taking the abovementioned state of art into consideration, my PhD thesis has been conceived to investigate both a possible alternative therapeutic approach for the pancreatic cancer, one of the deadliest malignancies, and the centromere protein A (CENP-A), the centromeric variant of canonical histone H3, which is fully involved in genome stability and promising therapeutic target for cancer care. For this reason, my thesis consists of two distinct parts.

The first part reports published data regarding the combination treatment AdipoRon plus Gemcitabine in pancreatic ductal adenocarcinoma (PDAC). PDAC accounts for 90% of all pancreatic cancers and even if its incidence is not among the highest, PDAC prognosis is fatal. As a result of either aggressiveness or metastatic stage at diagnosis, chemotherapy constitutes the only marginally effective therapeutic approach. Gemcitabine is still the cornerstone for PDAC management, even though the low response rate and the onset of resistant mechanisms claim for

additional therapeutic strategies. Recently, the first synthetic orally active adiponectin receptor agonist AdipoRon has been proposed as an anticancer agent in several tumors, including PDAC. To address its therapeutic potential and propose a potential therapeutic strategy for PDAC care, herein I investigated its pharmacodynamic interaction with Gemcitabine in human PDAC cell lines. Surprisingly, their simultaneous administration revealed a more effective action in contrasting PDAC cell growth and limiting clonogenic potential than single ones. Remarkably, the combination AdipoRon plus Gemcitabine persisted in being effective even in Gemcitabine-resistant MIA PaCa-2 cells. Moreover a different ability in braking cell cycle progression between AdipoRon and Gemcitabine supported their cooperating features in PDAC, and PD98059-mediated p44/42 MAPK ablation hindered combination effectiveness. Taken together, these findings propose AdipoRon as a suitable partner in Gemcitabine-based therapy and recognize the p44/42 MAPK pathway as potentially involved in combination outcomes.

The second part describes the state of art of the project about CENP-A, which I followed in the last year of my PhD during the internship with Max Planck Institute of Molecular Physiology in Dortmund, at the Department of Mechanistic Cell Biology directed by Prof. Dr. Andrea Musacchio. CENP-A is the epigenetic marker of the centromere in eukaryotic cells. It maintains centromere function ensuring the faithful chromosome segregation to daughter cells during cell division. CENP-A overexpression, in fact, directly perturbs genetic stability causing centromere dysfunction, chromosome instability and mitotic defects, which contribute in both tumorigenesis and its progession. Furthermore, its overexpression is a common feature of many cancers. Considering its crucial role in preserving genomic stability, CENP-A can be considered a potential future therapeutic target for cancer care. Particularly, a strong reduction of CENP-A nucleosomes dramatically increases the chance of centromere loss with severe consequences on the genomic stability of the cell. Additionally, the deposition of new CENP-A on chromatin is uncoupled from DNA replication and this implicates that the CENP-A pool is distributed, without new incorporation, to the sister chromatids during DNA replication and then restored after mitotic exit,

when deposition occurs, to guarantee the centromere identity. For understinding the molecular basis of centromere inheritance, the project is finalized to study CENP-A during S phase of cell cycle trying to shed light on the composition of the CENP-A nucleosome before and after DNA replication. To do this, I wanted to find a method to distinguish the pre-existing CENP-A protein from the new CENP-A protein deposited in the early G1 phase. This task requires development and standardization of a sophisticated synchronization protocol for differential labelling of the pre-existing and new CENP-A in human retinal pigment epithelial cells expressing CENP-A-SNAP, providing a predictable labelling schedule for additional validation experiments.

SOMMARIO

Nel corso degli anni, la Medicina di Precisione ha acquisito grande importanza affermandosi come "il futuro della medicina". Diversamente dall'approccio terapeutico tradizionale, che è universale e propone una cura uguale per tutti, usando strategie di trattamento e prevenzione basate sulla meta-analisi dei dati derivati dai pazienti, la Medicina di Precisione offre una terapia personalizzata che tiene conto dell'individualità di ciascun caso/paziente. Nonostante la sfida, questo approccio terapeutico è attualmente impiegato in diversi campi medici, in particolare in oncologia, dove ha dato inizio ad una vera rivoluzione nell'approccio terapeutico. Ad oggi, i tipi di trattamento appartenenti alla Medicina di Precisone più utilizzati nella cura del cancro sono: i) la terapia farmacologica mirata, che fa uso dei farmaci progettati per colpire un bersaglio specifico sulle cellule tumorali; ii) l'immunoterapia, che viene utilizzata per aiutare il sistema immunitario del paziente ad attaccare il cancro. Purtroppo, mentre determinati tipi di tumore hanno risposta limitata all'immunoterapia, l'identificazione di nuovi bersagli terapeutici è particolarmente lenta sia a causa dell'alto tasso di fallimento sia per i costi eccessivi. Pertanto, nuovi approcci terapeutici sono necessari per lotta contro il cancro. Prendendo in considerazione quanto sopra menzionato, la mia tesi di Dottorato studia sia un possibile approccio terapeutico alternativo per il cancro al pancreas, uno dei tumori più letali, sia la proteina centromerica A (CENP-A), la variante del canonico istone H3 tipica dei nucleosomi nella regione cromatinica, che è pienamente coinvolta nella stabilità del genoma e promettente bersaglio terapeutico per la cura del cancro. Per questo, la mia tesi si compone di due parti distinte.

La prima parte riporta i dati pubblicati riguardanti il trattamento combinatorio AdipoRon più Gemcitabina nell'adenocarcinoma duttale pancreatico (PDAC). Il PDAC rappresenta il 90% di tutti i tumori pancreatici e anche se la sua incidenza non è tra le più alte, la prognosi del PDAC è fatale. Come risultato dell'aggressività o della fase metastatica alla diagnosi, la chemioterapia costituisce l'unico approccio terapeutico marginalmente efficace. La Gemcitabina rimane di fatto

ancora oggi il farmaco dell'elezione per cura del PDAC, sebbene il basso tasso di risposta e l'insorgenza di meccanismi di resistenza richiedano ulteriori strategie terapeutiche. Recentemente, AdipoRon, il primo agonista sintetico oralmente attivo dei recettori del adiponectina, è stato proposto come agente anticancro in molti tumori, compreso il PDAC. Per avvalorare e supportare il suo potenziale terapeutico e proporre una potenziale strategia terapeutica per il PDAC, ho investigato sulla sua interazione farmacodinamica con la Gemcitabina nelle linee cellulari umane di PDAC. Sorprendentemente, la loro somministrazione simultanea ha rivelato un'azione più efficace nel contrastare la crescita delle cellule PDAC e limitare la loro capacità di formare colonie rispetto ai singoli agenti. Di particolare importanza, la combinazione si è dimostrata efficace anche in cellule MIA PaCa-2 resistenti alla Gemcitabina. Inoltre, la diversa capacità di bloccare la progressione del ciclo cellulare tra AdipoRon e Gemcitabina ha supportato la loro cooperazione in PDAC, e l'inibizione di p44/42 del pathway delle MAPK mediata da PD98059 ha ostacolato l'efficacia della combinazione. Complessivamente, i risultati ottenuti propongono AdipoRon come promettente partner per la Gemcitabina e individuano un potenziale coinvolgimento dei pathways delle MAPK, e in particolare quello di p44/42, nei meccanismi d'azione alla base dell'azione combinatoria.

La seconda parte, invece, descrive lo stato dell'arte del progetto su CENP-A, di cui mi sono occupata nell'ultimo anno del mio Dottorato di Ricerca durante l'internship con il Max Planck Institute of Molecular Physiology di Dortmund, presso il Dipartimento di Biologia Cellulare Meccanicistica diretto dal Prof. Dr. Andrea Musacchio. CENP-A è il marcatore epigenetico del centromero nelle cellule eucariotiche e determina la funzione del centromero, che assicura la corretta segregazione dei cromosomi tra le cellule figlie durante la divisione cellulare. La sovraespressione di CENP-A, infatti, perturba direttamente la stabilità genetica provocando disfunzione centromerica, instabilità centromerica e difetti nella mitosi, che contribuiscono sia alla tumorigenesi che alla sua progessione. Inoltre, la sua sovraespressione è una caratteristica comune di molti tumori. Considerando il suo ruolo cruciale nel preservare la stabilità genomica, CENP-A

può essere considerato un potenziale bersaglio terapeutico futuro per la cura del cancro. In particolare, una forte riduzione dei nucleosomi di CENP-A aumenta drasticamente la probabilità di perdita del centromero con gravi conseguenze sulla stabilità genomica della cellula. Inoltre, la deposizione di nuovo CENP-A sulla cromatina è disgiunta dalla duplicazione del DNA e questo implica che il pool di CENP-A è distribuito, senza nuova incorporazione, ai cromatidi fratelli durante la replicazione del DNA e poi ristabilito per garantire l'identità del centromero a termine della mitosi, quando il nuovo CENP-A viene depositato. Per comprendere la base molecolare dell'ereditarietà del centromero, il progetto è finalizzato a studiare CENP-A durante la fase S del ciclo cellulare cercando di far luce sulla composizione del nucleosoma di CENP-A prima e dopo la replicazione del DNA. Per fare questo, ho trovato un metodo per distinguere la forma preesistente di CENP-A dal nuovo CENP-A depositato agli inizi della fase G1. Questo metodo richiede lo sviluppo e la standardizzazione di un sofisticato protocollo di sincronizzazione, per l'etichettatura differenziale del preesistente e del nuovo CENP-A in cellulle epiteliali umane del pigmento retinico che esprimono CENP-A-SNAP, che fornisca un programma di possibili etichettature per ulteriori esperimenti di convalida.

PART I

1 INTRODUCTION TO INTEGRATING GEMCITABINE BASED-THERAPY WITH ADIPORON IN PDAC TREATMENT

1.1 PANCREATIC CANCER

1.1.1 PANCREATIC CANCER: AN OVERVIEW

Pancreatic cancer is one of the most fatal malignancies. Global Cancer Statics 2020 report 495,773 new cases and 466,003 deaths for pancreatic cancer and classify it as the seventh leading cause of cancer death worldwide due to its high mortality rate in spite of the incidence is far below the "*top cancers*", that are breast, lung and colorectum (Figure 1). (Sung et al., 2021)

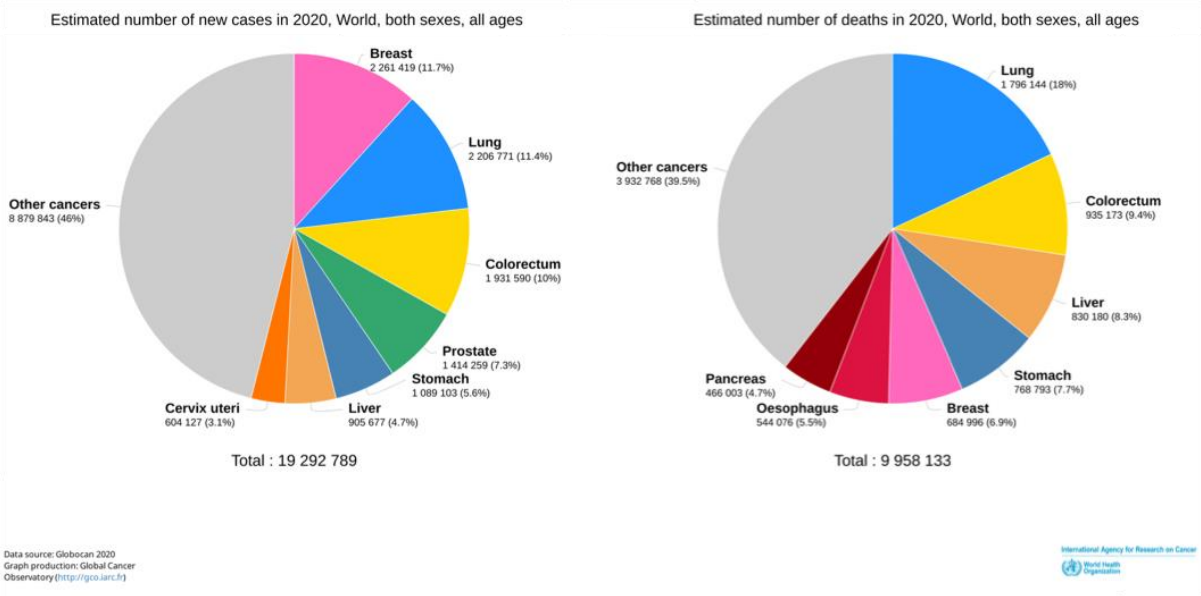

Figure 1. ***Global Cancer Statics 2020.*** (Adapted from Global Cancer Observatory – International Agency for Research in Cancer)

Pancreatic cancer has 5-years survival rate of approximately 10% and estimated projection give it as the second cause of cancer-related deaths by 2030, just behind lung cancer in the United States. (Christenson et al., 2020) Moreover, the median age at diagnosis is around 70 years and it is slightly more common in men than in women with 262,865 against 232,908 recorded cases in

2020. (Wang et al., 2020) In addition to age and gender, other risk factors for developing pancreatic cancer are race, tobacco use, diet, diabetes, alcohol consumption, family history and inherited genetic syndromes. (Klein, 2021) The incidence, for example, is lowest in Africa while higher in Australia, Northern America and Europe maybe because of the exposition to some other determinants associated with higher economic status, such as diabetes and being overweight; smoking as well as obesity are modifiable factors which increase the likelihood of developing pancreatic cancer; the germline mutations in the genes *BRCA1/2, ATM, MLH1, TP53,* or *CDKN2A*, represent further risk factors. In the end, pathological and molecular analysis of this type of tumor has identified around 63 genetic mutations, especially in *KRAS*, *TP53*, *CDKN2A*, and *SMAD4* genes, which contribute to the dysregulation of at least 12 altered signaling pathways in pancreatic tumors, such as Raf-MEK-ERK and PI3K/Akt, and cause heterogeneity leading to aggressiveness and lack of targeted therapy (Table 1). (Pompella et al., 2020; Wang et al., 2021)

	Frequency (%)*	Role in tumorigenesis
KRAS	91%	Constitutive activation of RAS–MAPK pathway promoting proliferation
TP53	70%	Impaired recognition of DNA damage and cell cycle arrest
CDKN2A	46%	Loss of regulation of the CDK4 and CDK6 growth checkpoint
SMAD	38%	Alteration in TGFβ signalling permitting increased proliferation
ATM	3%	Dysfunctional homologous recombination repair
BRAF	2·2%	Constitutive activation of RAS–MAPK pathway promoting proliferation
BRCA1	1·3%	Dysfunctional homologous recombination repair
BRCA2	1·3%	Dysfunctional homologous recombination repair
MSI family	0·8%	Impaired mismatch repair
PALB2	0·7%	Dysfunctional homologous recombination repair
NRG1 fusion	0·5%	Increased HER3 dimerisation with HER2 causing RAS–MAPK activation
NTRK fusion	0·3%	Upregulation of TRK activity
ALK amplification	0·16%	Constitutive activation of RAS–MAPK pathway promoting proliferation

*Percentage of pancreatic cancers with genomic aberrations.

Table 1. ***Genetic mutations in Pancreatic cancer*** (Adapted from *Christenson et al., 2020)*

1.1.2 PDAC: PREVENTION, DIAGNOSIS AND TREATMENT

Pancreatic cancer can develop from exocrine cells and neuroendocrine cells, such as islet cells. The most common subtype of exocrine cancer is pancreatic ductal cell adenocarcinoma (PDAC), which accounts for 90% of all pancreatic malignancies, while tumors derived from islet cells are almost uncommon and constitute 5% of the pancreatic neoplasms. (Gao et al., 2020)

As the totality of pancreatic tumors, PDAC is difficult to prevent given that some risk factors, like age, gender, race and familiarity, cannot be controlled. However, others which depend mainly on lifestyle can be modulate so as to lower the risk to develop it. At this purpose, in accordance with the increased likelihood, the most important avoidable risk factor is smoking. Next, it is recommended to stay in healthy weight, perform regular physical activity and limit alcohol consumption as much as possible. (Klein, 2021)

Unfortunately, the screening also is very tricky and unwarranted by the current available technologies. Actually, screening is often applied only in high-risk population for predisposition because of the lack of high specificity noninvasive tests. The detection of precursor lesions, and consequently the early diagnosis, in these individuals is achieved thanks to the diagnostic accuracy of endoscopic ultrasound-guided fine-needle aspiration (EUS-FNA), which is the gold standard for pancreatic cancer diagnosis. (Yang et al., 2021) Additionally, tardive diagnosis aggravates the scenario: patients with PDAC have no specific symptoms until advanced stage.

At the time of diagnosis, PDAC patients can be classified into four categories based on extent of disease: resectable, borderline resectable, locally advanced and metastatic. The major part of them (almost 50%) are diagnosticated with metastatic stage in which the tumor has already spread to other organs, such as the liver, lungs, or distant parts of the abdomen; then, the patients with a locally advanced stage, in which cancer is still located only in the area around the pancreas and it has grown close to nearby arteries, veins, or organs. For these groups, the surgical resection is chiefly impossible while remains the best chance, sometimes in association with neoadjuvant therapies, in the other two cases, when the tumor is localized or borderline localized. (Mizrahi et

al., 2020) In fact, the surgery, preceded or followed by chemotherapy with or without radiation, represents the only chance for recovery in PDAC and the chemotherapy is the only one solution to improve survival rate when the advanced stage leaves no longer chances of recovery. (Huang et al., 2019; Qian et al., 2020)

1.1.3 GEMCITABINE AND COMBINATION THERAPY

Across the years, the combination therapy has received great attention as a potential successful strategy to overcome resistance and mitigate toxicity targeting different pathways in cancer care. The agents used in combination can works in synergistic or additive manner, and therefore a lower therapeutic dosage of each single drug is required. (Bayat et al., 2017; Plana et al., 2022)

Regarding the pancreatic cancer, chemotherapy is a fundamental aspect of the comprehensive treatment and systemic chemotherapy combinations including FOLFIRINOX (5-fluorouracil, leucovorin, irinotecan, and oxaliplatin) and Gemcitabine plus nab-Paclitaxel remain the mainstay of treatment for patients with advanced disease (Figure 2). (Riedl et al., 2021)

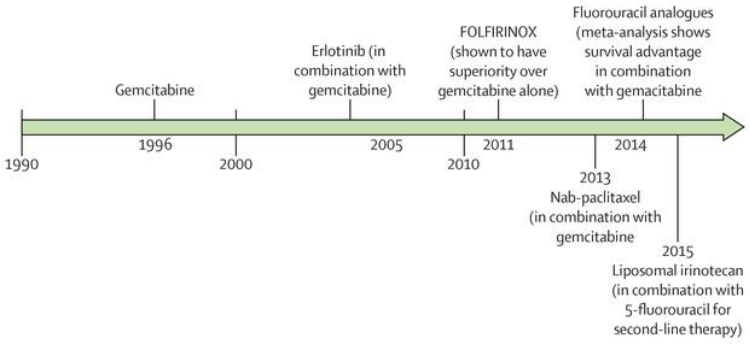

Figure 2. ***Timeline of U.S. Food and Drug Administration (FDA) approvals for the treatment of metastatic pancreatic cancer.*** (Adapted from *Christenson et al., 2020*)

Although FOLFIRINOX provides significant results in improving both overall and median progression-free survival, its side effects limit the administration only in patients with good performance status. (Damm et al., 2021) Unfortunately, this limitation is very common in PDAC patients given that the diagnosis happens in the major part of cases when the general health is

already compromised. If the patient is not suitable for combination chemotherapy, the best therapeutic regimen is Gemcitabine, which remains the standard of care for advanced PDAC. (Oba et al., 2020)

Gemcitabine, or 2',2'-difluoro 2'-deoxycytidine (dFdC), is the most important cytidine analogue developed by cytosine arabinoside displaying distinctive pharmacological properties and a wide spectrum of antitumor activity in many cancers, including PDAC. (de Sousa Cavalcante et al., 2014) To be effective, Gemcitabine requires cellular uptake and intracellular phosphorylation. Inside the cell, the prodrug Gemcitabine is first phosphorylated to Gemcitabine monophosphate (dFdCMP) by deoxycytidine kinase (dCK) and then converted to the two active metabolites, Gemcitabine di- and triphosphate (dFdCDP and dFdCTP, respectively). Moreover, Gemcitabine has multiple intracellular targets and its antiproliferative activity is the result of several inhibitory actions on DNA synthesis: dFdCTP competes with deoxycytidine triphosphate (dCTP) as an inhibitor of DNA polymerase and its incorporation leads to termination of chain elongation; dFdCDP is a potent inhibitor of ribonucleoside reductase, resulting in depletion of deoxyribonucleotide pools necessary for DNA synthesis and, thereby potentiating the effects of dFdCTP (Figure 3). (Principe et al., 2021) Due to its low membrane permeability, the prerequisite for clinically efficacy of Gemcitabine is the presence of nucleoside transporters (NTs) located in the cell plasma membrane which guarantee its uptake. Consequently, when the NTs are not well-expressed or inhibited, patients are resistant to Gemcitabine. In addition, activating and inactivating enzymes and competitive substrates involved in the activation of metabolites also play a crucial role in the mechanism of resistance to this drug. Regrettably, the extensive administration of Gemcitabine and its limited toxicity usually conflict with a very low response rate and resistant mechanism acquisition. (Amrutkar and Gladhaug, 2017; Fu et al., 2021)

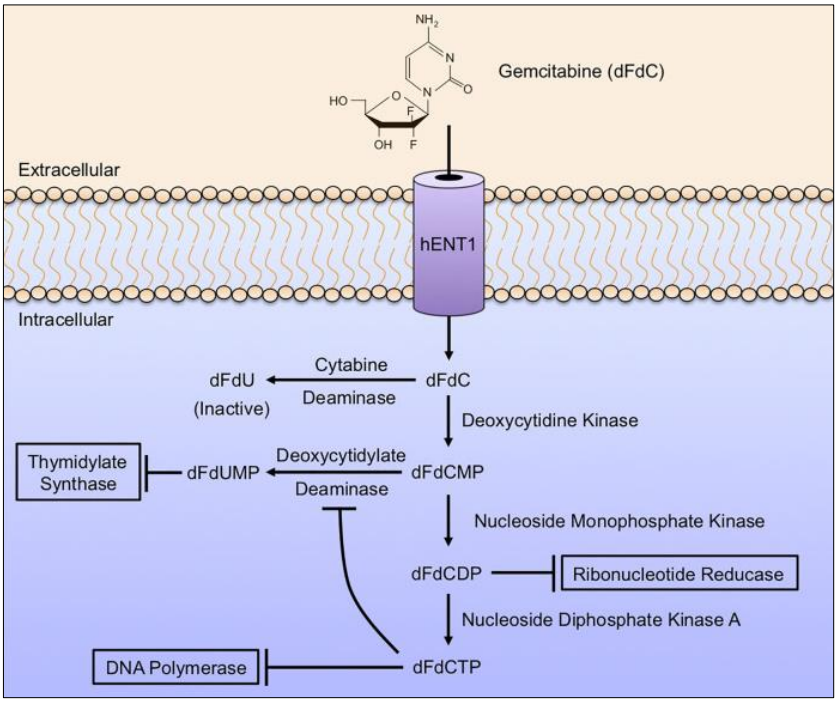

Figure 3. ***Gemcitabine mechanism of action.*** (Adapted from *Principe et al.,2021*)

1.1.4 Clinical challenges in PDAC care

Despite the huge efforts made to improve PDAC treatment over the last years, the number of PDAC related deaths is dramatically on the rise and it is projected to be the second cause of cancer-related deaths in the next years. (Lippi and Mattiuzzi, 2020) Generally, 1-year survival rate for PDAC patients is 60.1% while the median survival is 16 months (Braun et al., 2022).

Low survival rate mainly derives from a late diagnosis, high recurrence rate as well as lack of effective treatments for advanced stages. In fact, only a minority of patients (about 20%) is eligible for surgery at the time of diagnosis and the greatest step towards an improvement of treatment for nonresectable PDAC has been made with the introduction of the two combination chemotherapy regimens FOLFIRINOX and Gemcitabine plus nab-Paclitaxel, respectively. (Vernuccio et al., 2021; Riedl et al., 2021) Therefore, in order to improve the outcomes of PDAC, an early diagnosis is mandatory and more effective therapies are urgently required.

Regarding the first clinical challenge, there is an urgent need for biomarkers and tools for detecting PDAC at initial stage. At this purpose, non-invasive biomarkers have been widely investigated in

blood and urine human samples, but only carbohydrate antigen 19-9 (CA19-9) has received approval by FDA. (Yong and Wirama, 2022) CA19-9, also known as Sialylated Lewis antigen (Sla), is produced by a deregulated glycosylation. In the normal condition, glycosylated proteins play various crucial functions including protection and lubrication of the pancreatic ducts. However, during cancer progression, aberrant glycosylation, one of the hallmarks of cancer, provokes the formation of various glycosylated residues such as CA19-9.

Unfortunately, the sensitivity and specificity of CA19-9 are inadequate for PDAC diagnosis, and its clinical use is restricted to monitoring treatment response and recurrence in patients with PDAC already diagnosed.

Regarding the second challenge, PDAC shows significant resistance to chemotherapy, targeted therapy and immunotherapy due to its distinctive features, including heterogeneity of genetic mutation and complex tumor immune microenvironment. (Bai et al., 2022)

In contrast to other solid tumors, like breast and lung cancer, where clinical and molecular classification systems permit a better patient management, the clinical and prognostic impact of tumor genetics in PDAC still remains under investigation for the low prevalence and the great genetic heterogeneity among different tumors and between the different cells of the same tumor. (Gutiérrez et al., 2021; Pompella et al., 2020; Orth et al., 2019)

In addition, PDAC is the only tumor in which neoplastic cells are surrounded by an abundant and dense stroma associated with tissue inflammation. In details, the dense stroma may represent up to 90% of the whole tumor mass and it is characterized by an extensive fibrosis, reduced vascularization, a hypoxic environment with a highly variable number of tumor-infiltrating immune cells (TILs). Moreover, the fibrotic tumor tissue, also called desmoplasia, consists of cancer-associated fibroblasts (CAFs), endothelial cells, and pancreatic stellate cells (PSCs) immersed in a highly variable extracellular matrix (ECM) of collagen, glycosaminoglycans, proteoglycans, and growth factors. As result, the stroma contributes to produce a barrier for drug delivery and influences cancer cell behaviors so that the tumor is defended instead of affected by

immunotherapeutic drugs. These peculiarities all together make PDAC one of the most resistant tumors to immunotherapy. (Sapio et al., 2022)

Nevertheless, current research is aimed at developing new treatment options, such as the use of agents targeting the oncogenic network signaling of KRAS, the most mutated gene in PDAC, or modifying tumor microenvironment to overcome resistance in immunotherapeutic approach. (He et al., 2022; Zhu et al., 2022)

1.2 AdipoRon

1.2.1 Characteristics and possible therapeutic uses

AdipoRon is the first oral active adiponectin receptor agonist. As a result of chemical library screening, it was discovered in 2013 by Okada-Iwabu and colleagues at the Open Innovation Center for Drug Discovery of the University of Tokyo thanks to its capability of bonding both adiponectin receptors, AdipoR1 and AdipoR2, and turning on AMPK in C2C12 murine myeloblast cells. (Okada-Iwabu et al., 2013)

AdipoRon was synthesized by Enamine Ltd. (Kiev, Ukraine) starting from the alkylation of hydroxybenzophenone with methyl chloroacetate. On the whole, it consists of three distinct functional groups arranged together as follows: 1-benzyl 4-substituted 6-membered cyclic amine moiety, carbonyl group and a terminal aromatic ring. Indeed, according with radioactive binding and Scatchard analysis, AdipoRon has a specificity in binding both AdipoR1 and AdipoR2 in vitro with a constant value for the dissociation (Kd) of about 1.8 and 3.1 μM, respectively. (Nigro et al., 2021)

Unfortunately, the lack of its crystal structure hampered the proper recognition of the binding site during discovery and, even if the 3D structures of receptors are currently well known, this information is still missing. Certainly, the suitable distance between the carbonyl group and the cyclic amine, as well as within the cyclic amine and the aromatic ring(s), could provide the right

spatial arrangement for both AMPK activation and AdipoRon-dependency. Moreover, since specific structural motifs have also been observed in other ligands of G-protein-coupled receptors (GPCR), such as the aromatic rings binding via cyclic amine, similarities in ligand recognition cannot be ruled out between these two types of membrane receptors.

AdipoRon has been proven to possess pharmacological properties similar to adiponectin (Acrp30), an adipose tissue-derived hormone, and its ability to bind and activate AdipoR1 and AdipoR2 receptors make it a suitable candidate for the treatment of several disorders. (Bath et al., 2020) In this regard, AdipoRon exhibits strong anti-obesity, -diabetic, -cancer, -depressant, -ischemic, -hypertrophic properties in experimental systems and also improves conditions like post-traumatic stress disorder, anxiety, and systemic sclerosis.

1.2.2 AdipoRon as anticancer molecule: evidence from literature

An increasing number of studies provides consistent evidence supporting AdipoRon as potential anti-tumoral agent in a wide variety of preclinical cancer models, particularly PDAC, myeloma, breast and ovarian cancer. (Messaggio et al., 2017: Ramzan et al., 2019; Wang et al., 2020; Akimoto et al, 2018; Wang et al., 2017) Recently, we also described how AdipoRon can strongly inhibit cell proliferation in osteosarcoma cells. (Sapio et al., 2020)

Beyond the canonical activation of AMPK and its related downstream target acetyl-CoA carboxylase (ACC), AdipoRon has been described to module both AMPK-dependent and -independent pathways as signal transducer and activator of transcription 3 (STAT3), protein kinase B (PKB), extracellular signal-regulated kinase 1/2 (ERK1/2), and p38. (Messaggio et al., 2017; Akimoto et al., 2018)

Based on the existing knowledge, the G0/G1 phase delay or blockage exerted by AdipoRon seems to be the functional key mechanism by which it induces growth arrest in vitro and in vivo. (Nigro et al., 2021) Nevertheless, the cytotoxic-mediated effects are not totally clear: albeit an increase in apoptosis-related proteins has been observed in reaction to AdipoRon administration in PDAC,

myeloma and ovarian cancer, the programmed cell death does not appear to be the only signaling engaged by AdipoRon. Indeed, conflicting evidence exist on the involvement of the apoptosis, especially in PDAC. In this respect, characterizing AdipoRon consequences in human and mouse pancreatic cancer models, Messaggio and colleagues recognized the Annexin V positive cell increase as a direct marker of apoptosis induction. On the contrary, using Z-VAD-FMK as a pan-caspase inhibitor, Akimoto and coworkers did not observe any amelioration in AdipoRon-induced cytotoxicity, thus excluding caspase-dependent apoptosis as the main cause of death. (Messaggio et al., 2017; Akimoto et al., 2018)

Besides apoptosis, other findings report different types of cell death in response to AdipoRon administration, including RIPK1/ERK-dependent necroptosis and AMPK-mediated autophagy, however. (Wang et al., 2020; Akimoto et al., 2018)

2 RESULTS

2.1 EFFECTS OF ADIPORON AND GEMCITABINE ON PDAC CELLS

Recently, two studies have reported the AdipoRon ability in suppressing tumor growth in PDAC. (Messaggio et al., 2017; Akimoto et al. 2018) In order to extend and corroborate these findings, we first established the impact of AdipoRon in two human PDAC cell lines, namely, MIA PaCa-2 and PANC-1, which are extensively accepted as representative PDAC models.

In line with the previous published results, AdipoRon exposure induced a remarkable cell growth decrease in PDAC cells, almost in a dose-dependent manner, without substantial differences between MIA PaCa-2 and PANC-1 cell types (Figure 4A). Choosing 10 μg/mL as a subsequent effective working dosage, time course experiments up to 72 hours showed a near time dependency in MIA PaCa-2. In this case, a cell number decrease of 20, 42, and 57% was recorded at 24, 48, and 72 hours, respectively (Figure 4B). Instead, a different trend was obtained in PANC-1, where no considerable responsiveness to AdipoRon was observed at 24 hours (Figure 4B).

Remarkably, AdipoRon-mediated antiproliferative properties were supported by an increase in the G0/G1 phase and a concomitant decrease of both S and G2/M phases in MIA PaCa-2 (Figure 4C). In details, the cell amount in G0/G1 moved from 35 to 48% after 24 hours of treatment with 10 μg/mL AdipoRon, while both S and G2/M phases decreased by around 6%, concurrently.

Interestingly, although 10 μg/mL AdipoRon was not effective in impacting PANC-1 cell growth after 24 h, changes in cell cycle phases distribution were detected. Like to MIA PaCa-2 cells, AdipoRon causes a G0/G1 intensification and an S-phase depletion in PANC-1 although with a less sharp magnitude. Unlike, no G2/M involvement seems to occur.

Before exploring the consequences of the combination treatment AdipoRon plus Gemcitabine (Combo) in these PDAC cell lines, we preliminarily addressed the Gemcitabine-mediated cell growth impact on both employed cells.

Evaluating a wide concentration range, Figure 4D displays a different aptitude in reacting to the chemotherapy drug between MIA PaCa-2 and PANC-1. While MIA PaCa-2 showed great responsiveness to Gemcitabine already at very low concentration, the PANC-1 ability in resisting Gemcitabine was further confirmed when high dosages were applied. Exposing MIA PaCa-2 to 50 or 100 nM Gemcitabine for 48 hours, for instance, nearly affected the totality of the cells, differently from PANC-1, in which the inhibition rate was roughly 40 and 60%, respectively.

Overall, these findings further recognize AdipoRon as an antiproliferative compound in PDAC, support the peculiarity of AdipoRon in slowing-down cell cycle and remark an effective yet different Gemcitabine sensitivity between the examined PDAC cells.

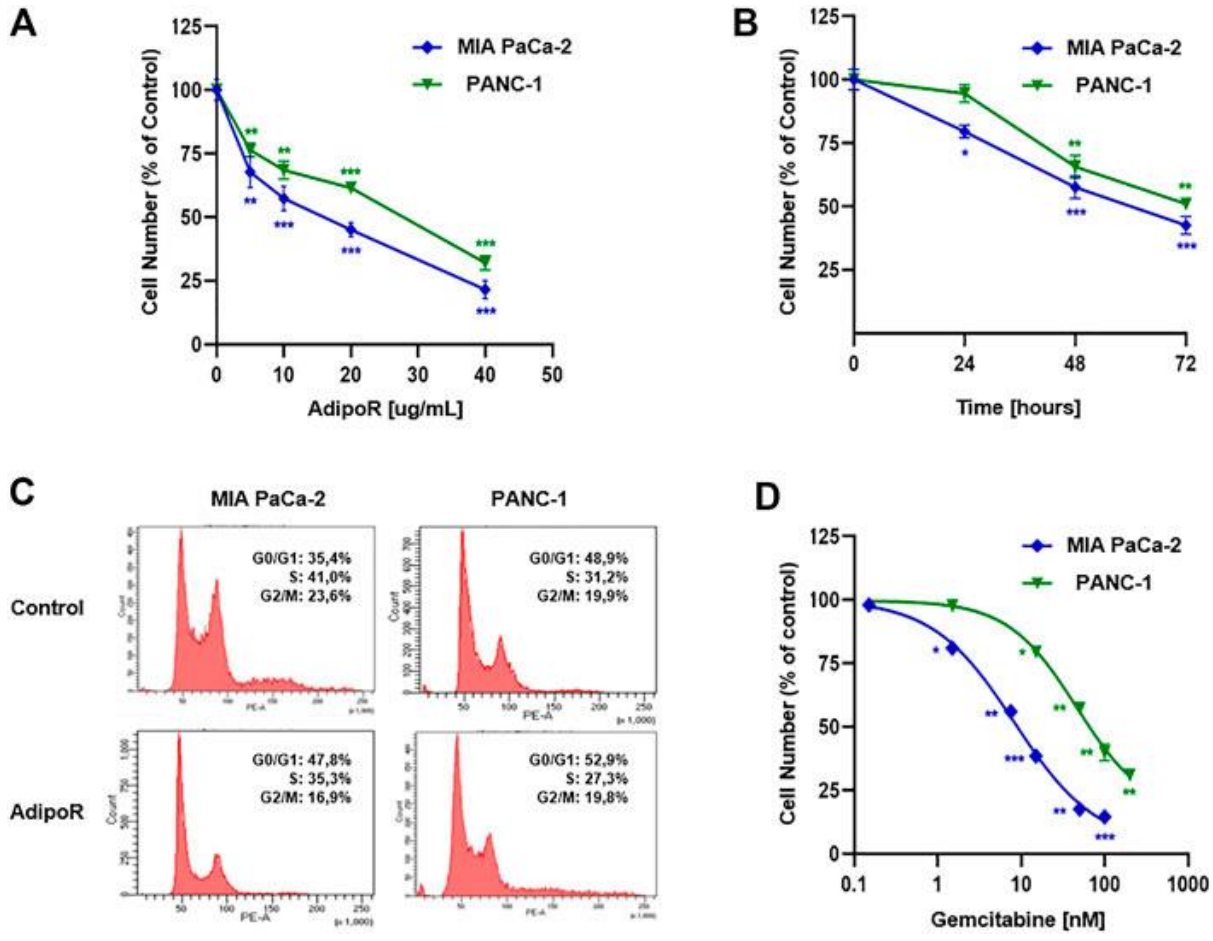

FIGURE 4. ***Evaluation of single drug-mediated effects in PDAC cells.*** **(A)** MIA PaCa-2 and PANC-1 cells were exposed for 48 h to increasing AdipoRon (AdipoR) concentrations (10–40 μg/mL). **(B)** Cell growth curves were established in reaction to 10 μg/ml AdipoR over a period of 72 h. **(C)** Representative cell cycle profiles were obtained in MIA PaCa-2 and PANC-1 cells treated and not (control) with 10 μg/mL AdipoR for 24 h. **(D)** Dose effect induced by 48 h of Gemcitabine administration in MIA PaCa-2 and PANC-1 cells. In each experimental condition, the relative cell number was estimated in triplicate and expressed in figure as % of control. *$p < 0.05$, **$p < 0.01$, ***$p < 0.001$ by unpaired Student's t-test. (Adapted from *Ragone et al.,2022*)

2.2 Effects of combination AdipoRon plus Gemcitabine on PDAC cells

2.2.1 Combination improves single outcomes

To address the potential cooperating effects between AdipoRon and Gemcitabine in PDAC models, we subsequently combined effective concentrations of both molecules in a constant dilution ratio, and the relative outcomes in cell growth were later assessed.

Specifically, three different doses of both AdipoRon (5, 10, and 20 μg/mL) and Gemcitabine (7.5, 15, and 30 nM) were employed in MIA PaCa-2 cells, which exhibit a clear dose dependency (Figure 5A). Even more interestingly, the concomitant use of AdipoRon and Gemcitabine further counteracted the proliferation in MIA PaCa-2 cells, suggesting a positive interplay between the two compounds.

Comparing the combination condition of 5 μg/mL AdipoRon and 7.5 nM Gemcitabine with corresponding agents, the combination treatment improved single outcomes by nearly 33% and 20% in respect of AdipoRon and Gemcitabine, respectively. This tendency became even more pronounced at the highest tested doses, raising inhibition values of 47% versus AdipoRon and 34% versus Gemcitabine (Figure 5A).

The different Gemcitabine responsiveness has required the use of higher concentrations in PANC-1 (25, 50, and 100 nM), while no changes in AdipoRon doses were applied.

In keeping with MIA PaCa-2 results, all three tested combination conditions enhanced the anticancer effects of single treatments also in PANC-1 (Figure 5B). Minimal fluctuations were observed in response to the increasing combinations in PANC-1.

CompuSyn analysis was subsequently performed with the purpose of defining both drug-drug interaction and the relative combination index (CI). Plotting dose-effect curves of both single and combination agents, the Chou-Talalay method discriminates among additive (CI = 1), synergism (CI < 1), and antagonism (CI >1) effects, using the median-effect equation. (Chou, 2010)

Based on Fa-CI plots of analysis, AdipoRon and Gemcitabine exercised a robust synergism in MIA PaCa-2 already at very low concentrations, maintaining a constant trend even when combination affected 90% of cells (Figure 5C). On contrary, the Fa-CI plot unveiled a different tendency in PANC-1 albeit in all tested conditions CI estimation supported a synergic action (Figure 5D).

Then, we performed time-course experiments, using 10 μg/mL AdipoRon plus 15 nM Gemcitabine in MIA PaCa-2 or 50 nM Gemcitabine in PANC-1. Although co-administration improved cell reduction mediated by single drugs in both PDAC models, different curves were outlined over time. Whilst a time dependency was revealed in reaction to both single and combination treatments in MIA PaCa-2 (Figure 5E), no clear reliance on treatment duration was observed in reaction to Gemcitabine in PANC-1. Indeed, comparing combination versus AdipoRon, the time exposure did not amplify the gap (Figure 5F).

Collectively, these data show that the combination impairs MIA PaCa-2 and PANC-1 cell growth more effectively than the singles. In addition, as suggested by CompuSyn analysis, a potential synergism might exist between AdipoRon and Gemcitabine.

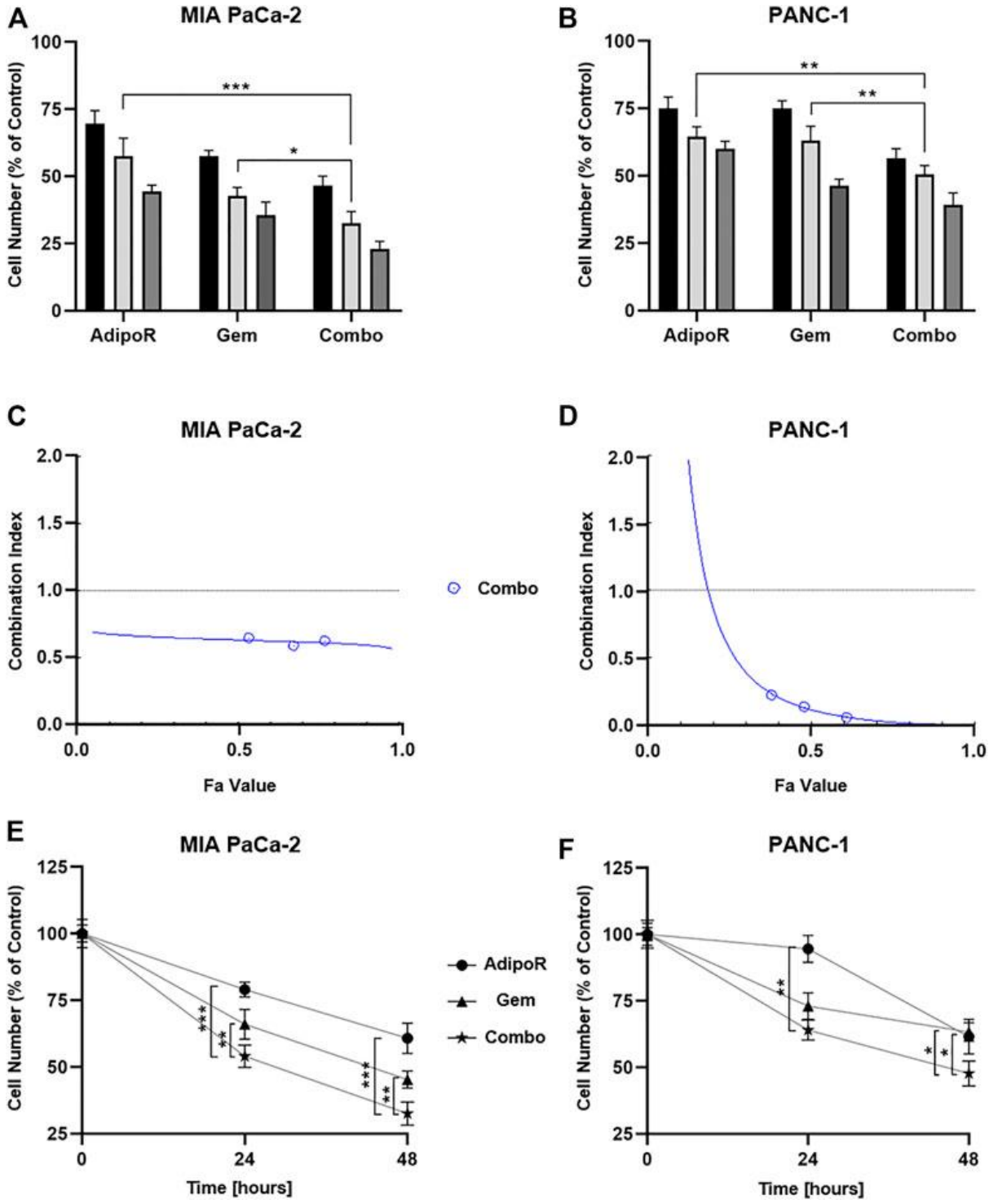

FIGURE 5. ***Assessment of single and combinatory outcomes in PDAC cells.*** **(A)** 5 (black bar), 10 (light gray), and 20 µg/mL (gray) of AdipoR were added to MIA PaCa-2 cell medium for 48 h, either alone or in combination with 7.5 (black bar), 15 (light gray), and 30 nM (gray) Gemcitabine (Gem). Colors of the columns reflect those of single drug concentrations in combination setting. **(B)**Identical AdipoR amounts were instead mixed with 25 (black bar), 50 (light gray), and 100 nM (gray) Gem in PANC-1. Representative Fa-CI report obtained in MIA PaCa-2 **(C)** and PANC-1 **(D)**. **(E)** MIA PaCa-2 growth curves achieved after 24 and 48 h under 10 µg/mL AdipoR, 15 nM Gem, and AdipoR plus Gem, respectively. The same AdipoR concentration (10 µg/ml) and a different Gem amount (50 nM) were applied in PANC-1 time course experiments **(F)**. For each stimulation, cell number was estimated at least in triplicate and reported in figure as average ± SD in % of control. *$p < 0.05$, **$p < 0.01$, ***$p < 0.001$ by Tukey's multiple comparisons test. (Adapted from *Ragone et al.,2022*)

2.2.2 COMBINATION MINIMIZES THE CLONOGENIC POTENTIAL

The clonogenic assay is considered a valuable in vitro assay for monitoring undifferentiated potential and anchorage-independent growth. (Rajendran and Jain, 2018) Given that Gemcitabine and AdipoRon have been proved to act as effective agents in mitigating colony formation, we successively addressed the potential impact of the combination on this PDAC cells. (Messaggio et al., 2017; Alhothali et al., 2019; Zhou et al., 2019)

Aiming at defining the consequences of long-term exposure, PDAC cells were seeded at very low density and treated with AdipoRon and Gemcitabine, both individually and in combination, until newly-formed colonies became visible.

The employment of a small amount of AdipoRon and Gemcitabine moderately impaired PDAC colony-forming ability, separately (Figure 6). Conversely, a very strong reduction in PDAC clonogenic potential was observed when the same doses of singles were put together (Figure 6A). Quantification analysis revealed a further enhancement in colonies reduction of nearly 40% compared to Gemcitabine in MIA PaCa-2, as a result of both number and size decrease (Figure 6B). Consistent results were also obtained in PANC-1 (Figure 6C).

Taken together, these results indicate a stronger and deeper outcome in limiting PDAC clonogenic potential made by combinatory treatment compared to single-agent administration.

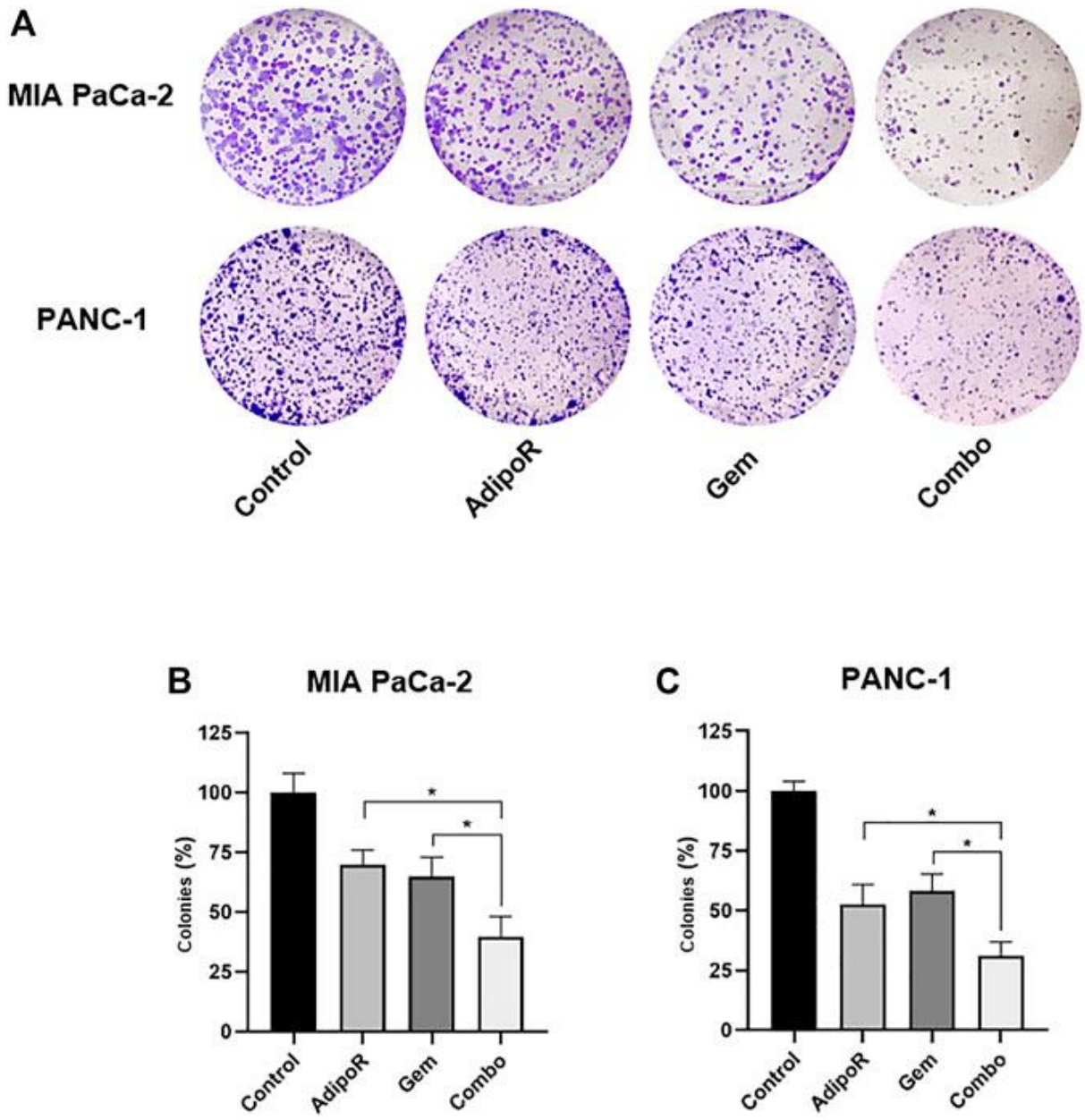

FIGURE 6. ***Estimation of single and combinatory impacts on clonogenic potential in PDAC cells.*** MIA PaCa-2 and PANC-1 were treated and not (control) with the same AdipoR concentration (2 µg/mL) but different Gem amounts (4 vs 6 nM), both individually and in combination, for 8 and 10 days, respectively. Representative stained wells are displayed in **(A)**, while the relative quantification analysis has been reported in **(B)**(MIA PaCa-2) and **(C)** (PANC-1). Experiments were reproduced thrice and plotted on a graph as mean value ± SD in % of control. *$p < 0.05$ by Tukey's multiple comparisons test. (Adapted from *Ragone et al.,2022*)

2.2.3 COMBINATION DIFFERENTLY AFFECTS CELL CYCLE

To figure out how the combination treatment AdipoRon plus Gemcitabine affected PDAC cell growth, we analyzed cell cycle to determine the distribution of phases in reaction to our *stimuli*. Comprehensively, single and combination treatments were performed in both PDAC models for

up to 48 hours, and the relative DNA content was later detected by flow cytometry using propidium iodide (PI) as basepair intercalating dye.

Depending on the concentration employed, Gemcitabine has been reported to induce both S and G2 phase arrest in PDAC models. (Miao et al., 2016; Montano et al., 2017; Passacantilli et al., 2018; Kumarasamy et al., 2020) In agreement with these findings, we observed a remarkable S phase accumulation in reaction to 24 hours of Gemcitabine administration in MIA PaCa-2 (Figures 7A,C). In respect of untreated cells, Gemcitabine raised S phase from 40 to 62% at the expense of G0/G1 (−14%) and partly G2/M (−7%). A more pronounced tendency was observed at 48 hours as a result of changes in both cell density and nutrients occurring in control cells, rather than a Gemcitabine-mediated action (Figure 7A). Quite the contrary, AdipoRon intensified the amount of cells in G0/G1 phase and decreased both S and G2/M phases at 24 hours, while at 48 hours, the G0/G1 enrichment was only supported by S phase reduction.

Looking at the cell phase distribution in reaction to the combination, different but intermediate features were detected in comparison with single agents. In this respect, after 24 hours, combination displayed a G0/G1 amount closer to AdipoRon, while conversely, their simultaneous presence for another 24 hours exhibited an S phase accumulation similar to Gemcitabine (Figures 7A,C). A quite comparable pattern was also obtained in PANC-1, especially following 24 hours of treatment (Figures 7B,C).

In agreement with the recorded cell cycle phases distribution, considerable changes were also detected in cyclin A1 and E1 levels, and cyclin-dependent kinase inhibitor $p27^{KIP1}$, in reaction to both single and combined *stimuli* (Figure 7D and Supplementary Figure S1).

Analysis of subG1 population, which usually includes hypodiploid cells undergoing DNA fragmentation, showed a substantial increase in reaction to both Gemcitabine and combination at 48 hours in respect of the untreated cells (Figure 7E). The absence of significant additive cytotoxic effects between Gemcitabine and combination was also confirmed in trypan blue exclusion assay,

which revealed only minimal changes in dead vs alive cells in response to these two conditions (Figure 7F).

Comprehensively, these findings reveal a different ability in braking cell cycle progression among AdipoRon, Gemcitabine, and combination.

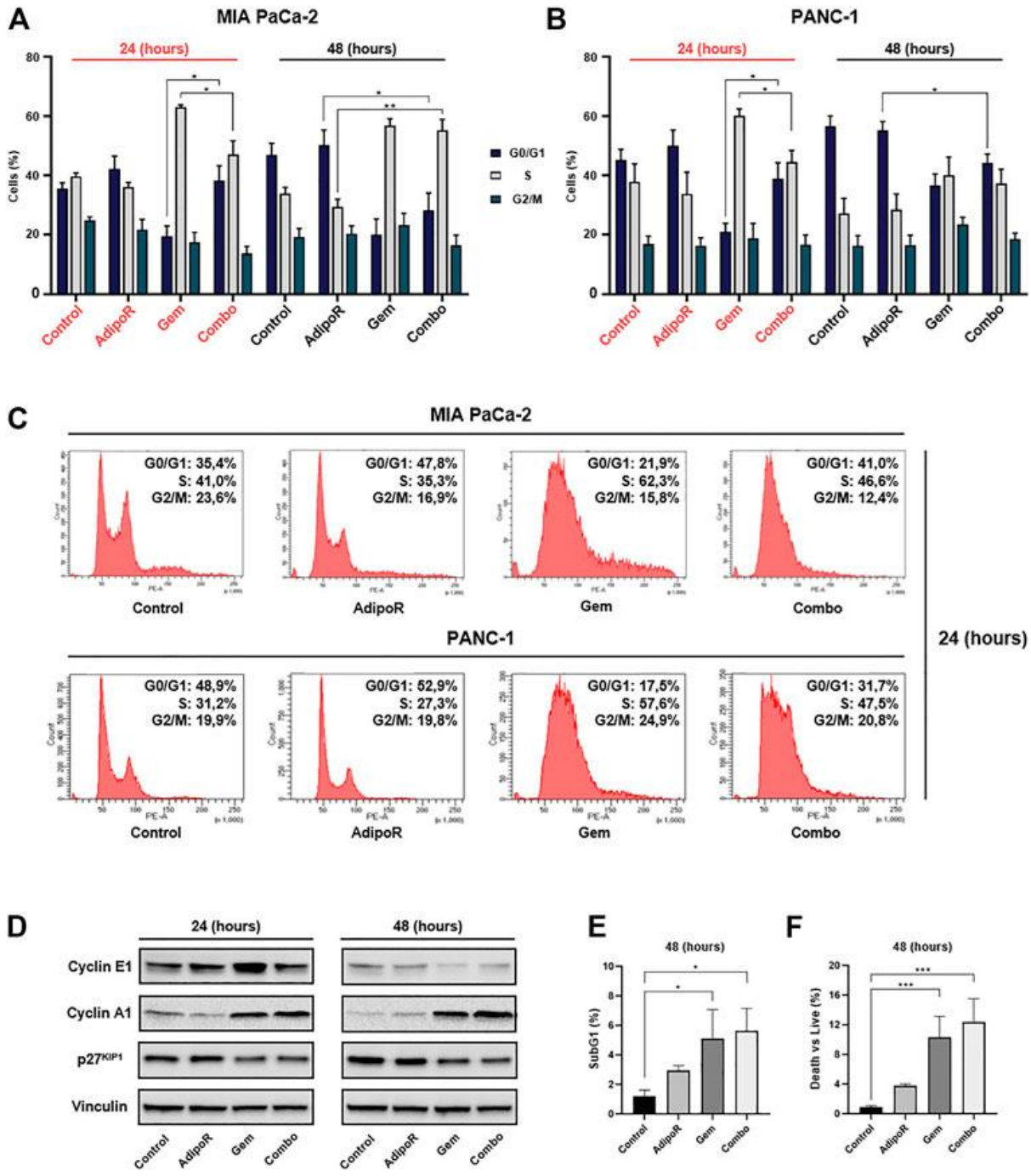

FIGURE 7. ***Investigation of single and combinatory consequences on cell cycle distribution in PDAC cells.*** MIA PaCa-2 was exposed and not (control) to 10 µg/mL AdipoR, 15 nM Gem, and AdipoR plus Gem over a period of 24 and 48 h **(A)**. PANC-1 cells, instead, were treated and not (control) with 10 µg/mL AdipoR, 50 nM Gem, and combination for the same temporal extension **(B)**. Subsequently, the relative cell phase distribution was defined by FACSCelesta™ using PI as DNA staining. MIA PaCa-2 and PANC-1 representative histogram plots at 24 h **(C)**. **(D)** Cyclin A1, cyclin E1, and $p27^{KIP1}$ expression levels were obtained in reaction to 10 µg/mL AdipoR,

15 nM Gem, and combination in MIA PaCa-2. **(E)** Relative subG1 amount. **(F)** Trypan blue discrimination analysis. Either **(E)** or **(F)** show MIA PaCa-2 results cultured in media containing AdipoR, Gem, and AdipoR plus Gem under the same **(B)** experimental conditions. Displayed data are expressed in percentage as average value ± SD of three independent experiments. *$p < 0.05$, **$p < 0.01$, ***$p < 0.001$ by Tukey's multiple comparisons test. (Adapted from *Ragone et al.,2022*)

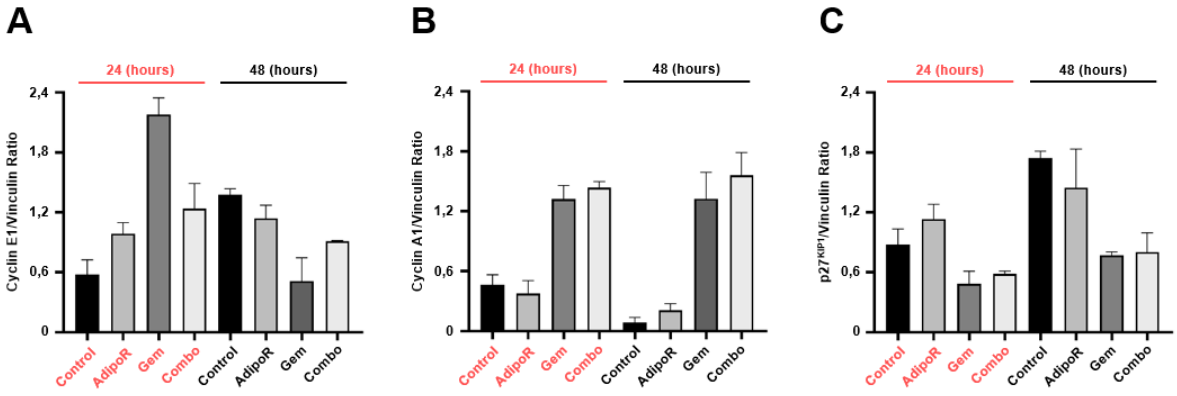

Supplementary Figure 1. ***Quantification analysis of the cell cycle related proteins.*** **(A)** Cyclin E1/Vinculin Ratio. **(B)** Cyclin A1/Vinculin Ratio. **(C)** p27KIP1/Vinculin Ratio. ImageJ-mediated quantification analysis has been performed processing three distinct Western blotting experiments for every cell cycle related protein, and housekeeping protein (Vinculin). Median value ± SD of the relative Ratio is reported in chart. Representative Western blotting films are displayed in Figure 7D. (Adapted from *Ragone et al.,2022*)

2.3 Involvement of p44/42 MAPK pathway in Combination outcome in PDAC cells

2.3.1 Combination activates p44/42 MAPK

As the most frequent mutated gene, abnormal KRAS hyperactivation occurs recurrently in PDAC. (Buscail et al., 2020) Consequently, dysregulation of the p44/42 MAPK pathway has been recognized in PDAC, assuming a possible correlation between its expression and tumor prognosis. (Furukawa, 2015)

Modulation of p44/42 MAPK has also been detected in response to Gemcitabine administration in both in vitro and in vivo PDAC models, and in patients. (Jin et al., 2017; Ryu et al., 2021) Correspondingly, despite the AdipoRon-related molecular mechanisms remain largely unknown, its antiproliferative action has been linked to p44/42 MAPK activation in PDAC. (Akimoto et al.,

2018) Additionally, we also observed AdipoRon-mediated p44/42 MAPK stimulation in osteosarcoma cell lines. (Sapio et al., 2020)

Taking into consideration the mentioned findings and the relevance of this pleiotropic pathway in regulating the cell functions (Guo et al., 2020), we first addressed the involvement of p44/42 MAPK in reaction to the combination.

For this purpose, MIA PaCa-2 and PANC-1 cells were treated with AdipoRon and Gemcitabine, alone and in co-administration, for up to 48 hours and subsequently analyzed for p44/42 MAPK phosphorylation status.

In the absence of substantial protein amount variations, we recognized a different combination capability in modulating p44/42 MAPK phosphorylation between MIA PaCa-2 and PANC-1 cell lines. Specifically, while the concomitant administration of AdipoRon and Gemcitabine resulted in p44/42 MAPK activation at 48 hours in MIA PaCa-2 (Figure 8A), the phospho-p44/42 MAPK upregulation was already apparent at 24 hours and maintained up to 48 hours in PANC-1 (Figure 8B).

On the whole, these findings suppose an involvement of p44/42 MAPK pathway in AdipoRon plus Gemcitabine combination response.

2.3.2 p44/42 MAPK pathway perturbation counteracts Combination effectiveness

To further investigate the p44/42 MAPK involvement in combination-mediated effects, we subsequently tested the impact of MEK1/MEK2 inhibitor PD98059 on combination outcome.

Bearing in mind that long-term exposure to downstream blockade of MAPK deeply impairs PDAC cell growth (Wong et al., 2016), we chose 10 μM for 24 hours as effective dosage of PD98059 and time to mitigate p44/42 MAPK signaling and affect MIA PaCa-2 cell growth, marginally (Figure 8C and Supplementary Figure S2A).

Albeit the combination increased cell growth inhibition compared to single ones, PD98059 partially counteracted combination effectiveness, reducing the inhibition rate of approximately 25% relative to p44/42 MAPK-proficient counterpart (Figure 8D). Comparable experiments performed in PANC-1 also revealed a PD98059-mediated capacity in hindering the combination anticancer action (Figure 8E) although MEK1/MEK2 inhibitor alone affected cell growth in a more effective manner in PANC-1 than in MIA PaCa-2 (Supplementary Figures S2B,C).

So overall, these findings support the possible involvement of p44/42 MAPK pathway in combination response.

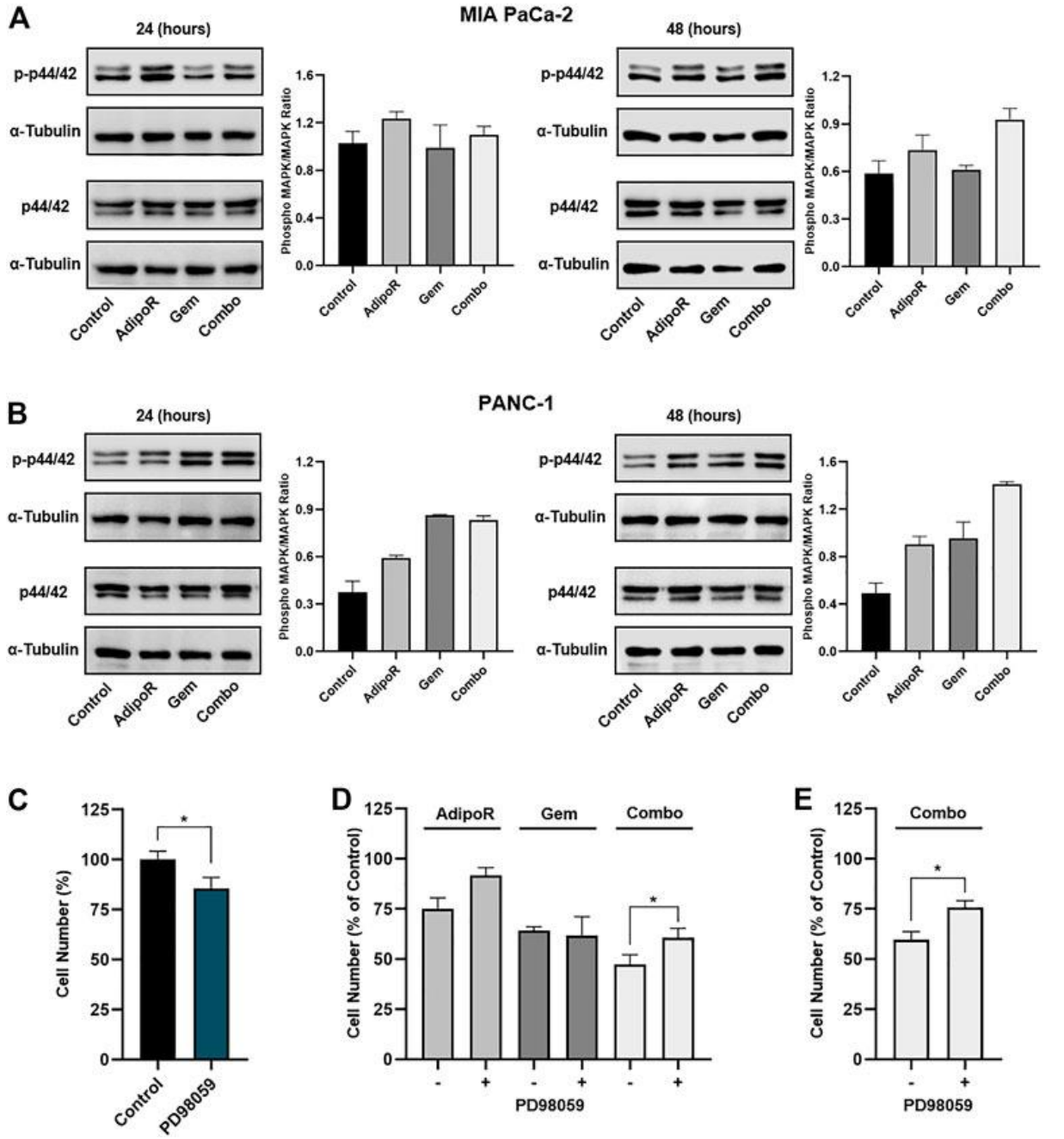

FIGURE 8. ***Evaluation of p44/42 MAPK involvement in AdipoR plus Gem effects.*** MIA PaCa-2 **(A)** and PANC-1 **(B)** were treated and not (control) with 10 μg/mL AdipoR, 15 nM (MIA PaCa-2) or 50 nM (PANC-1) Gem, and AdipoR plus Gem over a period of 48 h. Thereafter, either single or combination consequences on p44/42 MAPK activation (phosphorylation) were estimated by Western blotting. Phospho-MAPK/MAPK ratio results from the quotient of phospho-p44/42 MAPK and its relative housekeeping on the gel divided by a quotient of p44/42 and its relative α-tubulin. **(C)** MIA PaCa-2 was exposed and not (control) to 10 μM PD98059 for 24 h, and the cell growth percentage was established. **(D)** MIA PaCa-2 single and combination treatments in MAPK-proficient and -hampered background. **(E)**Combination treatments containing 10 μg/mL AdipoR plus 50 nM Gem were carried out in PANC-1 cells with or without PD98059 inhibitor. Two hours of PD98059 pretreatment preceded and not individual and combinatory administration. Results are depicted in percentage as mean ± SD of three independent experiments. *$p <$ 0.05 by Tukey's multiple comparisons or Student's t-test. (Adapted from *Ragone et al.,2022*)

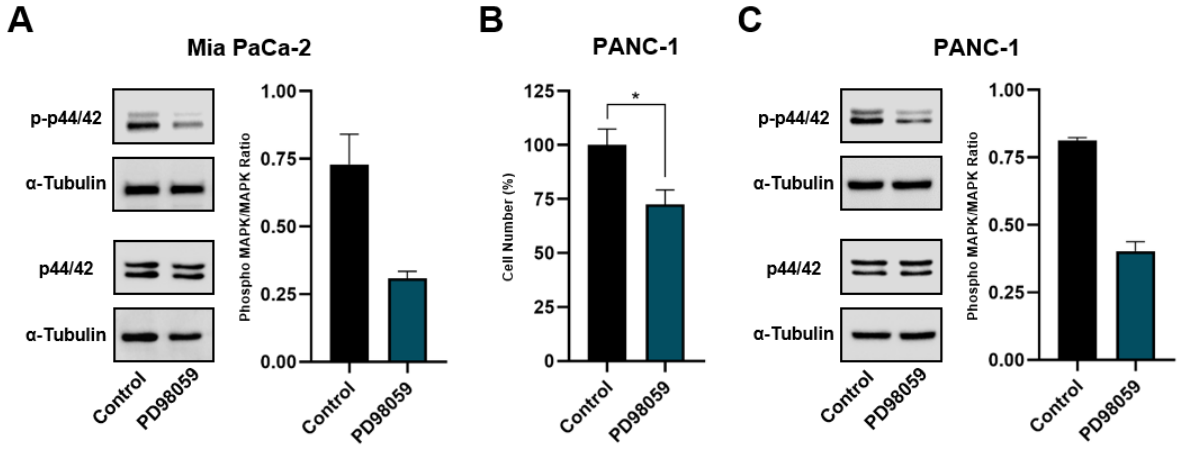

Supplementary Figure 2. ***Effects of PD98059 inhibitor on p44/42 MAPK phosphorylation in PDAC cells.*** MIA PaCa-2 **(A)** and PANC-1 **(C)** were treated and not (control) with 10 μM PD98059 for 2 h with the purpose of assessing both phospho-p44/42 and p44/42 levels by Western Blotting. **(B)** Growth impact of 10 μM PD98059 for 24 h in PANC-1 cells, expressed in percentage of control as mean ± SD of three independent experiments. *p < 0.05 by unpaired Student's t-test. (Adapted from *Ragone et al.,2022*)

2.4 COMBINATION EFFECTIVENESS IN GEMCITABINE-RESISTANT CELLS

Although Gemicitabine displays one of the highest response rates compared to other anticancer agents in PDAC, mechanisms of resistance occur already within few weeks from starting of therapy. (Amrutkar and Gladhaug, 2017) As a result of unresponsiveness, PDAC becomes more aggressive causing an extra reduction in overall survival. (Quiñonero et al., 2019)

To further speculate the usefulness of AdipoRon in PDAC care, we first developed stable MIA PaCa-2 cell lines resistant to Gemicatibine (MIA Paca-2 Gem-Res). Thereafter, MIA PaCa-2 Gem-Res cells were cultured in a medium containing 10 μg/mL AdipoRon and 15 nM Gemcitabine, either alone and in combination for up to 48 hours, in tandem with MIA PaCa-2 cells.

In line with the previous results obtained in MIA PaCa-2, combination treatment resulted in an additional cell growth reduction compared to single treatments at 24 hours and even 48 hours (Figures 9A,B). Particularly relevant, even though Gemcitabine was ineffective in reducing the cell number in MIA PaCa-2 Gem-Res cells, AdipoRon alone induced a 25% growth inhibition, and even more interestingly, co-administration affected cell proliferation by another 18% in respect of AdipoRon alone at 48 hours (Figure 9B).

Using a higher dose than that employed in Figure 6, Gemcitabine strongly counteracted the colony forming ability in MIA PaCa-2, while conversely the same amount marginally affected the growing colony in Gem-Res cells. (Figure 9C). Interestingly, AdipoRon reduced clonogenic potential by 45% in single treatment and 55% in combination with Gemcitabine (Figure 9D).

Additionally, flow cytometry analysis showed AdipoRon persistence in braking cell cycle progression even in MIA PaCa-2 Gem-Res, though in a less pronounced manner. Like the sensitive cells, a G0/G1 phase increase was observed in the resistant ones supplemented with AdipoRon (Figure 9E). But even more interesting, reducing both S and G2/M phases, the combination enhanced the G0/G1 accumulation compared to AdipoRon alone (Figure 9E). Remarkably, no substantial changes were detected between Gem-treated and untreated cells, confirming the loss of chemotherapy responsiveness by this cell line.

Taken together, these data indicate that the combination AdipoRon plus Gemcitabine is effective in preventing growth and colony formation even in Gem-resistant MIA PaCa-2 cells.

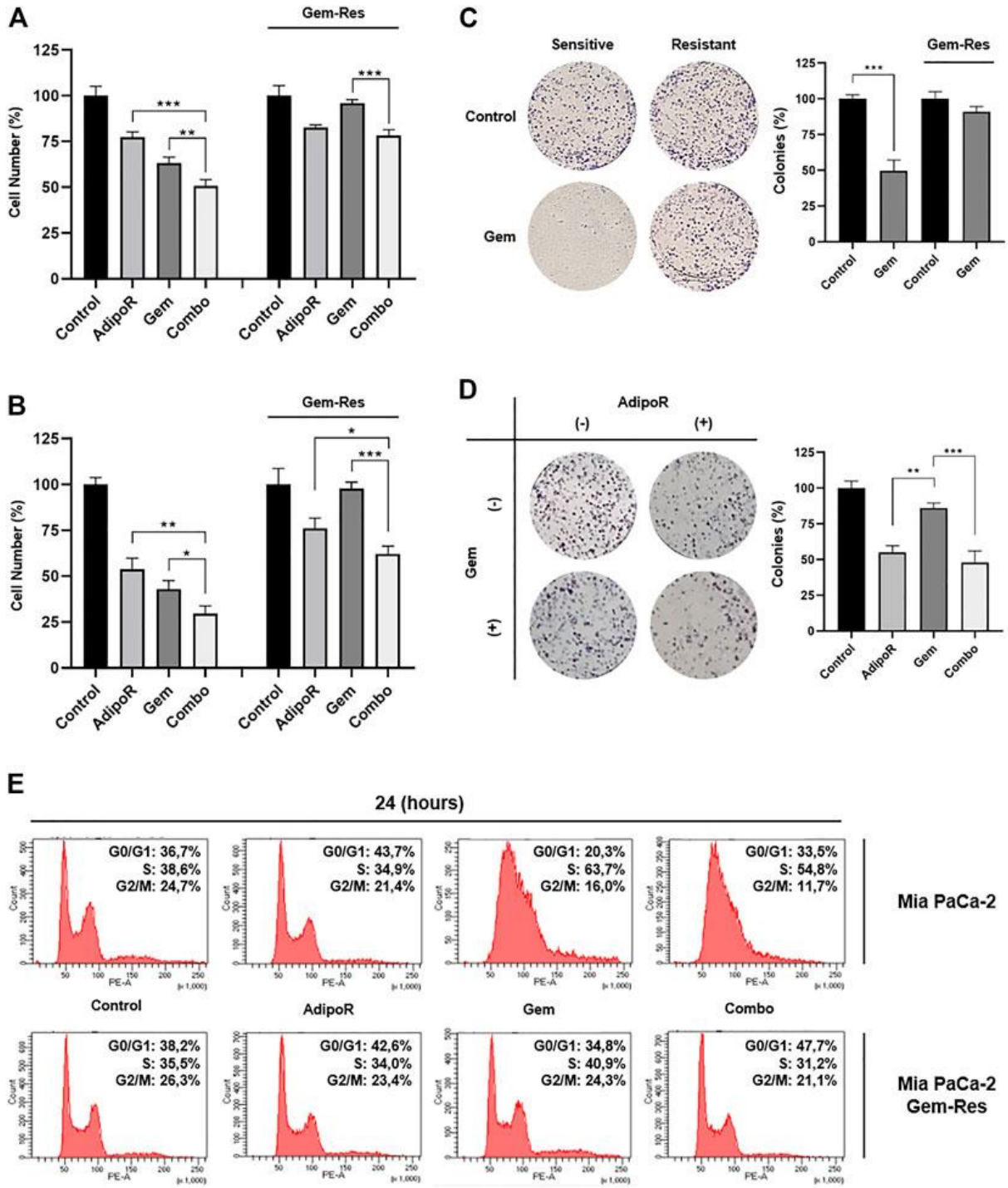

FIGURE 9. ***Responsiveness of MIA PaCa-2 Gem-resistant cells to single and combinatory treatments.*** Either MIA PaCa-2 Gem-sensitive and -resistant cells were treated and not (control) with 10 µg/mL AdipoR, 15 nM Gem, and AdipoR plus Gem for 24 **(A)** and 48 h **(B)**; thereafter, the relative impact on cell growth was addressed. **(C)** Cell media of both MIA PaCa-2 Gem-sensitive and -resistant cells were supplemented with and without (control) 10 nM Gem for 8 days. Illustrative violet-stained wells are shown on the left side, the relative quantification on the right. **(D)** MIA PaCa-2 Gem-resistant cells undergoing AdipoR (10 µg/mL) and Gem (5 nM) individually and combinatory treatments were tested for colony-forming ability. Images and quantification assay are provided in Figure. **(E)** MIA PaCa-2 Gem-sensitive and -resistant were incubated either with single or combination drugs as indicated in **(A)**. FACSCelesta™ analysis was later performed with the purpose of defining the drug-induced consequences on cell phase distribution. Reported results are indicated in percentage as median value ± SD of triplicate experiments. *$p <$ 0.05, **$p <$ 0.01, ***$p <$ 0.001 by Tukey's multiple comparisons or Student's t-test. (Adapted from *Ragone et al.,2022*)

3 DISCUSSION

The existing therapeutic options have failed to provide an appropriate response in PDAC, reinforcing the unlucky privilege of being one of the deadliest cancers worldwide. (Latenstein et al., 2020) Regrettably, even immunotherapy, which has recently revolutionized the drug regimes in cancer treatment, has shown few successful chances in PDAC due to tumor-related stroma abundance. (Makaremi et al., 2021; Panchal et al., 2021)

Therefore, besides radiation and surgical resection, chemotherapy represents the only partially effective pharmacological approach in PDAC, irrespective of tumor stage. (Qian et al., 2020) Despite the clinical approval of novel chemotherapeutics and formulations, Gemcitabine still remains a cornerstone for PDAC management, and Gemcitabine-based therapy constitutes the widely used partner in combination therapy. (Christenson et al., 2020) Unfortunately, the limited success rate of Gemcitabine treatment and the relative ease in developing chemoresistance warrant for more effective therapeutic approaches in PDAC.

Recently, the first synthetic adiponectin receptor agonist is emerging as a promising anticancer compound in several tumors, including myeloma, breast, prostate, and ovarian cancers. (Nigro et al., 2021) Convincing evidence is also emerging in PDAC, where AdipoRon suppresses tumor growth and induces cell death, mainly through apoptosis and necroptosis induction. (Messaggio et al., 2017; Akimoto et al., 2018)

With the purpose of further addressing the AdipoRon candidacy in PDAC treatment, herein we investigated the potential outcome of its dynamic interaction with Gemcitabine in MIA PaCa-2 and PANC-1 cells. Albeit quite preliminary, our results reveal no shortcomings in using these two compounds together; quite to the contrary, their combination could have a greater therapeutic impact compared with single ones. Moreover, as suggested by CompuSyn analysis, potential synergistic action could exist between AdipoRon and Gemcitabine. The cooperative interaction is

clearly supported by cell growth and colony results, which shows a combination-mediated stronger and deeper outcome in limiting PDAC tumorigenicity. Additionally, either AdipoRon or combination kept their therapeutic effectiveness even in MIA PaCa-2 cells that developed resistance to Gemcitabine administration.

Although countless other compounds have been tested over the last years, only two Gemcitabine-based combination therapies have been approved and employed in clinical for advanced PDAC treatment, namely, Erlotinib and nab-Paclitaxel. (Elsayed and Abdelrahim, 2021) However, while the successful rate of combination Gemcitabine plus Erlotinib is strictly dependent on the EGFR status and other potential signatures, serious side effects have been reported in PDAC patients treated with Gemcitabine plus nab-Paclitaxel, including neutropenia, peripheral neuropathy, and fatigue. (Hoyer et al., 2021; Blomstrand et al., 2019) In addition to supporting its antineoplastic role in PDAC, our findings first recognize AdipoRon as a novel potential candidate in Gemcitabine-based multidrug therapy. If subsequently confirmed by in vivo and trial studies, combination AdipoRon plus Gemcitabine could represent an additional pharmacological choice in PDAC, especially for metastatic unresectable patients whose survival is currently under 1 year, even with an optimal chemotherapy regimen.

Mechanistically, the combination action could be explained by a different capability in slowing down cell cycle progression between AdipoRon and Gemcitabine. Although in different cancer types, both Akimoto and Ramzan reported an AdipoRon-mediated G0/G1 phase delay, which results in tumor growth arrest. (Akimoto et al., 2018; Ramzan et al., 2019) More recently, we also observed a similar functional mechanism in the AdipoRon-induced osteosarcoma stunting. (Sapio et al., 2020) In agreement with the exhibiting findings, our results confirmed the ability of this compound in affecting G0/G1, as well as of Gemcitabine in blocking the S phase. (Miao et al., 2016; Montano et al., 2017; Waissi et al., 2021) Surprisingly, each compound retains its respective peculiarity even when combined. Indeed, the simultaneous administration showed intermediate features between AdipoRon and Gemcitabine, wherein Gemcitabine is still arresting in S phase

and AdipoRon in G0/G1. Therefore, rather than inducing cytotoxic effects, our findings could suggest an experimental model in which a sum of different phase slowdown, mediated by single agents, further reduces PDAC growth.

Signaling pathway examination revealed a possible involvement of p44/42 MAPK in the responses elicited by AdipoRon plus Gemcitabine in PDAC cells. In this regard, while combination stimulated p44/42 MAPK activation, PD98059-mediated p44/42 MAPK impairment partially counteracted its effectiveness. Interestingly, analog results were also observed in reaction to AdipoRon, thus supposing that a proficient activation of this pathway is functional for this compound.

Different studies have reported an AdipoRon-mediated p44/42 MAPK hyperphosphorylation in different pathological conditions, including in cancer. (Messaggio et al., 2017; Akimoto et al., 2018) In this regard, in our previous study, we also reported how AdipoRon induces a robust p44/42 MAPK activation in osteosarcoma cells. (Sapio et al., 2020) In accordance with Akimoto's results, herein we demonstrated that p44/42 MAPK activation is needed to allow a proper AdipoRon antitumor action and combination outcome. Even though not in cancer models, additional studies further support the functional p44/42 MAPK role in either AdipoRon- or adiponectin-mediated effects. (Akimoto et al., 2018; Koskinen et al., 2011; Alvarez et al., 2012; Wang et al., 2020) In this respect, Wang and coworkers have recently proved that ameliorating cell viability, apoptosis, and reactive oxygen species (ROS) production, AdipoRon stimulates bone regeneration in ATDC5 cells via p44/42 MAPK pathway. (Wang et al., 2020) Interestingly, when p44/42 MAPK was irreversibly suppressed by PD98059, AdipoRon failed to rescue impaired apoptosis and chondrogenesis of cells. Although our results recognize this pathway as potentially involved in combination effectiveness; we cannot rule out that other signaling pathways that might be involved in, especially because the PD98059-mediated action just results in an incomplete combination rescue. In this respect, as far as known, the most common multidrug resistances are related to ATP-binding cassette (ABC) transporters, which, regulating

drug absorption, distribution, and excretion, play a crucial role in overcoming drug-induced cytotoxicity. (Robey et al., 2018) Recently, different ABC family members have been reported to be involved in Gemcitabine resistance, expressly in PDAC. (Xu et al., 2013; Lu et al., 2019; Okada et al., 2021) Interestingly, a positive correlation between adiponectin and ABCA1 levels has been observed in visceral adipose tissue. (Vincent et al., 2019) Moreover, adiponectin has been described to increase both mRNA and protein levels of ABCA1 in HepG2 hepatocellular carcinoma cells. (Matsuura et al., 2007) Despite no evidence currently reports AdipoRon-induced ABC modulation yet, this association could explain how this receptor agonist overcomes Gemcitabine ineffectiveness in MIA PaCa-2-resistant cells. Therefore, targeting experiments aimed at defining their relative engagement will be performed shortly.

4 CONCLUSION

In conclusion, we first provide evidence of enhanced performances in constraining PDAC progression when AdipoRon and Gemcitabine are combined. Apart from supporting the antineoplastic feature, our results recognize an additional and newly AdipoRon therapeutic usage in PDAC, potentially as a partner in Gemcitabine-based combination therapy.

Considering the current orphan status for this illness, finding out novel and more effective pharmacological strategies could help in improving both PDAC prognosis and survival. In this regard, our promising in vitro results may encourage the development of future supplementary studies aimed at addressing the feasibility of AdipoRon plus Gemcitabine approval in clinical practice.

5 MATERIALS & METHODS

5.1 CHEMICALS & ANTIBODIES

Chemicals: AdipoRon (#SML0998; Sigma-Aldrich), Gemcitabine (#G6423, Sigma-Aldrich), trypan blue (#T8154; Sigma-Aldrich), propidium iodide (#P4864; Sigma-Aldrich), crystal violet (#C0775; Sigma-Aldrich), PD98059 (#P215; Sigma-Aldrich), dimethyl sulfoxide (DMSO) (A3672; AppliChem), and ethanol absolute anhydrous (308603; Carlo Erba). Antibodies: α-Tubulin (#3873; Cell Signaling Technology), cyclin E1 (#4129; Cell Signaling Technology), p44/42 MAPK (#9102; Cell Signaling Technology), phospho-p44/42 MAPK (#9101; Cell Signaling Technology), cyclin A1 (sc-751; Santa Cruz Biotechnology), vinculin (sc-73614; Santa Cruz Biotechnology), and $p27^{KIP1}$ (ab3203; Abcam).

5.2 CELL CULTURE AND EXPERIMENTAL PROCEDURES

MIA PaCa-2 and PANC-1 human PDAC cell lines were purchased by the American Type Culture Collection (ATCC) and maintained at 37°C in a 5% CO_2 humidified atmosphere, using Dulbecco's Minimum Essential Medium (DMEM) (ECM0728L; Euroclone) supplemented with 10% fetal bovine serum (FBS) (ECS0180L; Euroclone) and 1% penicillin/streptomycin (ECB3001D; Euroclone) as culture medium. Typically, cells were equally seeded and kept under standard growing conditions for 24 hours. The following day, AdipoRon and Gemcitabine were supplemented to fresh media, either individually or in combination, and PDAC cells were incubated for times and concentrations provided in each experimental condition. Ultimately, adherent cells were trypsinized and collected with potential floating ones, before being centrifuged

for 5 minutes at 1,500 RPM. Since AdipoRon and Gemcitabine were dissolved in DMSO and H_2O, respectively, an equal solvent rate (% v/v) was used as a negative control.

5.3 Development of Gemcitabine-Resistant MIA PaCa-2 cells

MIA PaCa-2 cells were chronically exposed to increasing Gemcitabine concentration over a period of 4 months. Specifically, starting from 1 nM, cells were cultured in media containing Gemcitabine until they grew steadily. A higher cumulative Gemcitabine dosage was subsequently applied, and the resistant procedure was repeated as long as a final concentration of 200 nM was reached. At each step, cells were amplified, harvested, and cryopreserved in liquid nitrogen or an ultralow-temperature freezer. The obtained MIA PaCa-2 Gemcitabine- resistant cells were finally cultured in drug-free medium for up to 2 weeks before performing the reported experiments.

5.4 Assessment of drug-mediated effects on alive and dead cells

A total number of 8×10^4 MIA PaCa-2 and 1×10^5 PANC-1 cells were moved in 6-well plates and kept in a standard growing state for 24 hours. AdipoRon and Gemcitabine, either alone or in combination, were subsequently added to new media and allowed to act in PDAC cells. Usually, pelleted cells were resuspended in 1.5 ml DMEM and diluted 1:1 with trypan blue, which, crossing damaged membrane, discriminates living from dead cells. Specifically, 10 µL of both media containing cells and blue dye (0.4%, v/v) were mixed, and the relative cell content was established using a Bürker chamber, where the number of unstained (living) and stained (dead) cells was recorded. Each point has been counted at least twice in each experimental procedure.

5.5 FLOW CYTOMETRY ANALYSIS

Cytometric analysis was performed to define the respective cell phase distribution in reaction to different *stimuli*. For each experimental conditions, pelleted samples were resuspended first in 300 μL PBS (ECB4004lL; Euroclone) and then in 700 μL ice-cold absolute ethanol. Fixed cells were stored at −20°C until analysis. Before investigation, the samples were spun down for 5 minutes at 1,500 RPM and incubated with PI staining solution containing 15 μg/mL PI and 20 μg RNase A (R5503; Sigma-Aldrich) in PBS for 10 minutes at room temperature in the dark side. For each experimental condition, at least 20,000 events were acquired and analyzed by FACS-Celesta (BD Biosciences).

5.6 COLONY FORMING ASSAY

PDAC cells were seeded in 6-well plates at a density of 1.5×10^3 per well (MIA PaCa-2 and MIA PaCa-2 Gem-Res) or 2×10^3 (PANC-1) and exposed to different times and concentrations of AdipoRon, Gemcitabine, and combination. At the established endpoint, media was discarded, and newly formed colonies were stained with crystal violet solution (1% aqueous solution) for 10 minutes. The staining solution was later removed, and wells were washed several times in distillate water. Colonies have been allowed to air dry naturally and acquired by photographic equipment. Quantification analysis has been performed by determining the optical density (OD) of dissolved colony-bound crystal violet staining in 10% acetic acid at 590 nm by an Infinite 200 PRO Microplate Reader (Tecan Life Sciences).

5.7 WESTERN BLOTTING

Depending on the target protein, an amount of 10–30 μg of total extracts was loaded and separated by sodium dodecyl sulfate–polyacrylamide gel electrophoresis (SDS-PAGE) for each sample. Subsequently, sample proteins were transferred onto nitrocellulose membranes (GEH10600008; Amersham) by the Mini Trans-Blot system (Bio-Rad Laboratories). After washing in tris-buffered saline (TBS) supplemented with 0.05% Tween 20 (TC287; HIMEDIA), films were blocked 1 hour in 5% no-fat dry milk (A0530; AppliChem) aimed at covering potentially free spots into the nitrocellulose membrane. Incubation overnight at 4°C has been chosen for primary antibody binding. In the following days, horseradish peroxidase (HRP)-conjugated secondary antibodies, reacting against the related primary species, were applied to the membrane for 1 hour at room temperature. Each incubation step was preceded and followed by three 5 minutes-rinses in T-TBS. Finally, protein-related light signals were acquired by ChemiDocTM (Bio-Rad Laboratories) using the enhanced luminol-based chemiluminescent substrate (E-IR-R301; Elabscience) as a detection system for HRP.

5.8 PROTEIN EXTRACTION AND WESTERN BLOTTING SAMPLE PREPARATION

A number of 4.8×10^5 (MIA PaCa-2) or 6×10^5 (PANC-1) cells were plated in 100 mm plates and left free to attach for 24 hours. In the next day, media was replaced with a fresh one containing AdipoRon, Gemcitabine, and the combination in doses and timelines reported in the Results section, and Figure legends. At every experimental point, cells were collected and spun down at 1,500 RPM for 5 minutes. Pellets were later resuspended in 3–5 volumes of RIPA buffer (R0278; Sigma-Aldrich) supplemented with protease and phosphatase inhibitors cocktail (#5872; Cell Signaling Technology). After 30 minutes, samples were further centrifuged at 14,000 RPM for 15 minutes at 4°C, and the supernatant was recovered and assessed for the relative protein content by

Bradford Assay (39222; SERVA). Protein samples were first mixed 1:1 with Laemmli 2× (S3401; Sigma-Aldrich) and later boiled at 95°C for 6 minutes.

5.9 STATISTICAL ANALYSIS

Results are indicated as average value ± SD of biological independent replicates. Significance has been defined using either Student's t-test, to compare the mean of two samples, or analysis of variance (ANOVA) followed by Turkey's test, to discriminate differences between more than two experimental groups. In both cases, values of less than 0.05 were recognized as significant. Densitometric analyses have been carried out by ImageJ (NIH, Bethesda).

PART II

6 INTRODUCTION TO THE INHERITANCE OF CENTROMERE IN GENOME STABILITY

6.1 THE CENTROMERE

The centromere is a chromosomal locus essential for the equal and faithful segregation of genetic material to daughter cells during cell division. It is defined as the "primary constriction" of the chromosome and its principal function is to both provide the foundation for the assembly of the kinetochore, the protein complex which connects chromosomes to microtubules of the mitotic and meiotic spindles, and serve as the site of sister chromatid cohesion until proper chromosome separation occurs. (Fukagawa and Earnshaw, 2014) Although the word "*centromere*" can be translated as "*central part*", centromeres are not necessarily positioned in the center of chromosomes. In fact, only five chromosomes of the human set are defined metacentric with the centromere located in the middle so that the chromosome is divided into two arms of equal length. In the other chromosomes, the centromere is either submetacentric, close to the center, or acrocentric, situated near the end determining that one arm is shorter than the other.

The size of a centromere varies largely between species. In *S. cerevisiae*, the centromere of each chromosome counts 125 bps and it is known as point centromere. (Clarke and Carbon, 1980) However, the centromeres of many eukaryotes are more complex and organized in a configuration termed regional centromere. These centromeres are characterized by complex tandemly repeated DNA sequences flanked by pericentromeric heterochromatin. In human regional centromeres, the 171 bp α-satellite DNA, which is organized in higher order repeats of AT-rich DNA, spans regions from several 100 kbps to 5 Mbps and make up ~3% of the genome. (Manuelidis, 1978; Fukagawa and Earnshaw, 2014) A third type of centromere, called holocentromere, exists in some insects, lower plants and nematodes like *Caenorhabditis elegans* and extends along the entire

length of the chromosome. (Marques and Pedrosa-Harand, 2016) Thus, point centromeres and holocentromeres seem to be an evolutionary adaptation from the regional centromere configuration.

The initial understanding of regional centromeres as repetitive α-satellite sequences was soon challenged and has changed in a way that the underlying DNA sequence moved out of focus. Although repetitive DNA sequences are a common feature of regional centromeres, several findings raised doubt that the centromere is strictly specified by its underlying DNA sequence. The most obvious evidence are the lack of repetitive DNA sequences in at least one chromosome in various species, like chicken or orangutan, and the discovery of neocentromeres, which form at non-centromeric loci due to *de novo* rearrangements of chromosomes. (Locke et al., 2011; Shang et al., 2010; Amor and Choo, 2002)

The discovery of autoantibodies against centromeres in patients suffering from the autoimmune syndrome CREST (Calcinosis, Reynaud's syndrome, Esophageal dysmotility, Sclerodactyly, Telangiectasia) represented the crucial turning point for the molecular understanding of the centromere. (Moroi et al., 1980) In fact, three different antigens, which are respectively known as CENP-A, CENP-B and CENP-C (where CENP stands for centromeric protein), were recognized by the sera of these patients and, among them, CENP-A has been finally identified as a histone H3 variant. (Earnshaw and Rothfield, 1985; Palmer et al., 1987) Currently, CENP-A is considered the molecular determinant of the centromere in eukaryotes since it is present in virtually all organisms from *S. cerevisiae* (where CENP-A is called Cse4) to humans. As a consequence, the centromere is defined rather epigenetically than by a specific DNA sequence.

The point centromere of *S. cerevisiae* is a notable exception, because it is genetically defined by three centromere DNA elements (CDE) CDEI, CDEII and CDEIII forming together the 125 bp centromere sequence. (Clarke and Carbon, 1980) The CDEIII element is specifically recognized by CBF3, a critical complex necessary for proper kinetochore function and for the recruitment of kinetochore proteins. (Lechner and Carbon, 1991) Quantitative chromatin immunoprecipitation

experiments could detect one single Cse4 nucleosome present at each point centromere in *S. cerevisiae*. (Furuyama and Biggins, 2007) Cse4 could furthermore be mapped to the 80 bp CDEII element in all 16 budding yeast chromosomes. (Krassovsky et al., 2012) In contrast to budding yeast, higher organisms with regional centromeres do not possess specific genetic elements which define the centromere region. As consequence, in these organisms, centromeric DNA sequence is not sufficient to maintain centromere position, but rather centromeres are epigenetically identified. So, the histone H3 variant CENP-A is the epigenetic mark for centromere identity and function.

6.2 CENP-A

CENP-A is the molecular, epigenetic determinant of the centromere in all higher eukaryotes. It functions as the foundation for kinetochore assembly given that it harbors specific features recognized by members of the inner kinetochore, a meshwork comprising 16 centromere proteins, which is termed constitutive centromere associated network (CCAN) given that most of its components permanently reside at the centromere throughout the cell cycle (Figure 10). (Weir et al., 2016; Musacchio and Desai, 2017)

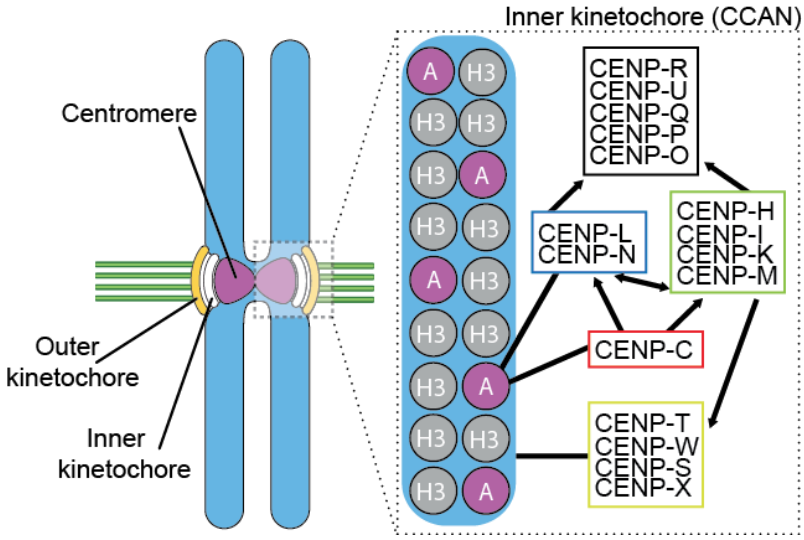

Figure 10. ***Organization of the Constitutive Centromere Associated Network (CCAN)***. (Adapted from *Weir et al., 2016*)

Furthermore, CENP-A is a variant of histone H3 found in the centromeric chromatin, wherein it replaces its canonical nucleosome counterpart in a significant fraction of the nucleosomes. The number of CENP-A nucleosomes is estimated to be approximately 200 per centromere in human cells, with a CENP-A:H3 ratio of 1:25. (Bodor et al., 2014) Although more than two thirds of the nuclear CENP-A pool were found at non-centromeric sites, taking into account the size of the human genome, the quantified number of centromeric CENP-A nucleosomes still represents nearly a 50-fold enrichment over non-centromeric CENP-A (Figure 11).

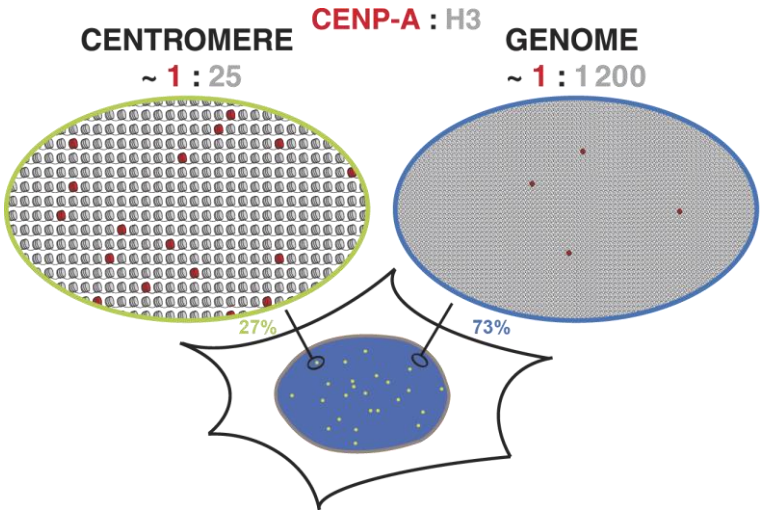

Figure 11. ***The quantitative architecture of centromeric chromatin***. (Adapted from *Bodor et al.,2014*).

CENP-A was identified as the first kinetochore protein by the sera of patients with CREST syndrome in 1985 and, over the years, several provocative forms of the CENP-A nucleosome have been postulated including tetrameric and hexameric forms, nucleosomes with opposite handedness and heterotypic nucleosomes containing both H3 and CENP-A. (Dalal et al., 2007; Dimitriadis et al., 2010; Furuyama and Henikoff, 2009; Mizuguchi et al., 2007)

The crystal structure of a reconstituted human CENP-A nucleosome revealed that CENP-A retains several properties of histone H3 with only minor differences. (Tachiwana et al., 2011) It interacts tightly with histone H4, and it is incorporated in vitro and in vivo into canonical octameric nucleosomes with histones H2A and H2B that share many structural features of the canonical H3-

containing nucleosomes. The DNA writhe is left-handed as for H3 nucleosomes, but CENP-A nucleosomes have looser the terminal contacts allowing more flexible DNA ends and protect a shorter DNA core (~100–120 bps compared to the 147 bp in nucleosome containing H3) in nuclease protection assays. (Roulland et al., 2016) Therefore, given that the overall organization of the CENP-A nucleosome does not seem to be very distinct from H3 nucleosomes, the only substantial discriminants can be found in the CENP- A histone itself. In fact, compared to H3, the N-terminal helix of CENP-A contains three residues less, which results in a smaller protected DNA fragment in nuclease assays, and the N-terminal tail of CENP-A is highly variable due to several posttranslational modifications. The residues Ser7, Ser16, Ser18 and Ser68 have been shown to be phosphorylated, whereas Lys124 is a ubiquitination site. (Conde e Silva et al., 2007; Tachiwana et al., 2011; Srivastava and Foltz, 2018) Instead, the N-terminal methionine of CENP-A is removed and the Gly1 residue of the nascent CENP-A peptide is trimethylated. (Sathyan et al., 2017)

The CENP-A targeting domain, or CATD, is an important feature and consists of unique residues within loop 1 and the a2-helix. It contributes to the rigidity of the CENP-A nucleosomes and is necessary and sufficient for the centromere recruitment of CENP-A. (Ali-Ahmad and Sekulić, 2020) The loop 1 region contains two extra residues, Arg80 and Gly81, which form a surface-accessible bulge. This bulge serves as a recognition motif by the kinetochore member CENP-N. (Tian et al., 2018)

In addition, CENP-A displays a poorly conserved C-terminal tail but it has a considerably higher proportion of hydrophobic residues than the C-Terminus of H3, which are specifically recognized by the member of the inner kinetochore CENP-C. (Kato et al., 2013) Replacing the C-Terminus of histone H3 with the C-terminal tail of CENP-A enables the recruitment of CENP-C in vitro and in vivo. (Carroll et al., 2010; Guse et al., 2011) However, CENP-C can also be recruited to the centromere in HeLa cells by H3 carrying the CATD, but not the C-Terminus of CENP-A. (Black et al., 2007) Furthermore, both the CATD and the CENP-A C-terminus are required to recruit CENP-C to a LacO array. (Logsdon et al., 2015)

6.3 THE PROPAGATION OF CENTROMERIC CHROMATIN

The epigenetic specification of the centromere by CENP-A necessitates the pool of centromeric CENP-A be maintained through cell division. In vertebrates, incorporation of new CENP-A at centromeres takes place after mitotic exit, from telophase until to early G1 phase. The CENP-A pool is then distributed, without new incorporation, to the sister chromatids during DNA replication. Thus, sister chromatids enter mitosis with halved CENP-A content in respect of the parental chromosome before replication. (Jansen et al., 2007) The resulting gaps are most likely filled with histone H3.3, that act as a placeholder. (Dunleavy et al., 2011)

Once the number of CENP-A nucleosomes drops to low, the chance of centromere loss increases dramatically with severe consequences on the genomic stability of the cell. (Bodor et al., 2014) Indeed, incorporation of CENP-A at non-centromeric sites has to be minimized to prevent the formation of ectopic kinetochores causing chromosomal segregation aberrations and genomic instability. (Sharma et al., 2019) Therefore, to guarantee the centromere identity and accordingly ensure the genome stability, the original CENP-A concentration has to be restored (Figure 12).

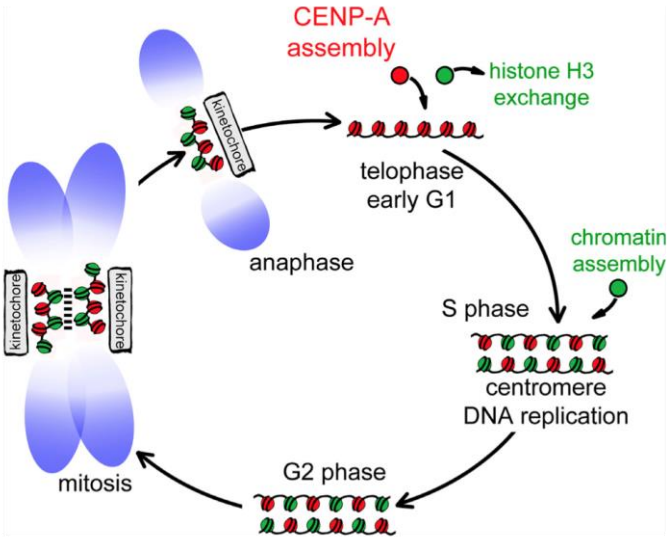

Figure 12. ***CENP-A deposition is uncoupled from DNA replication and takes place in early G1 phase***. (Adapted from *Jansen et al., 2007*)

This spatial regulation of CENP-A inheritance is mediated by the pool of pre-existing CENP-A nucleosomes recruiting. The CENP-A replenishment process, which is uncoupled from DNA replication, happens in early G1 phase when the CENP-A specific chaperone Holliday Junction Recognition Protein (HJURP) associates with Mis18α, Mis18β, and Mis18-binding protein (M18BP1), also known as the Mis18 complex, to target centromeres and deposit new CENP-A. (Pan et al.,2019) To note, the depletion of any member causes severe CENP-A loading defects. (Mahlke and Nechemia-Arbely, 2020)

The CENP-A deposition process can be schematized into three main steps. (Musacchio and Desai, 2017) First, the Mis18 complex localizes at the centromere directly after mitotic exit and modifies the chromatin to a permissive state for CENP-A deposition. In a second step, HJURP binds to the Mis18 complex and recruits prenucleosomal CENP-A to the centromere. The prenucleosomal CENP-A is a soluble complex made by one copy of HJURP binding to a CENP-A/H4 heterodimer. After, CENP-A is deposited and incorporated into the final nucleosome structure and in the last step of the replenishment process, these nascent CENP-A nucleosomes have to be stabilized or maintained. Precisely, after their initial deposition in early G1 phase, CENP-A nucleosomes require further stabilization to avoid their loss from the centromeric chromatin. Super-resolution microscopy analyses revealed, that newly incorporated CENP-A forms rosette-like clusters with HJURP being located in the middle as a nucleation point. Interestingly, in late G1 these clusters have a shape similar to the clusters of pre-existing CENP-A due to a structural transition. (Andronov et al., 2019) At this regard, several factors have been found to be involved in the maintenance process of newly incorporated CENP-A nucleosomes. Particularly, the loss of centromeric CENP-A over time is induced by the depletion of one of remodelling and spacing factor (RSF) complex-subunits, which localizes at the centromere in mid G1 phase. (Perpelescu et al., 2009) More generally, factors implicated in CENP-A deposition, or in its stable maintenance at centromeres, also include the chromatin remodeling FACT complex, the histone chaperone NPM1/nucleophosmin, the GTPase-activating protein MgcRacGAP, And-1, and Condensin II.

Additionally, several DNA and histone post-translational modifications have been implicated in CENP-A loading, including DNA methylation by DNMT3B, possibly through interactions with the C-terminal region of CENP-C and with Mis18α, acetylation, and histone H3K4 dimethylation. In analogy with the licensing events that limit the initiation of DNA replication to once per cell cycle, several factors have been proposed to promote licensing steps that limit CENP-A deposition to once per cycle. (Mahlke and Nechemia-Arbely, 2020) Among the factors required for deposition, positive and negative regulation by the kinase activities of the polo-like kinase 1 (PLK1) and cyclin-dependent kinases 1 and 2 (CDK1/2), respectively, have emerged for their prominence. In vertebrates, incorporation of new CENP-A is limited to telophase and early G1 phase, when CDK activity is suppressed. Inhibition of CENP-A deposition, implicating pre-mitotic Cdk2 kinase activity in complex with Cyclin E and Cyclin A as potential negative regulators of this process. A major target of this regulation is M18BP1, which CDKs phosphorylate at multiple sites, preventing its interaction with Mis18 subunits and its kinetochore recruitment. Inhibition of CENP-A deposition through phosphorylation of HJURP and CENP-A has also been described. On the other hand, PLK1 associates with the Mis18 complex at kinetochores in telophase/early G1 phase, and its activity is required for deposition (Figure 13).

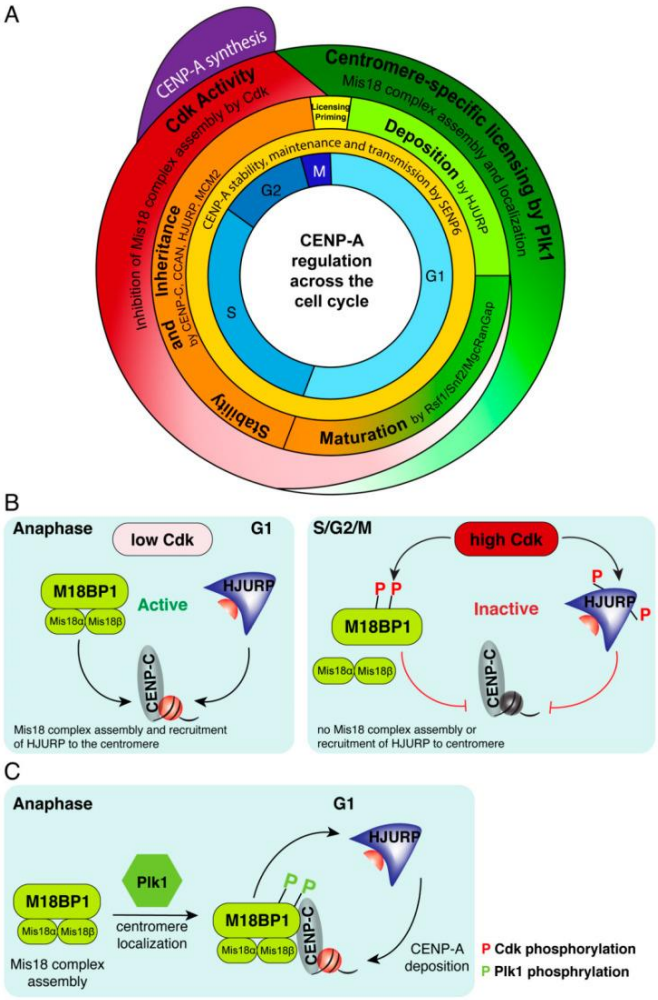

Figure 13.***Centromere protein A (CENP-A) deposition and maintenance are cell-cycle dependent.*** (**A**) CENP-A synthesis, deposition and maturation occur in distinct cell cycle phases and are regulated by coordinated activity of deposition, maturation factors and cell cycle kinases. (**B**) Cyclin-dependent kinase (CDK) regulation of Mis18 complex assembly. Phosphorylation of M18BP1 and HJURP by CDK1/2 renders them inactive, inhibits assembly of the Mis18 complex, and prevents HJURP recruitment to centromeres, preventing CENP-A deposition. At anaphase, low CDK1/2 levels result in active M18BP1 and assembly of Mis18 complex, recruitment of active HJURP and deposition of new CENP-A at the next G1. (**C**) Phosphorylation of M18BP1 by Plk1 is required for the assembly of the Mis18 complex and its localization to G1 centromeres. Once localized at centromeres by binding to CENP-C, HJURP is recruited to centromeres by binding to the Mis18 complex, leading to the subsequent deposition of new CENP-A. (Adapted from *Mahlke and Nechemia-Arbely, 2020*)

Lastly, CENP-C seems to be the most probable centromere receptor in human, but the concrete binding site has not been identified. Since CENP-C has two nucleosome binding motifs, the conserved C-terminal CENP-C motif, that has a lower binding affinity towards CENP-A than the central motif, might be temporarily occupied by the H3.3 placeholder nucleosome, which is recognized by the Mis18 complex and exchanged against CENP-A in early G1 phase. However, the concrete molecular details remain to be investigated and the chromatin remodelling complexes,

that promote the nucleosome exchange reaction, have not been identified yet. (Mahlke and Nechemia-Arbely, 2020)

6.4 THE GENOMIC INSTABILITY

Faithful chromosome segregation is essential for the maintenance of genomic integrity. During each cell cycle, cells duplicate their genetic material before cell division, so that genetic information is equally distributed among daughter cells. (Pesenti et al., 2022) To permit this, all eukaryotes have developed a strategy by which chromosomes are attached by microtubule fibers organized in a spindle that physically pull the two sister chromatids towards opposite poles during division. In this process, the functional centromeres are the key elements. Consequently, a centromere subjected to alterations contributes to chromosome instability and so to the onset of diseases. (Ovejero et al., 2020) Defects in any of the pathways which regulate centromere assembly and function can lead to chromosome mis-segregation and aneuploidy, the common features of cancer cells. Additionally, the repetitive centromeric DNA sequence is often prone to aberrant to rearrangements, leading to structural abnormalities. These could potentially induce replication fork stalling, topological problems causing sites of breakage. (Black et al., 2018)

Albeit it has widely known that alterations in chromosome number participate in early steps of tumorigenesis and in cancer heterogeneity, the mechanisms underlying mitotic errors that lead to structural chromosome alterations still remain elusive. Nevertheless, whole-chromosome arm gain, loss, or translocation are in fact common alterations in tumors. (Barra and Fachinetti, 2018) In this scenario, CENP-A is fully involved in health and diseased states playing a key role in the identity of centromere. For this reason, both its expression and loading occur through a very tightly regulated process. Varying expression levels of CENP-A has been shown to have opposite effects on cells: while down-regulation promotes both cell proliferation arrest and senescence, upregulation can lead to cancer transformation, although via molecular mechanisms which need

to be clarified. Notably, overexpression of CENP-A increases rates of CENP-A deposition ectopically causing mitotic defects, centromere dysfunction and chromosomal instability (CIN), a typical hallmark of cancer. (Mahlke and Nechemia-Arbely, 2020) Generally, CENP-A and HJURP protein levels are tightly co-regulated in accordance with cell cycle progression and CENP-A overexpression is often accompanied by overexpression of its chaperone. CENP-A expression might be regulated by tumor suppressor genes such as Retinoblastoma protein (pRB). Indeed, increased levels of CENP-A and HJURP are found in several tumors like hepatocellular carcinoma, breast cancer and colorectal cancer. Consistent with the fact that their genes are both negatively regulated indirectly by p53, both CENP-A and HJURP are transcriptionally up-regulated in p53-null human tumors. In addition, CENP-A and HJURP have reciprocal stabilizing effects on each other. Specifically, siRNA-mediated depletion of CENP-A promote proteasome-dependent degradation of HJURP and HJURP stabilizes CENP-A. When expression of either CENP-A or HJURP is reduced in normal cells, deposition of new CENP-A at exit of mitosis is diminished, causing loss of centromere identity and increased segregation errors and micronuclei. Additionally, degradation of HJURP in early S phase impairs retention of CENP-A at centromeres throughout S phase. All of this demonstrates that co-regulation of CENP-A and HJURP is important for maintaining a fine balance which preserves centromere identity. Alterations in CENP-A posttranslational modifications are also linked to chromosome segregation errors and CIN. Collectively, CENP-A is pivotal to genomic stability through centromere maintenance, perturbation of which can lead to tumorigenesis. (Renaud-Pageot et al., 2022)

6.5 CENP-A IN CANCER CARE

Across the last two decades, several scientific evidence report CENP-A is closely correlated with cancer progression and patient outcome. (McGovern et al., 2012; Wu et al., 2012; Li et al., 2011; Gu et al., 2014; Qiu et al., 2013; Tomonaga e al., 2003; Rajput et al., 2011; Sun et al., 2016; Amato

et al., 2009; Xu et al., 2020; Saha et al., 2020) The CIN induced by CENP-A overexpression provokes an incrementation in chromosomal rearrangements and mutagenesis which in turn increase the heterogeneity of the cell population. This easily promotes the selection of advantageous clones and cancer progression. In addition, the pivotal role of CENP-A in mitotic progression strongly sustains the correlation between CENP-A and cancer progression. (Shrestha et al., 2021; Giunta et al., 2021) At this regard, it has demonstrated that a partial or complete depletion of CENP-A in cancer cells, which overexpress it, reduces proliferation, blocks cell-cycle progression, promotes apoptosis and decreases invasiveness of cancer cells. (Renaud-Pageot et al., 2022) So, the hyperproliferative cells need sufficient expression of CENP-A along with its chaperone HJURP to proliferate resulting "addicted" to CENP-A. (Filipescu et al., 2017)

The correlation of high CENP-A levels with clear therapeutic response is not simple, instead. Disagreeing evidence exit in this regard: i.e., a reduced therapeutic response is reported when CENP-A is overexpressed in osteosarcoma while a better outcome correlates to its expression in breast and lung cancers. (Gu et al., 2014; McGovern et al., 2012; Sun et al., 2016; Zhang et al., 2016) To note, CENP-A overexpression promotes distinct fates in human cells, depending on p53 status. (Jeffery et al., 2021) In details, Jeffery and coworkers have demonstrated that CENP-A overexpression strongly increased sensitivity to X-ray irradiation of several p53-WT cell lines but not of p53-defective cell lines as well as the inactivation of p53 was sufficient to counteract the CENP-A induced radio-sensitivity phenotype. Thus, CENP-A acts like a double-edged sword: its overexpression enhances radio-sensitivity in cells with wild type p53 while p53-defective cells show a more tolerant state to X-ray irradiation.

Furthermore, regarding CENP-A role in cancer care, it has been proposed as a biomarker for tumor aggressiveness in ovarian, osteosarcoma, lung and breast estrogen receptor positive cancer. (Qiu et al., 2013; Gu et al., 2014; Wu et al., 2012; Liu et al., 2018; McGovern et al., 2012) Additionally, also the localization of CENP-A seems a promising feature. At this regard, the subnuclear distribution of CENP-A at the time of diagnosis of locally advanced head and neck squamous cell

cancer is emerging as an independent predictive marker of local disease control and curability by concurrent chemoradiation therapy. In the last year, Verrelle and colleagues have demonstrated the feasibility of a strategy in this type of tumor enabled to reveal a nuclear CENP-A localization pattern assessed by immunohistochemistry, as a predictive marker of local disease control at 2 years by concurrent chemoradiation therapy (CCRT) with 96% accuracy. (Verrelle et al., 2021)

6.6 OBJECTIVES OF THE PROJECT

CENP-A is the centromere-specific variant of histone H3 and plays a central role in both directing kinetochore assembly and maintaining centromere function. Considering its great importance in preserving genomic stability in eukaryote cells, CENP-A is continually the focus of intensive research finalized to understand its intrinsic peculiarities and the mechanisms which involve itself in tumorigenesis. For this reason, the project is finalized to study CENP-A nucleosome before and after DNA replication to further gain other insights on CENP-A for helping to better clarify its contribution to the maintenance of the centromere identity.

The cellular model used for the project is the human retinal pigment epithelial RPE-1 (hTERT RPE-1) cell line. RPE-1 cells are genetically stable with a near-diploid karyotype of 46 chromosome and largely accepted as a representative model for normal cell division studies. Given that the CENP-A translation occurs during G2 phase and its deposition in the time-frame ranging from telophase to early G1 phase, we want to distinguish the existing CENP-A-SNAP proteins in cell at the end of G1 phase from the new ones produced in the subsequent G2 and deposited then in the next early G1 phase, identifying them as “old CENP-A” and “new CENP-A” respectively. This approach will allow to find out if the CENP-A nucleosome, which includes two copies of CENP-A, reassembles so as to have one “old CENP-A” and one “new CENP-A” (mixed nucleosome - 1st Hypothesis) or two “old” and two “new CENP-A” (non-mixed nucleosome – 2nd

Hypothesis) for each sister chromatids after the DNA replication which follows the deposition of "new CENP-A" (Figure 14).

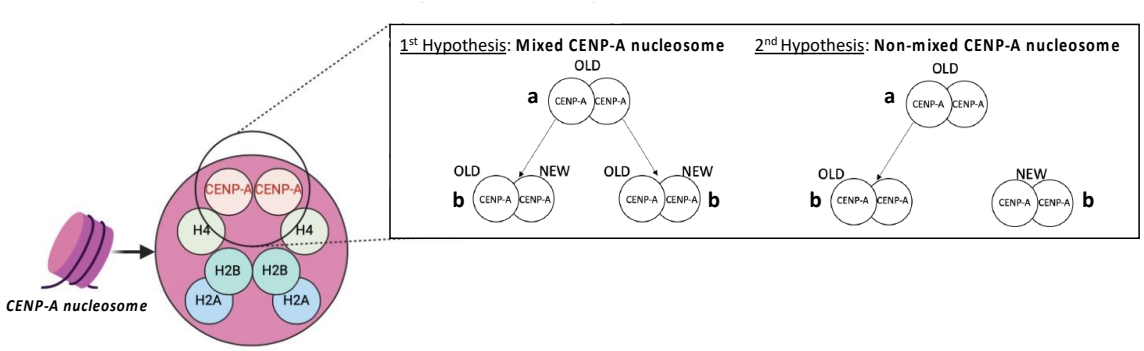

Figure 14. ***Graphical abstract (1/2).*** In S-phase, the CENP-A nucleosome could reassemble in two different manners. According to the 1st Hypothesis, the nucleosome of pre-replication chromosome, which is made by two "old" copies of CENP-A, split and each sister chromatid has both one "old" copy and "new" one of CENP-A respectively; according to the 2nd Hypothesis, the nucleosome of pre-replication chromosome does not split and it passes entirely to one of sister chromatids, as a consequence the remaining sister chromatid has CENP-A nucleosome constituted by two copies of "new" CENP-A protein. In the figure, **a** indicates nucleosome of pre-replication chromosome while **b** indicates the nucleosome of sister chromatid.

To distinguish old and new form of CENP-A, we have generated RPE-1 cell line expressing CENP-A covalently linked to SNAP-tag. This tag is based on human O6-alkylguanine-DNA-alkyltransferase (hAGT), a DNA repair protein, which was re-engineered to allow covalent intra-cellular labelling with various fluorophores (Dreyer et al., 2023). In this way, the two forms of CENP-A will be labelled with different colours (fluorescent dyes) to be distinguished. This requires development and standardization of a sophisticated synchronization protocol which permits differential labelling in CENP-A-SNAP RPE-1 cells in correspondence with both production and deposition CENP-A timing. In addition, it will enable to collect samples before and after DNA replication for analysing and understanding the achieved results.

Due to the complexity of cellular model used, the individuation of fluorescent dyes for labelling old and new CENP-A in these cells was also required. For this purpose, a screening of different molecules, both commercial and non-commercial, was carried out to identify dyes capable of overcoming cellular barriers and so marking CENP-A-SNAP on chromatin.

Finally, CENP-A mononucleosome will be purified from the chromatin, co-immunoprecipitated and the fluorescence of each mononucleosome will be visualize for verifying the nature of nucleosome. If the 1st Hypothesis is true, the immunoprecipitated CENP-A will show both

different fluorescent signals used for labelling, otherwise, the fluorescence signal will be unique and the mononucleosome is constituted only by “the old CENP-A” or “the new CENP-A” in according to the signal colour (Figure 15).

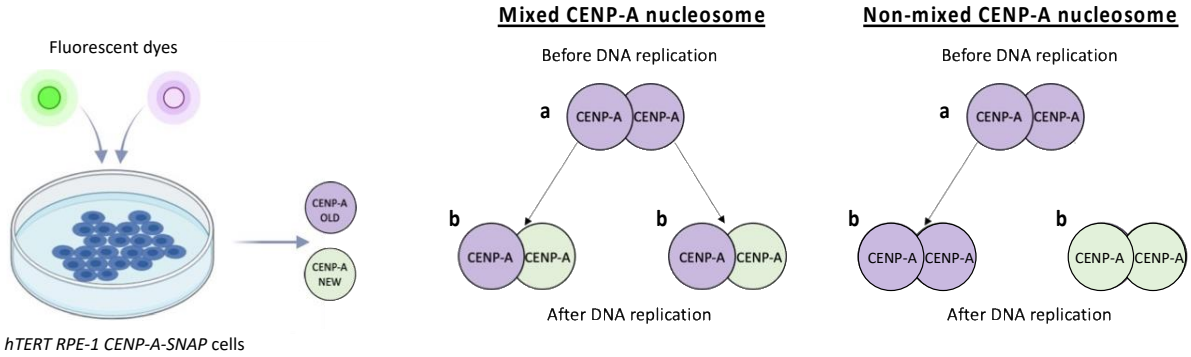

Figure 15. ***Graphical abstract (2/2).*** Our strategy permit to distinguish the two forms of CENP-A thanks to a differential labelling of the “old” (in purple) and “new” (in green) CENP-A by two fluorescent dyes. In the figure, **a** indicates nucleosome of pre-replication chromosome while **b** indicates the nucleosome of sister chromatid.

7 RESULTS

7.1 GENERATION OF A STABLE CENP-A-SNAP RPE-1 CELL LINE

Human retinal pigment epithelial RPE-1 (hTERT RPE-1) cells are genetically stable, near diploid cells widely used as model to study cell division in a non-transformed context. (Scott et al., 2020) For our studies, we needed RPE-1 cell line expressing CENP-A as a fusion protein with a tag permitting sequential labelling of CENP-A required to distinguish old and new CENP-A. To this end, we chose the SNAP-tag system, which is based on a 20 kDa mutant of DNA repair enzyme O6-alkylguanine-DNA-alkyltransferas. The SNAP tag reacts specifically and rapidly with benzylguanine derivatives, leading to irreversible covalent labelling of the SNAP-tag with a synthetic probe, including probes coupled to a fluorophore.

First of all, we generated a stable RPE-1 cell line expressing CENP-A with SNAP-tag through CRISPR/Cas9 system following the protocol published by Ghetti and colleagues and the strategy illustrated in figure 16A. (Ghetti et al., 2021) For genome-editing, two different RNA guides were tested. Guide #2 proved to be the one with the highest cutting efficiency (Figure 16B). After knock-in, the electroporated cells were cultured and selected for antibiotic resistance. The isolated clones were characterized by PCR reactions of their genomic DNA to identify those with insertions of the expected molecular weight (Figure 16C). This allowed us to select three potential candidate clones, namely clones #35, #42, #45, respectively. The expression level of CENP-A was imaged using SNAP-Cell® 647-SiR fluorescent labelling and using a Deltavision Elite fluorescence microscope. Clone #42 was found to have the best signal quality (Figure 16D).

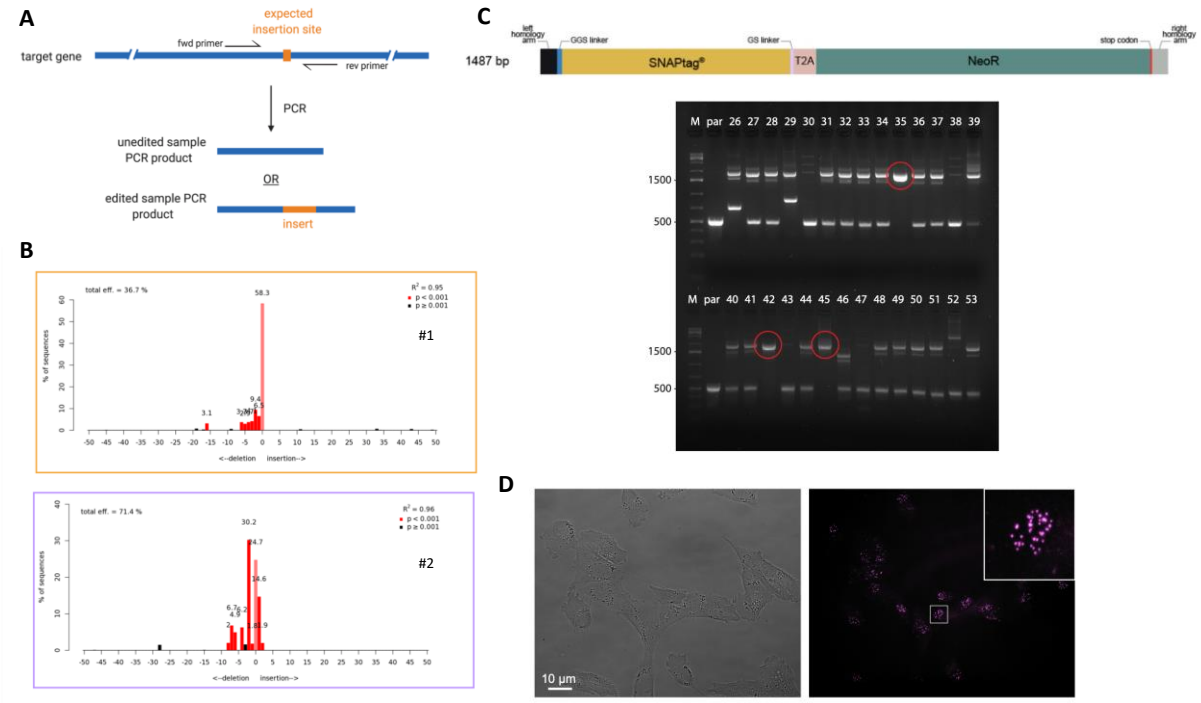

Figure 16. ***Generation of the stable CENP-A-SNAP RPE-1 cell line.*** (**A**) Genome-editing was performed following the strategy illustrated in panel **A**. (**B**) Two different guides were tested for the knock-in. (**C**) The characterization of clones was performed by PCR reactions of their genomic DNA for identifying those with inserted site at the expected weight. (**D**) Representative image of the selected clone was obtained at Deltavision Elite System using SNAP-Cell® 647-SiR for labelling.

7.2 Labelling of CENP-A-SNAP in RPE-1cells

To identify two dyes capable of labelling CENP-A in RPE-1 cell line expressing CENP-A-SNAP, we screened different commercial and customized reagents. At the beginning, we aimed to identify two substrates which, in addition to labelling CENP-A, could also be used to immuno-precipitate the resulting adducts with CENP-A. For this reason, we screened three dyes, including the commercial SNAP-Cell® Oregon Green® and two additional fluorophores generated in collaboration with the Department of Chemical Biology at the Max Planck Institute for Medical Research in Heidelberg. These molecules were chosen because the first could be immunoprecipitated using the Fluorescein/Oregon antibody, the other two using Streptavidin or Biotin antibody thanks to the presence of Biotin in their structure.

First, cells were seeded on coverslips and synchronized in G1 phase. Then, SNAP labelling was performed for each benzyl-substrates at different times and concentrations. After the labelling reaction, cells were fixed and imaged using a Deltavision Elite System. We also repeated these experiments with cells synchronized in mitosis, so to verify if the labelling efficiency would be facilitated by dissolution of the nuclear membrane during mitosis. Unfortunately, as a result of these screens, we concluded that only SNAP-Cell® Oregon Green® was suitable for CENP-A-SNAP labelling finalized to immunoprecipitation (Figure 17).

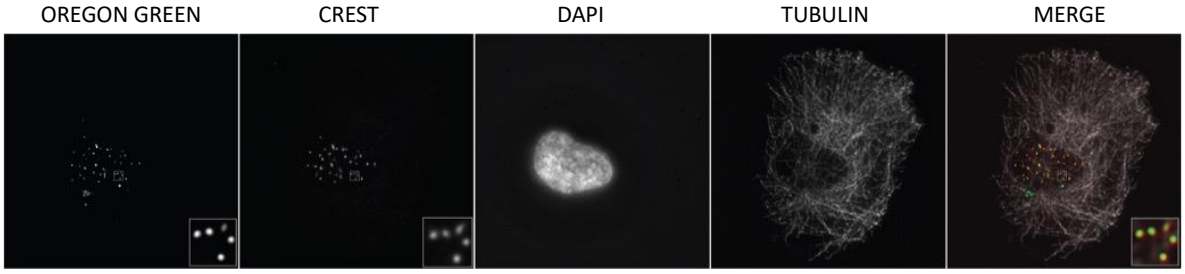

Figure 17. ***Fluorescent signal of CENP-A-SNAP labelled using SNAP-Cell® Oregon Green®.*** Representative image showing fluorescence of CENP-A labelled with SNAP-Cell® Oregon Green® (OREGON GREEN in green). Centromeres were visualized by CREST sera (red signal), DNA was stained by 4′,6-diamidino-2-phenylindole (DAPI) and cytoskeleton was recognized by tubulin. Scale bars, 10 μm.

The ability of SNAP-Cell® Oregon Green® to label CENP-A was also confirmed by Co-Immunoprecipitation as shown in figure 18.

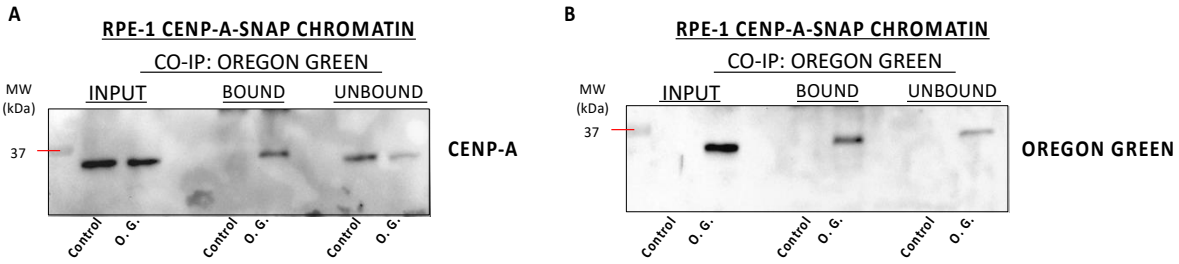

Figure 18. ***Co-Immunoprecipitation of CENP-A-SNAP labelled using SNAP-Cell® Oregon Green®.*** The purified chromatin of CENP-A-SNAP RPE-1 cells labelled and not (control) with SNAP-Cell® Oregon Green® (O.G.) was co-immunoprecipitated after incubation with Oregon Green antibody using protein A beads. The presence of CENP-A was evaluated by western blotting visualizing the chemiluminescence of CENP-A antibody (**A**) and Oregon Green antibody (**B**) in the different fractions. Two representative images are reported in figure.

As an alternative to the biotinylated compounds, we tested SNAP-Cell® 647-SiR, even if this compound does not allow precipitation of the labelled target protein. Also in this case, cells were seeded on coverslips and synchronized in G1 phase. Then, SNAP labelling was performed to

define both the right concentration and reaction time. After labelling, cells were fixed and imaged using the Deltavision Elite microscope (Figure 19A). Furthermore, we verified the presence of the SNAP-Cell® 647-SiR fluorescence signal in purified chromatin, as shown in figure 19B.

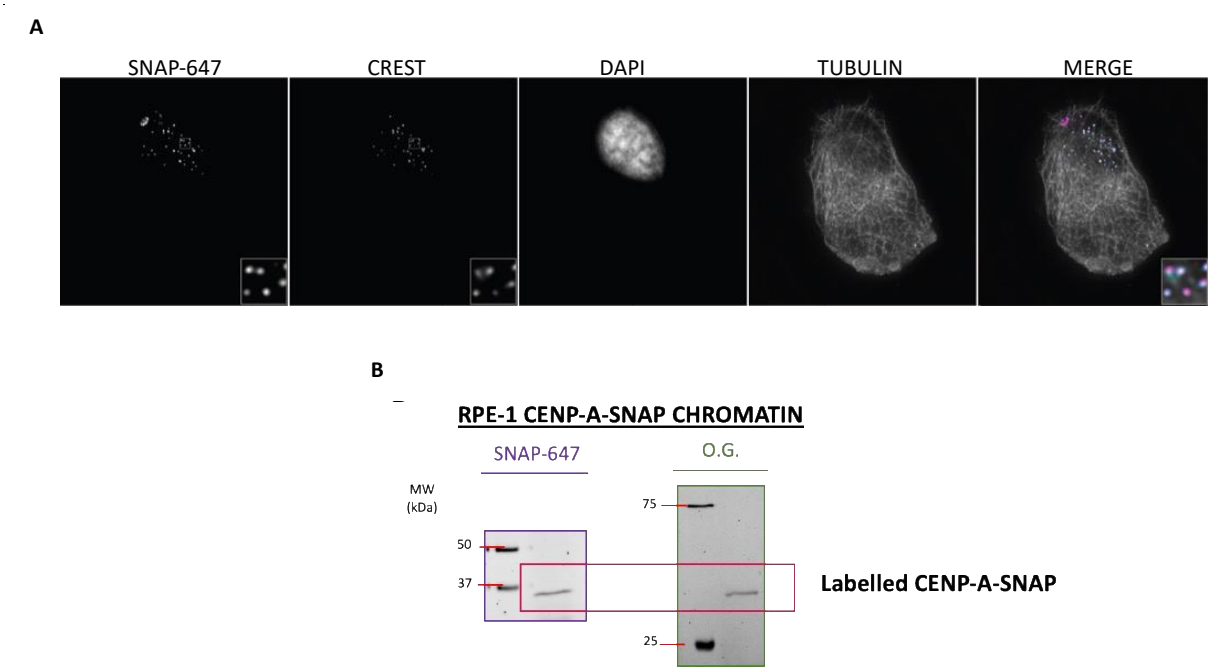

Figure 19. ***Fluorescent signal of labelled CENP-A-SNAP.*** (**A**) Representative image showing fluorescence of CENP-A labelled using SNAP-Cell® 647-SiR (SNAP-647 in magenta). Centromeres were visualized by CREST sera (cyan signal), DNA was stained by 4′,6-diamidino-2-phenylindole (DAPI) and cytoskeleton was recognized by tubulin. Scale bars, 10 μm. (**B**) The fluorescence of CENP-A-SNAP labelled with SNAP-Cell® 647-SiR (SNAP-647) and SNAP-Cell® Oregon Green® (O.G.) was evaluated in purified chromatin after electrophoresis on acrylamide gel. Two representative images are reported in figure.

Taken together, these results demonstrate that SNAP-Cell® Oregon Green® and SNAP-Cell® 647-SiR are suitable partners for CENP-A-SNAP labelling in CENP-A-SNAP RPE-1 cell line.

7.3 STANDARDIZATION OF THE SYNCHRONIZATION PROTOCOL FOR LABELLING OF CENP-A-SNAP IN RPE-1 CELLS

The differential labelling of CENP-A is particularly important to figure out its fate during DNA replication. For the purpose of discriminating the old form of CENP-A from the newly deposited

one, a synchronization protocol in CENP-A-SNAP RPE-1 cells is required to label CENP-A according to the timing of its production and deposition on chormatin. For this, pre-existing CENP-A on chromatin should be labelled before the synthesis of new protein. Thus, the first labelling should happen in a timeframe ranging from late G1 phase, in which deposition has already occured, to S phase. Conversely, the second labelling should be performed immediately after production of new CENP-A, from G2 phase to the subsquent G1 phase. To achieve this, we tried to implement treatment blocking cells sequentially in the appropriate cell cycle phases. This synchronization takes approximately 5 days (Figure 20).

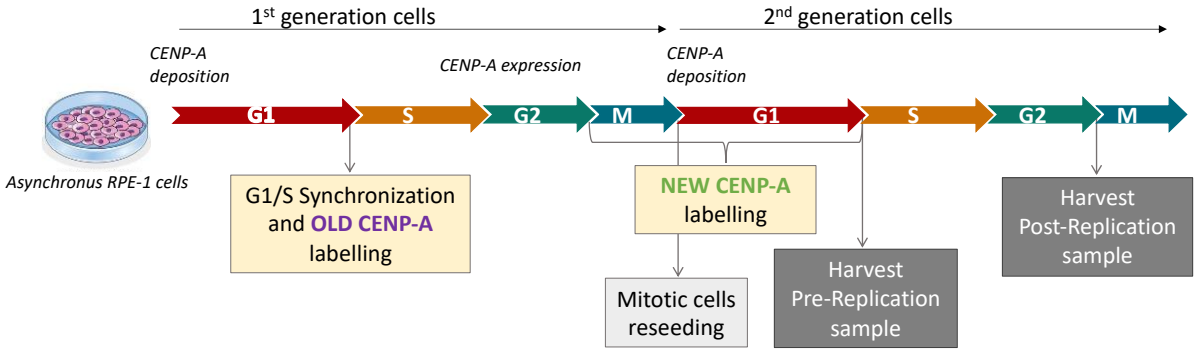

Figure 20. ***Schematic representation of synchronization protocol for CENP-A-SNAP RPE-1 cell line.***

RPE-1 are normal cells highly sensitive to stress, which complicates the synchronization protocols. Experiments to improve cell survival and and decreasing the undesired effects of cell cycle checkpoint are in progress. The preliminary results, reflecting optimization of the use of different drugs over multiple attempts, show that the most promising starting point is the implementation of a G1 phase arrest with the inhibitor of cyclin-dependent kinase 4 (Cdk4) and Cdk6 Palbociclib, as shown in Figure 20. Although Palbociclib is known for blocking RPE-1 cells in G1 phase, the concentrations used and duration of treatment had to be optimized for our conditions. (Trotter and Hagan, 2020) We first tested three concentrations of Palbociclib, 150, 500, and 1000 nM (Figure 21). Accumulation of cells in G1 phase after 24 hours was clearly visible already at the lowest dose tested (with an increase of G1 cells approximately close to 30% relative to control). Notably,

500 nM and 1000 nM of Palbociblib caused about 90% of the cell population to be arrested in G1, with no substantial difference between these two concentrations.

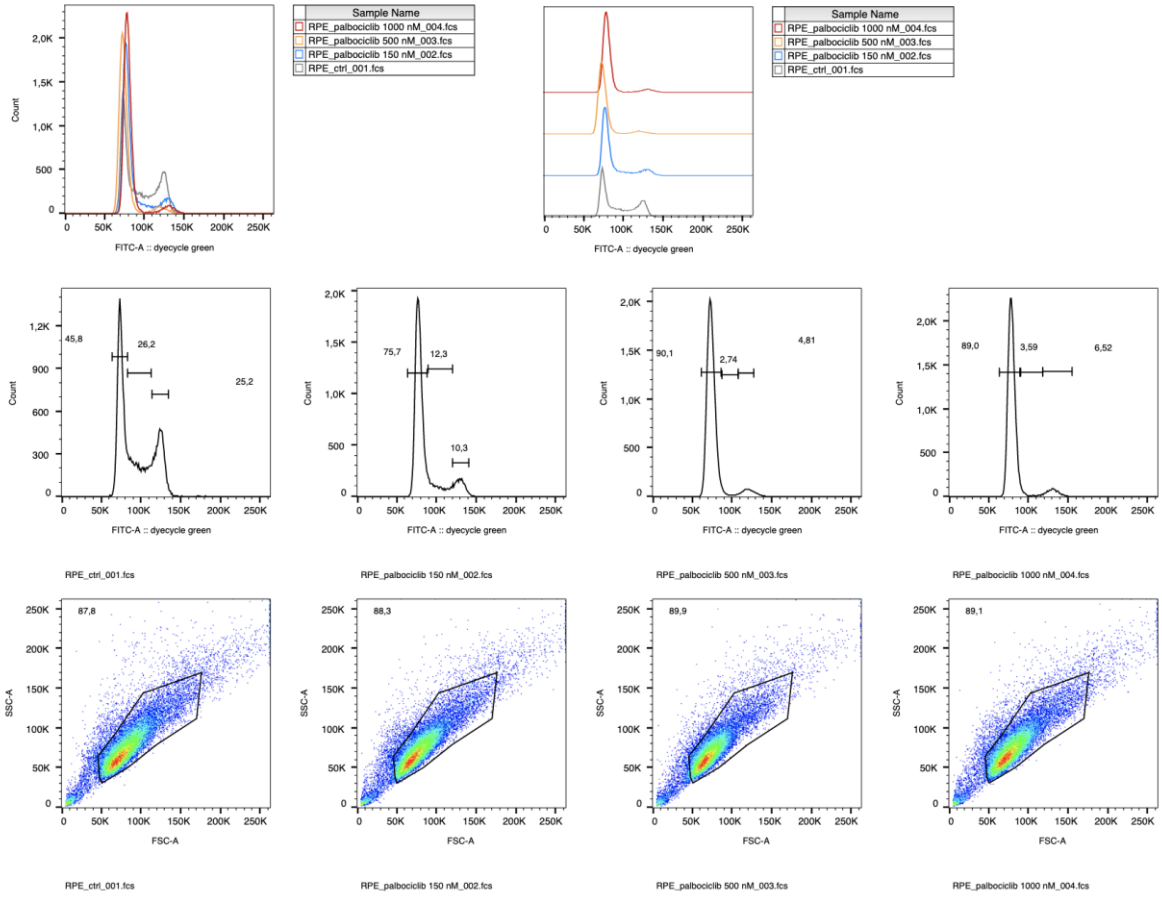

Figure 21. ***Representative cell cycle profiles of Palbociclib screening in CENP-A-SNAP RPE-1 cells.*** RPE-1 cells were treated and not (control also indicated as "ctrl") with 150, 500 and 1000 nM of Palbociclib for 24 hours.

As reported by Trotter and Hagan, HeLa cells are unresponsive to Palbociclib treatments (Trotter and Hagan, 2020). We therefore used HeLa cells as a negative control, confirming these previous results.

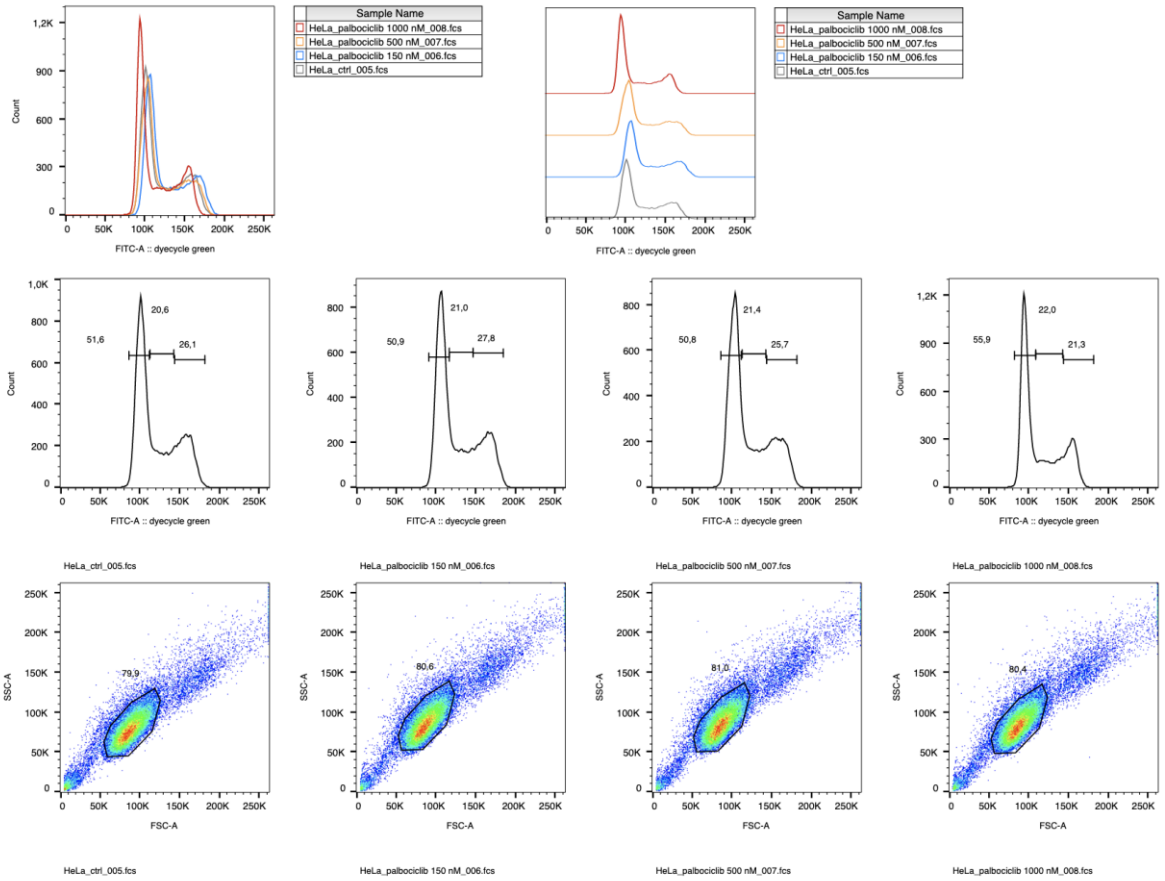

Figure 22. ***Representative cell cycle profiles of Palbociclib screening in HeLa cells.*** HeLa cells were treated and not (control also indicated as "ctrl") with 150, 500 and 1000 nM of Palbociclib for 24 hours.

Based on these results, we chose 500 nM Palbociclib as working concentration and further refined the protocol by setting different additional factors, such as confluence, treatment, release time and so on. Remarkably, almost the entire G1-arrested population following the treatment with 500 nM Palbociclib and release from the drug was found to be blocked in mitosis after an additional 24 hours in presence of 330 nM Nocodazole, which reversibly interferes with the polymerization of microtubules, or in presence of 5 μM STLC, which prevents the formation of mitotic spindle. No significant differences in the fraction of mitotic cells were observed among these two inhibitors. Given that cells round up during mitosis and are less firmly attached to the culture substratum, we were able to separate the mitotic fraction from non-mitotic cells by gently shaking and washing (mitotic shake-off), thus allowing us to select mitotic cells before reseeding them in a medium devoid of spindle poisons. Representative cell cycle profiles showed that at least 90% of reseeded

cells were in the G2/M peak after mitotic shake-off, underlining the efficiency of the method (Figure 23 – Day 3). After 6 hours from reseeding, cells had re-attached and the majority of the cell population was in G1-phase. Precisely, about 76% and 60 % of the cell population was in G1 after release from a Nocodazole or an STLC arrest, respectively (Figure 23 – Day 3). For our purposes, this sample could be considered as "Pre-Replication sample".

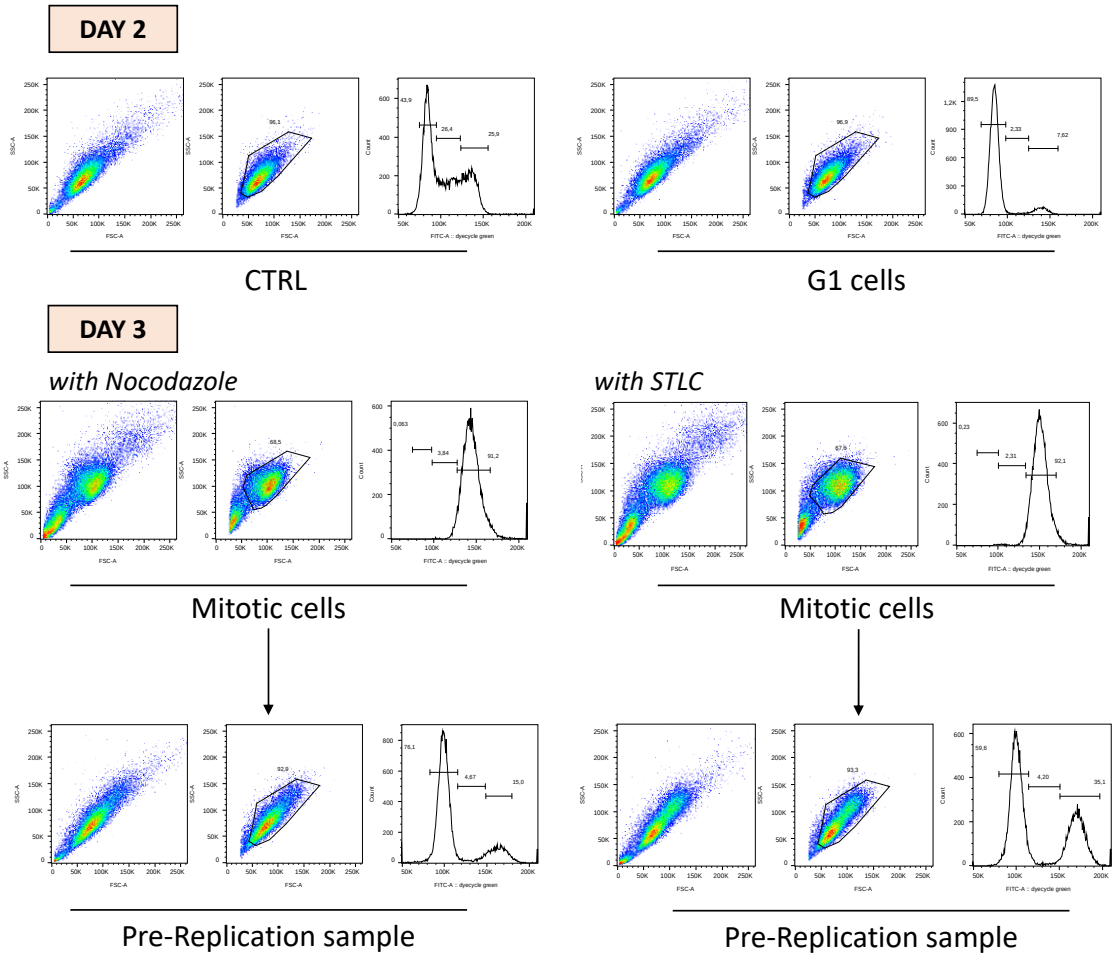

Figure 23. ***Representative cell cycle profiles of the time-points of interest.***

Overall, these results demonstrate the feasibility of a synchronization protocol in CENP-A-SNAP RPE-1 cells as shown in figure 24.

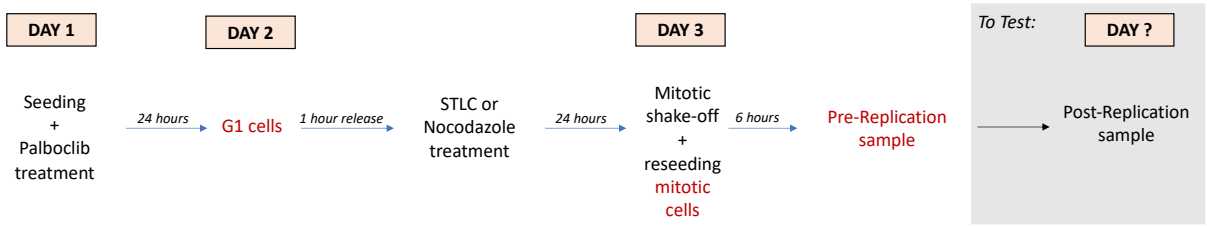

Figure 24. ***Scheme of the study protocol.*** The protocol takes at least 4 days. At day 1, RPE-1 cells are seeded in presence of 500nM of Palbociclib. After 24 hours, cells are release for 1 hour and then arrested in mitosis to collect only the mitotic cells (mitotic shake-off) and reseed them in order to exclude non-synchronized cells in day 3. After 6 hours, the "Pre-Replication" sample is fixed. Red samples are fixed for cytofluorimetric analysis.

8 DISCUSSION AND FUTURE PERSPECTIVES

CENP-A is a centromere-specific variant of histone H3. It plays a central role in directing kinetochore assembly and maintaining centromere function. (Musacchio and Desai, 2017) Specifically, CENP-A interacts selectively with proteins collectively identified as the constitutive centromere associated network (CCAN), which constitute the "inner" kinetochore and are necessary to build the microtubule-binding interface in the "outer" kinetochore. Recent structural work illuminated the organization of the CCAN subunits. (Pesenti et al., 2022) How CCAN interacts with CENP-A, however, has remained unknown. Several previous studies indicate that CENP-A, similarly to H3, interacts with histone H4 and can be assembled into "classic" octameric nucleosomes. (Tachiwana et al., 2011; Roulland et al., 2016) The localization of these CENP-A nucleosomes to centromeres, however, does not depend on any specific DNA sequence. Rather, it has been shown that CENP-A is inherited through an "epigenetic" mechanism (i.e., a mechanism that does not depend on a particular DNA sequence) that requires a dedicated CENP-A histone chaperone, HJURP, and additional machinery, the MIS18 complex. In human cells, deposition of new CENP-A by HJURP and the MIS18 complex occurs in the G1 phase of the cell cycle, and is therefore temporally uncoupled from the replication of DNA. The amount of new CENP-A deposited in G1 is similar to the amount of the existing CENP-A, suggesting that the existing CENP-A directs ("templates") the deposition reaction. This concept is consistent with an epigenetic mechanism, in which the pre-existing CENP-A, rather than any specific DNA sequence, directs new CENP-A deposition. This mechanism explains why the levels of CENP-A remain largely constant during successive cell divisions. (Pan et al., 2019)

The mechanism of CENP-A deposition remains poorly characterized. Prior to new deposition, the existing CENP-A on chromosomes is likely to be embedded in an octameric nucleosome containing two molecules (protomers) of CENP-A. Is the newly deposited CENP-A also part of a

nucleosome or does it adopt an unusual organization? Second, what happens to the newly deposited CENP-A during DNA replication, which is temporally disjoint from CENP-A deposition? Does new CENP-A mix with the pre-existing CENP-A in new hybrid nucleosome particles, or does it remain in distinct nucleosomes? These questions have very important implications for understanding the molecular basis of centromere inheritance and I tried to shed light on them. These questions are also of great importance when considering the crucial role of CENP-A in preserving genomic stability in eukaryotic cells. (Renaud-Pageot et al., 2022) It is important to understand how CENP-A performs its function, and how its deregulation may cause tumorigenesis. Thus, we are investigating CENP-A nucleosome composition before and after DNA replication.

To shed light on this problem, we wanted to find a method to distinguish the pre-existing CENP-A protein from the new CENP-A protein deposited in the early G1 phase (identified as "old CENP-A" and "new CENP-A" respectively). This, in turn, would allow establishing if the CENP-A nucleosomes on sister chromatids after DNA replication reassemble to have one "old CENP-A" and one "new CENP-A" (mixed nucleosome - 1st hypothesis), or they are rather inherited by sister chromatids as two "old" and two "new CENP-A", respectively, for each sister chromatids (non-mixed nucleosome – 2nd hypothesis) (Figure 14). To start the project, we used the CRISPR/Cas9 system to generate an hTERT RPE-1 cell line expressing a fusion protein of CENP-A and a small protein tag, the SNAP tag, which allow covalent intra-cellular labelling with various fluorophores. (Dreyer et al., 2023) CENP-A translation occurs during G2 phase and its deposition occurs in the time-frame ranging from telophase to early G1 phase. To succeed in our goal, we standardized the label of new and old forms of CENP-A with SNAP-Cell® Oregon Green® and SNAP-Cell® 647-SiR dyes. To overcome the impossibility of immunoprecipitated CENP-A with two different substrates, we will label first "old CENP-A" and then "new CENP-A" by Oregon Green® to check if the results is the same in both cases.

This task requires development and standardization of a sophisticated synchronization protocol for differential labelling of old and new CENP-A in hTERT RPE-1 cells expressing CENP-A-SNAP, providing a predictable labelling schedule for additional validation experiments. However, albeit they are genetically stable, near diploid cells, and widely used as model to study cell division in a non-transformed context, hTERT RPE-1 cells are highly sensitive to stress. This feature complicates the synchronization protocols taking a long time for setting up. (Scott et al., 2020) In this regard, minimal variations of cell number, treatment timing as well as the number of washes and releasing time strongly influnce the progression of cell cycle in RPE-1 cells and constitute the main obstacles to the finalisation of such a long protocol. For these reasons, further experiments are necessary to complete the protocol and also monitorate the expression levels of proteins like p53 and p21 for excluding a blockage of cell cycle. (Kumari and Jat, 2021) Finally, we intend to purify CENP-A mononucleosomes from the chromatin, and then visualize the fluorescence of each mononucleosome to verify whether old and new CENP-A mixed or not. We reasoned that if the 1st hypothesis were true, the immunoprecipitated CENP-A mononucleosomes will show both fluorescent colours used for labelling. Else, the immunoprecipitated CENP-A mononucleosomes will show only one of the two colours.

9 MATERIALS & METHODS

9.1 CHEMICALS & ANTIBODIES

Chemicals: Palbociclib (PZ0383; Sigma-Aldrich), Eg5 inhibitor S-trityl-L-cysteine (STLC) (164739; Sigma-Aldrich), Nocodazole (M1404; Sigma-Aldrich), SNAP-Cell® Oregon Green® (S9104S; New England Biolabs), SNAP-Cell® 647-SiR (S9102S; New England Biolabs), Benzonase (E8263; Sigma-Aldrich), Ethanol (BP2818100; Fisher Scientific), Methanol (322415; Sigma-Aldrich) 4′,6- diamidino-2-phenylindole (DAPI) (18860; Serva), Vybrant DyeCycle green (V35004; ThermoFisher), Mowiol (475904; Calbiochem). Antibodies: Oregon Green (A#889; Invitrogen), CENP-A (#2186; Cell Signaling Technology), CREST (15-234; Antibodies Incorporated) and Tubulin (T9026; Sigma-Aldrich)

9.2 CELL CULTURE AND SYNCHRONIZATION

Retinal pigmented epithelium (hTERT) RPE-1 cells were purchased by ATCC and CENP-A-SNAP cell line was generated by CRISPR/Cas9 genome editing as described in Ghetti et al., 2021. The cells were cultured in DMEM-F12 (BE12-719F; PAN-Biotech), supplemented with 10% FBS (P30-3306; PAN-Biotech,), 100 U/mL penicillin and 100 µg/mL streptomycin solution (DE17-602E; PAN-Biotech,) at 37°C with 5% CO_2.

In some experiments, cells were synchronized in different phases of the cell cycle. To synchronize cells at the G1/S phase border, cells were treated for 24 hours with Palbociclib at the concentrations reported in “Results” section. A mitotic arrest was induced by treating cells with 5 µM of STLC or with 330 nM of Nocodazole.

9.3 IMMUNOFLUORESCENCE

The cells on coverslips were fixed with ice-cold Methanol for 1 minute. Afterwards, the cells were first washed with 500 µL PBST three times and then blocked using the PBST solution supplemented with 5 % BSA for 20 minutes. The coverslips were incubated with 80 µL of master mix including primary antibody of interest for overnight. After the incubation, the coverslips were washed three times with PBST and the secondary antibody solution was added for 30 minutes to the samples. For the DNA staining was used 0.5 µg/mL of 4′,6- diamidino-2-phenylindole (DAPI). Lastly, the coverslips were washed thrice with PBST and once with ultrapure water and were mounted with Mowiol. The samples were let dry at room temperature for at least 16 hours and subsequently stored at 4 °C protected from light. Cells were imaged using a Deltavision Elite System (GE Healthcare) equipped with an IX-71 inverted microscope (Olympus). For each image, a z-stack containing 16 layers with a distance of 200 nm was acquired using the software softWoRx (GE Healthcare). The raw data were deconvolved and converted into average intensity projections for illustrative and quantification purposes. The images were edited and analyzed using the software FIJI.

9.4 CHROMATIN PURIFICATION

For each experimental point, cells were collected and spun down at 1,500 RPM for 5 minutes. Pellets were later resuspended in 5 volumes of lysis buffer in order to have a single-cell suspension. The samples were incubated for 2 minutes at room temperature and successively 10 minutes on ice. Then, 0.1% NP-40 was add to cells and the samples was mixed by gentle vortexing. Successively, the cytoplasmatic fraction was removed after centrifugation at 1,500 RPM for 10 minutes while the pellet, which is constituted by low purity *nuclei*, was resuspended in 5 volumes of washing buffer and sonicated for 5 cycles (1 cycle = 30 sec on/off) at low power. For chromatin

digestion, Benzonase was add to samples (0.1 μL of Benzonase for 200 μL of sample), which is mixed and incubated at 37°C for 5 minutes and then at 4°C with mild shaking. After 1 hour, NaCl was added to a final concentration of 420 mM and the samples were left in shaking for another 1 hour yet. Finally, the samples were spun-down at max speed for 20 minutes and the supernatant, or purified chromatin, was recovered. The protein concentration was evaluated using Nanodrop and the samples were stored at -20°C.

9.5 Co-Immunoprecipitation and sample preparation

For each sample, 1 mg of purified chromatin was incubated in mild rotation with Oregon Green antibody at 4°C overnight. The following day, 25 μL of protein-A beads was add to samples and they were incubated at 4°C with mild rotation for 1 hour. 6. Once the incubation was completed, the samples were spun-down at 1,500 RPM for 5 minutes at 4°C and the supernatant was recovered as "unbound" fraction. The pellets were washed thrice using washing solution by centrifugation at 1,500 RPM for 5 minutes at 4°C. 8. After the final wash, the supernatant was removed and 50 μL of 2X Leammli buffer were added to both pellets ("bound" fraction) and "unbound". In the end, all samples were boiled at 95 °C for 6 minutes and stored at -20°C until to western blotting.

9.6 Western Blotting

Generally, an amount of about 50 μg of chromatin was loaded and separated by SDS-PAGE. Then, sample proteins were transferred onto nitrocellulose membranes (GEH10600008; Amersham) by the Mini Trans-Blot system (Bio-Rad Laboratories). After washing in tris-buffered saline (TBS) supplemented with 0.05% Tween 20, membranes were blocked for 1 hour in 5% no-fat dry milk

(M7409; Sigma-Aldrich) and incubated overnight at 4°C with primary antibody. In the following days, HRP-conjugated secondary antibodies solution, reacting against the related primary species, were added to the membrane for 1 hour at room temperature. Each incubation step was preceded and followed by three 5-minutes washes in T-TBS. Finally, protein-related light signals were acquired by ChemiDocTM (Bio-Rad Laboratories) using the enhanced luminol-based chemiluminescent substrate (12994780; Cytiva Amersham) as a detection system for HRP.

9.7 FLOW CYTOMETRY ANALYSIS

Cytometric analysis was performed to define the respective cell phase distribution in reaction to different *stimuli*. Pelleted samples were resuspended first in 300 μL PBS and then in 700 μL ice-cold ethanol. Fixed cells were stored at −20°C until analysis. Before investigation, the samples were spun down for 5 minutes at 1,500 RPM and incubated with Vybrant DyeCycle green according manufacturing instruction. For each experimental condition, at least 20,000 events were acquired and analyzed by a BD LSRFortessa flow cytometer. Data were analyzed using FlowJo software.

BIBLIOGRAPHY

Akimoto M, Maruyama R, Kawabata Y, Tajima Y, Takenaga K. Antidiabetic adiponectin receptor agonist AdipoRon suppresses tumour growth of pancreatic cancer by inducing RIPK1/ERK-dependent necroptosis. Cell Death Dis. 2018 Jul 23;9(8):804. doi: 10.1038/s41419-018-0851-z. PMID: 30038429; PMCID: PMC6056513.

Alhothali M, Mathew M, Iyer G, Lawrence HR, Yang S, Chellappan S, Padmanabhan J. Fendiline Enhances the Cytotoxic Effects of Therapeutic Agents on PDAC Cells by Inhibiting Tumor-Promoting Signaling Events: A Potential Strategy to Combat PDAC. Int J Mol Sci. 2019 May 16;20(10):2423. doi: 10.3390/ijms20102423. PMID: 31100813; PMCID: PMC6567171.

Ali-Ahmad A, Sekulić N. CENP-A nucleosome-a chromatin-embedded pedestal for the centromere: lessons learned from structural biology. Essays Biochem. 2020 Sep 4;64(2):205-221. doi: 10.1042/EBC20190074. PMID: 32720682; PMCID: PMC7475651.

Alvarez G, Visitación Bartolomé M, Miana M, Jurado-López R, Martín R, Zuluaga P, et al. The effects of adiponectin and leptin on human endothelial cell proliferation: a live-cell study. J Vasc Res. 2012;49(2):111-22. doi: 10.1159/000332332. Epub 2012 Jan 13. PMID: 22249107.

Amato A, Schillaci T, Lentini L, Di Leonardo A. CENPA overexpression promotes genome instability in pRb-depleted human cells. Mol Cancer. 2009 Dec 10;8:119. doi: 10.1186/1476-4598-8-119. PMID: 20003272; PMCID: PMC2797498.

Amor DJ, Choo KH. Neocentromeres: role in human disease, evolution, and centromere study. Am J Hum Genet. 2002 Oct;71(4):695-714. doi: 10.1086/342730. Epub 2002 Aug 26. PMID: 12196915; PMCID: PMC378529.

Amrutkar M, Gladhaug IP. Pancreatic Cancer Chemoresistance to Gemcitabine. Cancers (Basel). 2017 Nov 16;9(11):157. doi: 10.3390/cancers9110157. PMID: 29144412; PMCID: PMC5704175.

Andronov L, Ouararhni K, Stoll I, Klaholz BP, Hamiche A. CENP-A nucleosome clusters form rosette-like structures around HJURP during G1. Nat Commun. 2019 Sep 30;10(1):4436. doi: 10.1038/s41467-019-12383-3. PMID: 31570711; PMCID: PMC6769019.

Bhat IA, Kabeer SW, Reza MI, Mir RH, Dar MO. AdipoRon: A Novel Insulin Sensitizer in Various Complications and the Underlying Mechanisms: A Review. Curr Mol Pharmacol. 2020;13(2):94-107. doi: 10.2174/1874467212666191022102800. PMID: 31642417.

Bai RL, Wang NY, Zhao LL, Zhang YF, Cui JW. Diverse and precision therapies open new horizons for patients with advanced pancreatic ductal adenocarcinoma. Hepatobiliary Pancreat Dis Int. 2022 Feb;21(1):10-24. doi: 10.1016/j.hbpd.2021.08.012. Epub 2021 Sep 8. PMID: 34538570.

Barra V, Fachinetti D. The dark side of centromeres: types, causes and consequences of structural abnormalities implicating centromeric DNA. Nat Commun. 2018 Oct 18;9(1):4340. doi: 10.1038/s41467-018-06545-y. PMID: 30337534; PMCID: PMC6194107.

Bayat Mokhtari R, Homayouni TS, Baluch N, Morgatskaya E, Kumar S, Das B, Yeger H. Combination therapy in combating cancer. Oncotarget. 2017 Jun 6;8(23):38022-38043. doi: 10.18632/oncotarget.16723. PMID: 28410237; PMCID: PMC5514969.

Black BE, Jansen LE, Maddox PS, Foltz DR, Desai AB, Shah JV, Cleveland DW. Centromere identity maintained by nucleosomes assembled with histone H3 containing the CENP-A targeting domain. Mol Cell. 2007 Jan 26;25(2):309-22. doi: 10.1016/j.molcel.2006.12.018. PMID: 17244537.

Black EM, Giunta S. Repetitive Fragile Sites: Centromere Satellite DNA As a Source of Genome Instability in Human Diseases. Genes (Basel). 2018 Dec 7;9(12):615. doi: 10.3390/genes9120615. PMID: 30544645; PMCID: PMC6315641.

Blomstrand H, Scheibling U, Bratthäll C, Green H, Elander NO. Real world evidence on gemcitabine and nab-paclitaxel combination chemotherapy in advanced pancreatic cancer. BMC Cancer. 2019 Jan 8;19(1):40. doi: 10.1186/s12885-018-5244-2. PMID: 30621618; PMCID: PMC6325739.

Bodor DL, Mata JF, Sergeev M, David AF, Salimian KJ, Panchenko T, et al. The quantitative architecture of centromeric chromatin. Elife. 2014 Jul 15;3:e02137. doi: 10.7554/eLife.02137. PMID: 25027692; PMCID: PMC4091408.

Braun R, Klinkhammer-Schalke M, Zeissig SR, Kleihus van Tol K, Bolm L, Honselmann KC, et al. Clinical Outcome and Prognostic Factors of Pancreatic Adenosquamous Carcinoma Compared to Ductal Adenocarcinoma-Results from the German Cancer Registry Group. Cancers (Basel). 2022 Aug 16;14(16):3946. doi: 10.3390/cancers14163946. PMID: 36010939; PMCID: PMC9406158.

Buscail L, Bournet B, Cordelier P. Role of oncogenic KRAS in the diagnosis, prognosis and treatment of pancreatic cancer. Nat Rev Gastroenterol Hepatol. 2020 Mar;17(3):153-168. doi: 10.1038/s41575-019-0245-4. Epub 2020 Jan 31. PMID: 32005945.

Carroll CW, Milks KJ, Straight AF. Dual recognition of CENP-A nucleosomes is required for centromere assembly. J Cell Biol. 2010 Jun 28;189(7):1143-55. doi: 10.1083/jcb.201001013. Epub 2010 Jun 21. PMID: 20566683; PMCID: PMC2894454.

Chou TC. Drug combination studies and their synergy quantification using the Chou-Talalay method. Cancer Res. 2010 Jan 15;70(2):440-6. doi: 10.1158/0008-5472.CAN-09-1947. Epub 2010 Jan 12. PMID: 20068163.

Christenson ES, Jaffee E, Azad NS. Current and emerging therapies for patients with advanced pancreatic ductal adenocarcinoma: a bright future. Lancet Oncol. 2020 Mar;21(3):e135-e145. doi: 10.1016/S1470-2045(19)30795-8. PMID: 32135117; PMCID: PMC8011058.

Clarke L, Carbon J. Isolation of a yeast centromere and construction of functional small circular chromosomes. Nature. 1980 Oct 9;287(5782):504-9. doi: 10.1038/287504a0. PMID: 6999364.

Conde e Silva N, Black BE, Sivolob A, Filipski J, Cleveland DW, Prunell A. CENP-A-containing nucleosomes: easier disassembly versus exclusive centromeric localization. J Mol Biol. 2007 Jul 13;370(3):555-73. doi: 10.1016/j.jmb.2007.04.064. Epub 2007 May 3. PMID: 17524417.

Dalal Y, Wang H, Lindsay S, Henikoff S. Tetrameric structure of centromeric nucleosomes in interphase Drosophila cells. PLoS Biol. 2007 Aug;5(8):e218. doi: 10.1371/journal.pbio.0050218. PMID: 17676993; PMCID: PMC1933458.

Damm M, Efremov L, Birnbach B, Terrero G, Kleeff J, Mikolajczyk R, et al. Efficacy and Safety of Neoadjuvant Gemcitabine Plus Nab-Paclitaxel in Borderline Resectable and Locally Advanced Pancreatic Cancer-A Systematic Review and Meta-Analysis. Cancers (Basel). 2021 Aug 27;13(17):4326. doi: 10.3390/cancers13174326. PMID: 34503138; PMCID: PMC8430874.

de Sousa Cavalcante L, Monteiro G. Gemcitabine: metabolism and molecular mechanisms of action, sensitivity and chemoresistance in pancreatic cancer. Eur J Pharmacol. 2014 Oct 15;741:8-16. doi: 10.1016/j.ejphar.2014.07.041. Epub 2014 Jul 30. PMID: 25084222.

Dimitriadis EK, Weber C, Gill RK, Diekmann S, Dalal Y. Tetrameric organization of vertebrate centromeric nucleosomes. Proc Natl Acad Sci U S A. 2010 Nov 23;107(47):20317-22. doi: 10.1073/pnas.1009563107. Epub 2010 Nov 8. PMID: 21059934; PMCID: PMC2996678.

Dreyer R, Pfukwa R, Barth S, Hunter R, Klumperman B. The Evolution of SNAP-Tag Labels. Biomacromolecules. 2023 Jan 6. doi: 10.1021/acs.biomac.2c01238. Epub ahead of print. PMID: 36607253.

Dunleavy EM, Almouzni G, Karpen GH. H3.3 is deposited at centromeres in S phase as a placeholder for newly assembled CENP-A in G_1 phase. Nucleus. 2011 Mar-Apr;2(2):146-57. doi: 10.4161/nucl.2.2.15211. PMID: 21738837; PMCID: PMC3127096.

Earnshaw WC, Rothfield N. Identification of a family of human centromere proteins using autoimmune sera from patients with scleroderma. Chromosoma. 1985;91(3-4):313-21. doi: 10.1007/BF00328227. PMID: 2579778.

Elsayed M, Abdelrahim M. The Latest Advancement in Pancreatic Ductal Adenocarcinoma Therapy: A Review Article for the Latest Guidelines and Novel Therapies. Biomedicines. 2021 Apr 6;9(4):389. doi: 10.3390/biomedicines9040389. PMID: 33917380; PMCID: PMC8067364.

Filipescu D, Naughtin M, Podsypanina K, Lejour V, Wilson L, Gurard-Levin ZA, et al. Essential role for centromeric factors following p53 loss and oncogenic transformation. Genes Dev. 2017 Mar 1;31(5):463-480. doi: 10.1101/gad.290924.116. Epub 2017 Mar 29. PMID: 28356341; PMCID: PMC5393061.

Fu Y, Ricciardiello F, Yang G, Qiu J, Huang H, Xiao J, et al. The Role of Mitochondria in the Chemoresistance of Pancreatic Cancer Cells. Cells. 2021 Feb 25;10(3):497. doi: 10.3390/cells10030497. PMID: 33669111; PMCID: PMC7996512.

Fukagawa T, Earnshaw WC. The centromere: chromatin foundation for the kinetochore machinery. Dev Cell. 2014 Sep 8;30(5):496-508. doi: 10.1016/j.devcel.2014.08.016. PMID: 25203206; PMCID: PMC4160344.

Furukawa T. Impacts of activation of the mitogen-activated protein kinase pathway in pancreatic cancer. Front Oncol. 2015 Feb 4;5:23. doi: 10.3389/fonc.2015.00023. PMID: 25699241; PMCID: PMC4316689.

Furuyama S, Biggins S. Centromere identity is specified by a single centromeric nucleosome in budding yeast. Proc Natl Acad Sci U S A. 2007 Sep 11;104(37):14706-11. doi: 10.1073/pnas.0706985104. Epub 2007 Sep 5. PMID: 17804787; PMCID: PMC1976213.

Furuyama T, Henikoff S. Centromeric nucleosomes induce positive DNA supercoils. Cell. 2009 Jul 10;138(1):104-13. doi: 10.1016/j.cell.2009.04.049. PMID: 19596238; PMCID: PMC2725230.

Gao HL, Wang WQ, Yu XJ, Liu L. Molecular drivers and cells of origin in pancreatic ductal adenocarcinoma and pancreatic neuroendocrine carcinoma. Exp Hematol Oncol. 2020 Oct 22;9:28. doi: 10.1186/s40164-020-00184-0. PMID: 33101770; PMCID: PMC7579802.

Ghetti S, Burigotto M, Mattivi A, Magnani G, Casini A, Bianchi A, et al. CRISPR/Cas9 ribonucleoprotein-mediated knockin generation in hTERT-RPE1 cells. STAR Protoc. 2021 Mar 24;2(2):100407. doi: 10.1016/j.xpro.2021.100407. PMID: 33855309; PMCID: PMC8025146.

Giunta S, Hervé S, White RR, Wilhelm T, Dumont M, Scelfo A, et al. CENP-A chromatin prevents replication stress at centromeres to avoid structural aneuploidy. Proc Natl Acad Sci U S A. 2021 Mar 9;118(10):e2015634118. doi: 10.1073/pnas.2015634118. PMID: 33653953; PMCID: PMC7958389.

Gu XM, Fu J, Feng XJ, Huang X, Wang SM, Chen XF, et al. Expression and prognostic relevance of centromere protein A in primary osteosarcoma. Pathol Res Pract. 2014 Apr;210(4):228-33. doi: 10.1016/j.prp.2013.12.007. Epub 2013 Dec 30. PMID: 24440098.

Gutiérrez ML, Muñoz-Bellvís L, Orfao A. Genomic Heterogeneity of Pancreatic Ductal Adenocarcinoma and Its Clinical Impact. Cancers (Basel). 2021 Sep 3;13(17):4451. doi: 10.3390/cancers13174451. PMID: 34503261; PMCID: PMC8430663

Guo YJ, Pan WW, Liu SB, Shen ZF, Xu Y, Hu LL. ERK/MAPK signalling pathway and tumorigenesis. Exp Ther Med. 2020 Mar;19(3):1997-2007. doi: 10.3892/etm.2020.8454. Epub 2020 Jan 15. PMID: 32104259; PMCID: PMC7027163.

Guse A, Carroll CW, Moree B, Fuller CJ, Straight AF. In vitro centromere and kinetochore assembly on defined chromatin templates. Nature. 2011 Aug 28;477(7364):354-8. doi: 10.1038/nature10379. PMID: 21874020; PMCID: PMC3175311.

He Q, Liu Z, Wang J. Targeting KRAS in PDAC: A New Way to Cure It? Cancers (Basel). 2022 Oct 11;14(20):4982. doi: 10.3390/cancers14204982. PMID: 36291766; PMCID: PMC9599866.

Hoyer K, Hablesreiter R, Inoue Y, Yoshida K, Briest F, Christen F, et al. A genetically defined signature of responsiveness to erlotinib in early-stage pancreatic cancer patients: Results from the CONKO-005 trial. EBioMedicine. 2021 Apr;66:103327. doi: 10.1016/j.ebiom.2021.103327. Epub 2021 Apr 13. PMID: 33862582; PMCID: PMC8054140.

Huang L, Jansen L, Balavarca Y, Molina-Montes E, Babaei M, van der Geest L, et al. Resection of pancreatic cancer in Europe and USA: an international large-scale study highlighting large variations. Gut. 2019 Jan;68(1):130-139. doi: 10.1136/gutjnl-2017-314828. Epub 2017 Nov 20. PMID: 29158237.

Jansen LE, Black BE, Foltz DR, Cleveland DW. Propagation of centromeric chromatin requires exit from mitosis. J Cell Biol. 2007 Mar 12;176(6):795-805. doi: 10.1083/jcb.200701066. Epub 2007 Mar 5. PMID: 17339380; PMCID: PMC2064054.

Jeffery D, Gatto A, Podsypanina K, Renaud-Pageot C, Ponce Landete R, Bonneville L, et al. CENP-A overexpression promotes distinct fates in human cells, depending on p53 status. Commun Biol. 2021 Mar 26;4(1):417. doi: 10.1038/s42003-021-01941-5. PMID: 33772115; PMCID: PMC7997993.

Jin X, Pan Y, Wang L, Ma T, Zhang L, Tang AH, et al. Fructose-1,6-bisphosphatase Inhibits ERK Activation and Bypasses Gemcitabine Resistance in Pancreatic Cancer by Blocking IQGAP1-MAPK Interaction. Cancer Res. 2017 Aug 15;77(16):4328-4341. doi: 10.1158/0008-5472.CAN-16-3143. Epub 2017 Jul 18. PMID: 28720574; PMCID: PMC5581962.

Kato H, Jiang J, Zhou BR, Rozendaal M, Feng H, Ghirlando R, et al. A conserved mechanism for centromeric nucleosome recognition by centromere protein CENP-C. Science. 2013 May 31;340(6136):1110-3. doi: 10.1126/science.1235532. PMID: 23723239; PMCID: PMC3763809.

Klein AP. Pancreatic cancer epidemiology: understanding the role of lifestyle and inherited risk factors. Nat Rev Gastroenterol Hepatol. 2021 Jul;18(7):493-502. doi: 10.1038/s41575-021-00457-x. Epub 2021 May 17. PMID: 34002083; PMCID: PMC9265847.

Koskinen A, Juslin S, Nieminen R, Moilanen T, Vuolteenaho K, Moilanen E. Adiponectin associates with markers of cartilage degradation in osteoarthritis and induces production of proinflammatory and catabolic factors through mitogen-activated protein kinase pathways. Arthritis Res Ther. 2011;13(6):R184. doi: 10.1186/ar3512. Epub 2011 Nov 11. PMID: 22077999; PMCID: PMC3334633.

Krassovsky K, Henikoff JG, Henikoff S. Tripartite organization of centromeric chromatin in budding yeast. Proc Natl Acad Sci U S A. 2012 Jan 3;109(1):243-8. doi: 10.1073/pnas.1118898109. Epub 2011 Dec 19. PMID: 22184235; PMCID: PMC3252899.

Kumarasamy V, Ruiz A, Nambiar R, Witkiewicz AK, Knudsen ES. Chemotherapy impacts on the cellular response to CDK4/6 inhibition: distinct mechanisms of interaction and efficacy in models of pancreatic cancer. Oncogene. 2020 Feb;39(9):1831-1845. doi: 10.1038/s41388-019-1102-1. Epub 2019 Nov 19. PMID: 31745297; PMCID: PMC7047578.

Kumari R, Jat P. Mechanisms of Cellular Senescence: Cell Cycle Arrest and Senescence Associated Secretory Phenotype. Front Cell Dev Biol. 2021 Mar 29;9:645593. doi: 10.3389/fcell.2021.645593. PMID: 33855023; PMCID: PMC8039141.

Latenstein AEJ, van der Geest LGM, Bonsing BA, Groot Koerkamp B, Haj Mohammad N, de Hingh IHJT, et al.; Dutch Pancreatic Cancer Group. Nationwide trends in incidence, treatment and survival of pancreatic ductal adenocarcinoma. Eur J Cancer. 2020 Jan;125:83-93. doi: 10.1016/j.ejca.2019.11.002. Epub 2019 Dec 13. PMID: 31841792.

Lechner J, Carbon J. A 240 kd multisubunit protein complex, CBF3, is a major component of the budding yeast centromere. Cell. 1991 Feb 22;64(4):717-25. doi: 10.1016/0092-8674(91)90501-o. PMID: 1997204.

Li Y, Zhu Z, Zhang S, Yu D, Yu H, Liu L, et al. ShRNA-targeted centromere protein A inhibits hepatocellular carcinoma growth. PLoS One. 2011 Mar 15;6(3):e17794. doi: 10.1371/journal.pone.0017794. PMID: 21423629; PMCID: PMC3058037.

Lippi G, Mattiuzzi C. The global burden of pancreatic cancer. Arch Med Sci. 2020 May 4;16(4):820-824. doi: 10.5114/aoms.2020.94845. PMID: 32542083; PMCID: PMC7286317.

Liu WT, Wang Y, Zhang J, Ye F, Huang XH, Li B, He QY. A novel strategy of integrated microarray analysis identifies CENPA, CDK1 and CDC20 as a cluster of diagnostic biomarkers in lung adenocarcinoma. Cancer Lett. 2018 Jul 1;425:43-53. doi: 10.1016/j.canlet.2018.03.043. Epub 2018 Mar 31. PMID: 29608985.

Locke DP, Hillier LW, Warren WC, Worley KC, Nazareth LV, Muzny DM, et al. Comparative and demographic analysis of orang-utan genomes. Nature. 2011 Jan 27;469(7331):529-33. doi: 10.1038/nature09687. Erratum in: Nature. 2022 Aug;608(7924):E36. PMID: 21270892; PMCID: PMC3060778.

Logsdon GA, Barrey EJ, Bassett EA, DeNizio JE, Guo LY, Panchenko T, Dawicki-McKenna JM, Heun P, Black BE. Both tails and the centromere targeting domain of CENP-A are required for centromere establishment. J Cell Biol. 2015 Mar 2;208(5):521-31. doi: 10.1083/jcb.201412011. Epub 2015 Feb 23. PMID: 25713413; PMCID: PMC4347640.

Lu Y, Xu D, Peng J, Luo Z, Chen C, Chen Y, et al. HNF1A inhibition induces the resistance of pancreatic cancer cells to gemcitabine by targeting ABCB1. EBioMedicine. 2019 Jun;44:403-418. doi: 10.1016/j.ebiom.2019.05.013. Epub 2019 May 15. PMID: 31103629; PMCID: PMC6606897.

Makaremi S, Asadzadeh Z, Hemmat N, Baghbanzadeh A, Sgambato A, Ghorbaninezhad F, et al. Immune Checkpoint Inhibitors in Colorectal Cancer: Challenges and Future Prospects. Biomedicines. 2021 Aug 24;9(9):1075. doi: 10.3390/biomedicines9091075. PMID: 34572263; PMCID: PMC8467932.

Mahlke MA, Nechemia-Arbely Y. Guarding the Genome: CENP-A-Chromatin in Health and Cancer. Genes (Basel). 2020 Jul 16;11(7):810. doi: 10.3390/genes11070810. PMID: 32708729; PMCID: PMC7397030.

Manuelidis L. Chromosomal localization of complex and simple repeated human DNAs. Chromosoma. 1978 Mar 22;66(1):23-32. doi: 10.1007/BF00285813. PMID: 639625.

Marques A, Pedrosa-Harand A. Holocentromere identity: from the typical mitotic linear structure to the great plasticity of meiotic holocentromeres. Chromosoma. 2016 Sep;125(4):669-81. doi: 10.1007/s00412-016-0612-7. Epub 2016 Aug 16. PMID: 27530342.

Matsuura F, Oku H, Koseki M, Sandoval JC, Yuasa-Kawase M, Tsubakio-Yamamoto K, et al. Adiponectin accelerates reverse cholesterol transport by increasing high density lipoprotein assembly in the liver. Biochem Biophys Res Commun. 2007 Jul 13;358(4):1091-5. doi: 10.1016/j.bbrc.2007.05.040. Epub 2007 May 15. PMID: 17521614.

McGovern SL, Qi Y, Pusztai L, Symmans WF, Buchholz TA. Centromere protein-A, an essential centromere protein, is a prognostic marker for relapse in estrogen receptor-positive breast cancer. Breast Cancer Res. 2012 May 4;14(3):R72. doi: 10.1186/bcr3181. PMID: 22559056; PMCID: PMC3446334.

Messaggio F, Mendonsa AM, Castellanos J, Nagathihalli NS, Gorden L, Merchant NB, VanSaun MN. Adiponectin receptor agonists inhibit leptin induced pSTAT3 and *in vivo* pancreatic tumor growth. Oncotarget. 2017 Aug 3;8(49):85378-85391. doi: 10.18632/oncotarget.19905. PMID: 29156726; PMCID: PMC5689616.

Miao X, Koch G, Ait-Oudhia S, Straubinger RM, Jusko WJ. Pharmacodynamic Modeling of Cell Cycle Effects for Gemcitabine and Trabectedin Combinations in Pancreatic Cancer Cells. Front Pharmacol. 2016 Nov 15;7:421. doi: 10.3389/fphar.2016.00421. PMID: 27895579; PMCID: PMC5108803.

Mizrahi JD, Surana R, Valle JW, Shroff RT. Pancreatic cancer. Lancet. 2020 Jun 27;395(10242):2008-2020. doi: 10.1016/S0140-6736(20)30974-0. PMID: 32593337.

Mizuguchi G, Xiao H, Wisniewski J, Smith MM, Wu C. Nonhistone Scm3 and histones CenH3-H4 assemble the core of centromere-specific nucleosomes. Cell. 2007 Jun 15;129(6):1153-64. doi: 10.1016/j.cell.2007.04.026. PMID: 17574026.

Montano R, Khan N, Hou H, Seigne J, Ernstoff MS, Lewis LD, Eastman A. Cell cycle perturbation induced by gemcitabine in human tumor cells in cell culture, xenografts and bladder cancer patients: implications for clinical trial designs combining gemcitabine with a Chk1 inhibitor. Oncotarget. 2017 Jun 28;8(40):67754-67768. doi: 10.18632/oncotarget.18834. PMID: 28978069; PMCID: PMC5620209.

Moroi Y, Peebles C, Fritzler MJ, Steigerwald J, Tan EM. Autoantibody to centromere (kinetochore) in scleroderma sera. Proc Natl Acad Sci U S A. 1980 Mar;77(3):1627-31. doi: 10.1073/pnas.77.3.1627. PMID: 6966403; PMCID: PMC348550.

Musacchio A, Desai A. A Molecular View of Kinetochore Assembly and Function. Biology (Basel). 2017 Jan 24;6(1):5. doi: 10.3390/biology6010005. PMID: 28125021; PMCID: PMC5371998.

Nigro E, Daniele A, Salzillo A, Ragone A, Naviglio S, Sapio L. AdipoRon and Other Adiponectin Receptor Agonists as Potential Candidates in Cancer Treatments. Int J Mol Sci. 2021 May 25;22(11):5569. doi: 10.3390/ijms22115569. PMID: 34070338; PMCID: PMC8197554.

Oba A, Ho F, Bao QR, Al-Musawi MH, Schulick RD, Del Chiaro M. Neoadjuvant Treatment in Pancreatic Cancer. Front Oncol. 2020 Feb 28;10:245. doi: 10.3389/fonc.2020.00245. PMID: 32185128; PMCID: PMC7058791.

Okada Y, Takahashi N, Takayama T, Goel A. LAMC2 promotes cancer progression and gemcitabine resistance through modulation of EMT and ATP-binding cassette transporters in pancreatic ductal adenocarcinoma. Carcinogenesis. 2021 Apr 30;42(4):546-556. doi: 10.1093/carcin/bgab011. PMID: 33624791; PMCID: PMC8086766.

Okada-Iwabu M, Yamauchi T, Iwabu M, Honma T, Hamagami K, Matsuda K, t al. A small-molecule AdipoR agonist for type 2 diabetes and short life in obesity. Nature. 2013 Nov 28;503(7477):493-9. doi: 10.1038/nature12656. Epub 2013 Oct 30. PMID: 24172895.

Orth M, Metzger P, Gerum S, Mayerle J, Schneider G, Belka C, et al. Pancreatic ductal adenocarcinoma: biological hallmarks, current status, and future perspectives of combined modality treatment approaches. Radiat Oncol. 2019 Aug 8;14(1):141. doi: 10.1186/s13014-019-1345-6. PMID: 31395068; PMCID: PMC6688256.

Ovejero S, Bueno A, Sacristán MP. Working on Genomic Stability: From the S-Phase to Mitosis. Genes (Basel). 2020 Feb 20;11(2):225. doi: 10.3390/genes11020225. PMID: 32093406; PMCID: PMC7074175.

Palmer DK, O'Day K, Wener MH, Andrews BS, Margolis RL. A 17-kD centromere protein (CENP-A) copurifies with nucleosome core particles and with histones. J Cell Biol. 1987 Apr;104(4):805-15. doi: 10.1083/jcb.104.4.805. PMID: 3558482; PMCID: PMC2114441.

Pan D, Walstein K, Take A, Bier D, Kaiser N, Musacchio A. Mechanism of centromere recruitment of the CENP-A chaperone HJURP and its implications for centromere licensing. Nat Commun. 2019 Sep 6;10(1):4046. doi: 10.1038/s41467-019-12019-6. PMID: 31492860; PMCID: PMC6731319.

Panchal K, Sahoo RK, Gupta U, Chaurasiya A. Role of targeted immunotherapy for pancreatic ductal adenocarcinoma (PDAC) treatment: An overview. Int Immunopharmacol. 2021 Jun;95:107508. doi: 10.1016/j.intimp.2021.107508. Epub 2021 Mar 13. PMID: 33725635.

Passacantilli I, Panzeri V, Terracciano F, Delle Fave G, Sette C, Capurso G. Co-treatment with gemcitabine and nab-paclitaxel exerts additive effects on pancreatic cancer cell death. Oncol Rep. 2018 Apr;39(4):1984-1990. doi: 10.3892/or.2018.6233. Epub 2018 Jan 25. PMID: 29393478.

Perpelescu M, Nozaki N, Obuse C, Yang H, Yoda K. Active establishment of centromeric CENP-A chromatin by RSF complex. J Cell Biol. 2009 May 4;185(3):397-407. doi: 10.1083/jcb.200903088. Epub 2009 Apr 27. PMID: 19398759; PMCID: PMC2700388.

Pesenti ME, Raisch T, Conti D, Walstein K, Hoffmann I, Vogt D, et al. Structure of the human inner kinetochore CCAN complex and its significance for human centromere organization. Mol Cell. 2022 Jun 2;82(11):2113-2131.e8. doi: 10.1016/j.molcel.2022.04.027. Epub 2022 May 6. PMID: 35525244; PMCID: PMC9235857.

Plana D, Palmer AC, Sorger PK. Independent Drug Action in Combination Therapy: Implications for Precision Oncology. Cancer Discov. 2022 Mar 1;12(3):606-624. doi: 10.1158/2159-8290.CD-21-0212. PMID: 34983746; PMCID: PMC8904281.

Pompella L, Tirino G, Pappalardo A, Caterino M, Ventriglia A, Nacca V, et al. Pancreatic Cancer Molecular Classifications: From Bulk Genomics to Single Cell Analysis. Int J Mol Sci. 2020 Apr 17;21(8):2814. doi: 10.3390/ijms21082814. PMID: 32316602; PMCID: PMC7215357.

Principe DR, Underwood PW, Korc M, Trevino JG, Munshi HG, Rana A. The Current Treatment Paradigm for Pancreatic Ductal Adenocarcinoma and Barriers to Therapeutic Efficacy. Front Oncol. 2021 Jul 15;11:688377. doi: 10.3389/fonc.2021.688377. PMID: 34336673; PMCID: PMC8319847.

Qian Y, Gong Y, Fan Z, Luo G, Huang Q, Deng S, et al. Molecular alterations and targeted therapy in pancreatic ductal adenocarcinoma. J Hematol Oncol. 2020 Oct 2;13(1):130. doi: 10.1186/s13045-020-00958-3. PMID: 33008426; PMCID: PMC7532113.

Qiu JJ, Guo JJ, Lv TJ, Jin HY, Ding JX, Feng WW, et al. Prognostic value of centromere protein-A expression in patients with epithelial ovarian cancer. Tumour Biol. 2013 Oct;34(5):2971-5. doi: 10.1007/s13277-013-0860-6. Epub 2013 May 28. PMID: 23712606.

Quiñonero F, Mesas C, Doello K, Cabeza L, Perazzoli G, Jimenez-Luna C, et al. The challenge of drug resistance in pancreatic ductal adenocarcinoma: a current overview. Cancer Biol Med. 2019 Nov;16(4):688-699. doi: 10.20892/j.issn.2095-3941.2019.0252. PMID: 31908888; PMCID: PMC6936232.

Ragone A, Salzillo A, Spina A, Naviglio S, Sapio L. Integrating Gemcitabine-Based Therapy With AdipoRon Enhances Growth Inhibition in Human PDAC Cell Lines. Front Pharmacol. 2022 Feb 22;13:837503. doi: 10.3389/fphar.2022.837503. PMID: 35273510; PMCID: PMC8902254.

Rajendran V, Jain MV. In Vitro Tumorigenic Assay: Colony Forming Assay for Cancer Stem Cells. Methods Mol Biol. 2018;1692:89-95. doi: 10.1007/978-1-4939-7401-6_8. PMID: 28986889.

Rajput AB, Hu N, Varma S, Chen CH, Ding K, Park PC, et al. Immunohistochemical Assessment of Expression of Centromere Protein-A (CENPA) in Human Invasive Breast Cancer. Cancers (Basel). 2011 Dec 6;3(4):4212-27. doi: 10.3390/cancers3044212. PMID: 24213134; PMCID: PMC3763419.

Ramzan AA, Bitler BG, Hicks D, Barner K, Qamar L, Behbakht K, et al. Adiponectin receptor agonist AdipoRon induces apoptotic cell death and suppresses proliferation in human ovarian cancer cells. Mol Cell Biochem. 2019 Nov;461(1-2):37-46. doi: 10.1007/s11010-019-03586-9. Epub 2019 Jul 10. PMID: 31292831; PMCID: PMC7490954.

Renaud-Pageot C, Quivy JP, Lochhead M, Almouzni G. CENP-A Regulation and Cancer. Front Cell Dev Biol. 2022 Jun 2;10:907120. doi: 10.3389/fcell.2022.907120. PMID: 35721491; PMCID: PMC9201071.

Riedl JM, Posch F, Horvath L, Gantschnigg A, Renneberg F, Schwarzenbacher E, et al. Gemcitabine/nab-Paclitaxel versus FOLFIRINOX for palliative first-line treatment of advanced pancreatic cancer: A propensity score analysis. Eur J Cancer. 2021 Jul;151:3-13. doi: 10.1016/j.ejca.2021.03.040. Epub 2021 May 2. PMID: 33951545.

Robey RW, Pluchino KM, Hall MD, Fojo AT, Bates SE, Gottesman MM. Revisiting the role of ABC transporters in multidrug-resistant cancer. Nat Rev Cancer. 2018 Jul;18(7):452-464. doi: 10.1038/s41568-018-0005-8. PMID: 29643473; PMCID: PMC6622180.

Roulland Y, Ouararhni K, Naidenov M, Ramos L, Shuaib M, Syed SH, et al. The Flexible Ends of CENP-A Nucleosome Are Required for Mitotic Fidelity. Mol Cell. 2016 Aug 18;63(4):674-685. doi: 10.1016/j.molcel.2016.06.023. Epub 2016 Aug 4. PMID: 27499292.

Ryu WJ, Han G, Lee SH, Choi KY. Suppression of Wnt/β-catenin and RAS/ERK pathways provides a therapeutic strategy for gemcitabine-resistant pancreatic cancer. Biochem Biophys Res Commun. 2021 Apr 16;549:40-46. doi: 10.1016/j.bbrc.2021.02.076. Epub 2021 Mar 1. PMID: 33662667.

Saha AK, Contreras-Galindo R, Niknafs YS, Iyer M, Qin T, Padmanabhan K, et al. The role of the histone H3 variant CENPA in prostate cancer. J Biol Chem. 2020 Jun 19;295(25):8537-8549. doi: 10.1074/jbc.RA119.010080. Epub 2020 May 5. PMID: 32371391; PMCID: PMC7307189.

Sapio L, Ragone A, Spina A, Salzillo A, Naviglio S. AdipoRon and Pancreatic Ductal Adenocarcinoma: a future perspective in overcoming chemotherapy-induced resistance? Cancer Drug Resist. 2022 Jun 21;5(3):625-636. doi: 10.20517/cdr.2022.34. PMID: 36176754; PMCID: PMC9511794.

Sapio L, Salzillo A, Illiano M, Ragone A, Spina A, et al. Chlorogenic acid activates ERK1/2 and inhibits proliferation of osteosarcoma cells. J Cell Physiol. 2020 Apr;235(4):3741-3752. doi: 10.1002/jcp.29269. Epub 2019 Oct 10. PMID: 31602671.

Sathyan KM, Fachinetti D, Foltz DR. α-amino trimethylation of CENP-A by NRMT is required for full recruitment of the centromere. Nat Commun. 2017 Mar 7;8:14678. doi: 10.1038/ncomms14678. PMID: 28266506; PMCID: PMC5343448.

Scott SJ, Suvarna KS, D'Avino PP. Synchronization of human retinal pigment epithelial-1 cells in mitosis. J Cell Sci. 2020 Sep 17;133(18):jcs247940. doi: 10.1242/jcs.247940. PMID: 32878943; PMCID: PMC7520456.

Shang WH, Hori T, Toyoda A, Kato J, Popendorf K, Sakakibara Y, et al. Chickens possess centromeres with both extended tandem repeats and short non-tandem-repetitive sequences. Genome Res. 2010 Sep;20(9):1219-28. doi: 10.1101/gr.106245.110. Epub 2010 Jun 9. PMID: 20534883; PMCID: PMC2928500.

Sharma AB, Dimitrov S, Hamiche A, Van Dyck E. Centromeric and ectopic assembly of CENP-A chromatin in health and cancer: old marks and new tracks. Nucleic Acids Res. 2019 Feb 20;47(3):1051-1069. doi: 10.1093/nar/gky1298. PMID: 30590707; PMCID: PMC6379705.

Shrestha RL, Rossi A, Wangsa D, Hogan AK, Zaldana KS, Suva E, et al. CENP-A overexpression promotes aneuploidy with karyotypic heterogeneity. J Cell Biol. 2021 Apr 5;220(4):e202007195. doi: 10.1083/jcb.202007195. PMID: 33620383; PMCID: PMC7905998.

Srivastava S, Foltz DR. Posttranslational modifications of CENP-A: marks of distinction. Chromosoma. 2018 Sep;127(3):279-290. doi: 10.1007/s00412-018-0665-x. Epub 2018 Mar 22. PMID: 29569072; PMCID: PMC6082721.

Sung H, Ferlay J, Siegel RL, Laversanne M, Soerjomataram I, Jemal A, Bray F. Global Cancer Statistics 2020: GLOBOCAN Estimates of Incidence and Mortality Worldwide for 36 Cancers in 185 Countries. CA Cancer J Clin. 2021 May;71(3):209-249. doi: 10.3322/caac.21660. Epub 2021 Feb 4. PMID: 33538338.

Sun X, Clermont PL, Jiao W, Helgason CD, Gout PW, Wang Y, Qu S. Elevated expression of the centromere protein-A(CENP-A)-encoding gene as a prognostic and predictive biomarker in human cancers. Int J Cancer. 2016 Aug 15;139(4):899-907. doi: 10.1002/ijc.30133. Epub 2016 Apr 21. PMID: 27062469.

Tachiwana H, Kagawa W, Shiga T, Osakabe A, Miya Y, Saito K, et al. Crystal structure of the human centromeric nucleosome containing CENP-A. Nature. 2011 Jul 10;476(7359):232-5. doi: 10.1038/nature10258. PMID: 21743476.

Tian T, Li X, Liu Y, Wang C, Liu X, Bi G, et al. Molecular basis for CENP-N recognition of CENP-A nucleosome on the human kinetochore. Cell Res. 2018 Mar;28(3):374-378. doi: 10.1038/cr.2018.13. Epub 2018 Jan 19. PMID: 29350209; PMCID: PMC5835772.

Tomonaga T, Matsushita K, Yamaguchi S, Oohashi T, Shimada H, Ochiai T, et al. Overexpression and mistargeting of centromere protein-A in human primary colorectal cancer. Cancer Res. 2003 Jul 1;63(13):3511-6. PMID: 12839935.

Trotter EW, Hagan IM. Release from cell cycle arrest with Cdk4/6 inhibitors generates highly synchronized cell cycle progression in human cell culture. Open Biol. 2020 Oct;10(10):200200. doi: 10.1098/rsob.200200. Epub 2020 Oct 14. PMID: 33052073; PMCID: PMC7653349.

Vernuccio F, Messina C, Merz V, Cannella R, Midiri M. Resectable and Borderline Resectable Pancreatic Ductal Adenocarcinoma: Role of the Radiologist and Oncologist in the Era of Precision Medicine. Diagnostics (Basel). 2021 Nov 22;11(11):2166. doi: 10.3390/diagnostics11112166. PMID: 34829513; PMCID: PMC8623921.

Verrelle P, Meseure D, Berger F, Forest A, Leclère R, Nicolas A, et al. CENP-A Subnuclear Localization Pattern as Marker Predicting Curability by Chemoradiation Therapy for Locally Advanced Head and Neck Cancer Patients. Cancers (Basel). 2021 Aug 4;13(16):3928. doi: 10.3390/cancers13163928. PMID: 34439087; PMCID: PMC8391827.

Vincent V, Thakkar H, Aggarwal S, Mridha AR, Ramakrishnan L, Singh A. ATP-binding cassette transporter A1 (ABCA1) expression in adipose tissue and its modulation with insulin resistance in obesity. Diabetes Metab Syndr Obes. 2019 Feb 25;12:275-284. doi: 10.2147/DMSO.S186565. Erratum in: Diabetes Metab Syndr Obes. 2019 Dec 11;12:2633. PMID: 30881070; PMCID: PMC6395069.

Waissi W, Amé JC, Mura C, Noël G, Burckel H. Gemcitabine-Based Chemoradiotherapy Enhanced by a PARP Inhibitor in Pancreatic Cancer Cell Lines. Int J Mol Sci. 2021 Jun 25;22(13):6825. doi: 10.3390/ijms22136825. PMID: 34201963; PMCID: PMC8269291.

Wang H, Liu J, Xia G, Lei S, Huang X, Huang X. Survival of pancreatic cancer patients is negatively correlated with age at diagnosis: a population-based retrospective study. Sci Rep. 2020 Apr 27;10(1):7048. doi: 10.1038/s41598-020-64068-3. PMID: 32341400; PMCID: PMC7184604.

Wang L, Collings CK, Zhao Z, Cozzolino KA, Ma Q, Liang K, et al. A cytoplasmic COMPASS is necessary for cell survival and triple-negative breast cancer pathogenesis by regulating metabolism. Genes Dev. 2017 Oct 15;31(20):2056-2066. doi: 10.1101/gad.306092.117. Epub 2017 Nov 14. PMID: 29138278; PMCID: PMC5733497.

Wang S, Zheng Y, Yang F, Zhu L, Zhu XQ, Wang ZF, et al. The molecular biology of pancreatic adenocarcinoma: translational challenges and clinical perspectives. Signal Transduct Target Ther. 2021 Jul 5;6(1):249. doi: 10.1038/s41392-021-00659-4. PMID: 34219130; PMCID: PMC8255319.

Wang SJ, Wang C, Wang WQ, Hao QQ, Liu YF. [Adiponectin Receptor Agonist AdipoRon Inhibits the Proliferation of Myeloma Cells via the AMPK/Autophagy Pathway]. Zhongguo Shi Yan Xue Ye Xue Za Zhi. 2020 Feb;28(1):171-176. Chinese. doi: 10.19746/j.cnki.issn.1009-2137.2020.01.029. PMID: 32027272.

Wang Z, Tang J, Li Y, Wang Y, Guo Y, Tu Q, et al. AdipoRon promotes diabetic fracture repair through endochondral ossification-based bone repair by enhancing survival and differentiation of chondrocytes. Exp Cell Res. 2020 Feb 15;387(2):111757. doi: 10.1016/j.yexcr.2019.111757. Epub 2019 Dec 12. PMID: 31838062; PMCID: PMC7722537.

Weir JR, Faesen AC, Klare K, Petrovic A, Basilico F, Fischböck J, et al. Insights from biochemical reconstitution into the architecture of human kinetochores. Nature. 2016 Sep 8;537(7619):249-253. doi: 10.1038/nature19333. Epub 2016 Aug 31. PMID: 27580032.

Wong MH, Xue A, Baxter RC, Pavlakis N, Smith RC. Upstream and Downstream Co-inhibition of Mitogen-Activated Protein Kinase and PI3K/Akt/mTOR Pathways in Pancreatic Ductal Adenocarcinoma. Neoplasia. 2016 Jul;18(7):425-35. doi: 10.1016/j.neo.2016.06.001. PMID: 27435925; PMCID: PMC5022074.

Wu Q, Qian YM, Zhao XL, Wang SM, Feng XJ, Chen XF, Zhang SH. Expression and prognostic significance of centromere protein A in human lung adenocarcinoma. Lung Cancer. 2012 Aug;77(2):407-14. doi: 10.1016/j.lungcan.2012.04.007. Epub 2012 Apr 28. PMID: 22542705.

Xu M, Li L, Liu Z, Jiao Z, Xu P, Kong X, et al. ABCB2 (TAP1) as the downstream target of SHH signaling enhances pancreatic ductal adenocarcinoma drug resistance. Cancer Lett. 2013 Jun 10;333(2):152-8. doi: 10.1016/j.canlet.2013.01.002. Epub 2013 Jan 20. PMID: 23340176.

Xu Y, Liang C, Cai X, Zhang M, Yu W, Shao Q. High Centromere Protein-A (CENP-A) Expression Correlates with Progression and Prognosis in Gastric Cancer. Onco Targets Ther. 2020 Dec 29;13:13237-13246. doi: 10.2147/OTT.S263512. PMID: 33402833; PMCID: PMC7778524.

Yang J, Xu R, Wang C, Qiu J, Ren B, You L. Early screening and diagnosis strategies of pancreatic cancer: a comprehensive review. Cancer Commun (Lond). 2021 Dec;41(12):1257-1274. doi: 10.1002/cac2.12204. Epub 2021 Jul 31. PMID: 34331845; PMCID: PMC8696234.

Yong BJC, Wirama Diyana M. Low Carbohydrate Antigen 19-9 (CA 19-9) Levels in a Patient Highly Suspected of Having Caput Pancreas Tumor. Cureus. 2022 Apr 21;14(4):e24357. doi: 10.7759/cureus.24357. PMID: 35611029; PMCID: PMC9124065.

Zhang W, Mao JH, Zhu W, Jain AK, Liu K, Brown JB, Karpen GH. Centromere and kinetochore gene misexpression predicts cancer patient survival and response to radiotherapy and chemotherapy. Nat Commun. 2016 Aug 31;7:12619. doi: 10.1038/ncomms12619. PMID: 27577169; PMCID: PMC5013662.

Zhou C, Qian W, Ma J, Cheng L, Jiang Z, Yan B, et al. Resveratrol enhances the chemotherapeutic response and reverses the stemness induced by gemcitabine in pancreatic cancer cells via targeting SREBP1. Cell Prolif. 2019 Jan;52(1):e12514. doi: 10.1111/cpr.12514. Epub 2018 Oct 19. PMID: 30341797; PMCID: PMC6430460.

Zhu YH, Zheng JH, Jia QY, Duan ZH, Yao HF, Yang J, et al. Immunosuppression, immune escape, and immunotherapy in pancreatic cancer: focused on the tumor microenvironment. Cell Oncol (Dordr). 2022 Nov 11. doi: 10.1007/s13402-022-00741-1. Epub ahead of print. PMID: 36367669.